TECHNICAL NOTES

NATIONAL ADVISORY COMMITTEE FOR AERONAUTICS

No. 893

LEAST-WORK ANALYSIS OF THE PROBLEM OF SHEAR LAG IN BOX BEAMS

By Francis B. Hildebrand and Eric Reissner
Massachusetts Institute of Technology

Washington
May 1945

NATIONAL ADVISORY COMMITTEE FOR AERONAUTICS

TECHNICAL NOTE NO. 893

LEAST-WORK ANALYSIS OF THE PROBLEM OF SHEAR LAG IN BOX BEAMS

By Francis B. Hildebrand and Eric Reissner

SUMMARY

The distribution of stress in the cover sheets of thin-wall box beams is analyzed, with regard to the effect of shear deformation in the cover sheets, by the method of least work.

Explicit results are obtained for a number of representative cases that show the influence of the following factors on the stress pattern:

1. Variation of stress in spanwise direction as given by elementary beam theory.

2. Value of a parameter called shear-lag aspect ratio which designates the product of span-width ratio of the beam and of the square root of the ratio of effective shear modulus and tension modulus of the cover sheets.

3. Value of ratio of cover-sheet stiffness to side-web stiffness.

4. Variation of beam height in span direction.

5. Variation of beam width in span direction.

6. Variation of cover-sheet thickness in span direction.

General conclusions are drawn from the results obtained. Among them the most important one appears to be the fact that the shear-lag effect depends primarily on the following two quantities:

1. the value of the shear-lag aspect ratio.

2. the shape of the curve representing the product of the stress of elementary beam theory and of the cover-sheet thickness.

The basic relations of the theory are presented in a form convenient for the determination of additional solutions.

While the main body of the work is concerned with the analysis of cantilever beams, there are also given examples of solutions for beams on two simple supports and for beams with statically indeterminate support. In the former case very simple approximate solutions are obtained for problems previously solved by exact methods. In the latter case, which has not been treated previously, it is found that not only the stress distribution but also the moment distribution of the elementary beam theory is modified by shear lag.

INTRODUCTION

Further applications and extensions of a method given by one of the authors (references 1 and 2) for the determination of shear lag in thin-wall box beams subjected to bending loads (fig. 1) are presented in this paper. The problem is that of determining the distribution of stress in the cover sheets of box beams when the shear deformation of the cover sheets is taken into account.

With regard to closed box beams the treatment is restricted to beams of doubly symmetrical rectangular cross section, it being understood that slight deviations from symmetry cause only slight deviations of the shear-lag pattern from that of the symmetrical beam. It is shown, however, that by simply modifying the definition of one of the parameters occurring in the analysis the developments are also applicable to the limiting case of asymmetry when one of the two cover sheets is entirely missing.

Part I of this work deals with shear lag in cantilever beams with one end fixed. By use of the basic equations, which have been derived in reference 2, explicit expressions are obtained for the stresses in the cover sheets. With the help of these expressions, the influence of the shape of the load curve and the influence of the cross-sectional characteristics of the beam on the shear-lag pattern are analyzed. In particular, information is obtained on the effect of height, width, and cover-sheet thickness taper. For a number of typical conditions, the results are evaluated numerically and are represented in form of diagrams.

In part II of this work the application of the basic equations of the theory to beams on two simple end supports is indicated, and a few such solutions are given although presumably they are of importance only for other than aeronautical applications.

The case of a beam with two fixed ends is considered as an example of beams with statically undeterminate support in part III of this paper. In this case, which to the authors' knowledge has not been treated before, it is found that not only is the transverse distribution of stress affected by shear lag but also the spanwise distribution of bending moments is modified if shear deformation of the cover sheets is taken into account.

Finally, explicit reference is made to the work of Kuhn and Chiarito (reference 3) in which approximate solutions of shear-lag problems are obtained by means of a method that is based on stronger simplifying assumptions than those made for the least-work method.

This investigation, conducted at Massachusetts Institute of Technology, was sponsored by, and conducted with financial assistance from the National Advisory Committee for Aeronautics.

SYMBOLS

σ_b cover-sheet bending stress of elementary beam theory $\left(\frac{M}{I}\frac{h}{2}\right)$

M bending moment

h height of beam

I moment of inertia of beam $(I_w + I_s)$

I_w principal moment of inertia of two side webs including flanges

I_s moment of inertia of two cover sheets about transverse beam axis

σ_x spanwise normal stress in cover sheets

x,y rectangular coordinates in plane of cover sheets; x (spanwise) measured from tip to root, y (transverse) measured from middle line to edge of sheet

m stiffness parameter $\left(\frac{3I_w + I_s}{I}\right)$

w half width of beam

s function giving effect of shear deformability of cover sheet $[\sigma_x(x,w) - \sigma_x(x,o)]$

t cover-sheet thickness

e_w distance of centroid of side webs from plane of cover sheet

A_w area of two side webs

σ_y transverse normal stress

G modulus of rigidity

E Young's modulus

w_d developed half width

n number of equally spaced longitudinals of area A

w_{eff} effective sheet width

l length of beam for cantilever; half length of beam with both ends supported

ξ dimensionless span coordinate $\left(\frac{x}{l_e}\right)$

l_e distance from origin of coordinate system to root of cantilever beam

H ratio of height of beam to height of beam at root $\left(\frac{h}{h_R}\right)$, called height function

h_R root height of beam

T ratio of cover-sheet thickness to cover-sheet thickness at root $\left(\frac{t}{t_R}\right)$, called thickness function

t_R cover-sheet thickness at root of beam

W ratio of width of beam to width of beam at root $\left(\frac{w}{w_R}\right)$, called width function

w_R half of root width of beam

F bending-moment function $\left(\frac{\sigma_b}{\sigma_o}\right)$

σ_o elementary bending stress at root section

f shear-lag function $\left(\frac{s}{\sigma_o}\right)$

m_R stiffness parameter at root section

ξ_o dimensionless coordinate of tip section

κ auxiliary parameter $\left(\lambda \frac{l_e}{w_R}\sqrt{\frac{6G}{E}}\right)$

λ auxiliary parameter $\sqrt{\frac{35m - 21}{35m^2 - 42m + 15}}$

η variable of integration

ξ_c dimensionless coordinate of point of concentrated load application

L distance of center of gravity of $(TF)''$ curve from root of beam

p_o uniform load

$-P_o$ concentrated load

δ ratio of successive cover-sheet thicknesses $\left(\frac{t_2}{t_1}\right)$

$p(\xi)$ particular integral of differential equation

A, B constants of integration

q exponent in width-taper law

γ auxiliary parameter $(\sqrt{m\lambda^2 - 1})$

n_1, n_2 exponents

c_1, c_2 constants of integration

d_1, d_2 constants of integration

M_R bending moment at root section

r exponent in sheet-thickness-taper law

$a_1, a_2, a_3, a_4 \ldots$ coefficients

M_e bending moment according to elementary beam theory (equal to M for statically determinate beams)

Subscripts:

l	left
r	right
R	at root section
m,n	general case numbers
part	particular
max	maximum
c	concentrated load
o	at tip section

I - DISTRIBUTION OF STRESS IN THE COVER SHEETS OF CANTILEVER BOX BEAMS

BASIC EQUATIONS USED IN SOLUTION OF PROBLEM

In reference 2, box beams with rectangular doubly symmetrical cross section acted upon by given distributions of bending moments were treated (fig. 1). A parabolic transverse distribution of the cover-sheet normal stresses σ_x was assumed

$$\sigma_x(x,y) = \sigma_b(x) - \left(\frac{m}{3} - \frac{y^2}{w^2}\right) s(x) \tag{1}$$

where

$$\sigma_b(x) = \frac{M(x)}{I(x)} \frac{h(x)}{2} \tag{2}$$

is the cover-sheet stress of elementary beam theory, obtained when the shear deformability of the sheets is disregarded. The function

$$s(x) = \sigma_x(x,w) - \sigma_x(x,o) \tag{3}$$

is a measure for the effect of the shear deformability of the sheet, and the value of the parameter

$$m = \frac{3I_w + I_s}{I_w + I_s}, \quad 1 \leq m \leq 3 \tag{4a}$$

insures that the state of stress in the beam due to the superposition of $s(x)$ does not give rise to a resultant moment about the neutral axis of the cross section.

If the neutral axis of the cross section is not at the same time an axis of geometrical symmetry, then in general the stress in the two cover sheets will be given by two different analytical expressions. An exception is formed by the limiting case of asymmetry of a beam with open cross section consisting of two side webs and one cover sheet. In this case the cover-sheet normal stress is given by one expression of the form of equation (1) with the parameter m defined by

$$m = \frac{3I_w + 2tw\, e_w^2 \left(1 + \dfrac{I_w}{e_w^2 A_w}\right)}{I_w + 2tw\, e_w^2 \left(1 + \dfrac{I_w}{e_w^2 A_w}\right)}, \quad 1 \leqslant m \leqslant 3 \qquad (4b)$$

where now I_w is the principal moment of inertia of the two side webs, A_w is their area, and e_w is the distance of their centroid from the plane of the cover sheet. This result is established by means of the condition of moment equilibrium in the form given by equation (12) in reference 4.

With the help of this result, it is established that if one cover sheet of a doubly symmetrical section is removed shear lag in the remaining cover sheet is very little modified. This permits the conclusion that also in the intermediate case of two unequal cover sheets the analysis of the doubly symmetrical section leads to relevant results.

The shear stress in the sheets corresponding to the normal stress of equation (1) is determined from equilibrium conditions. The function $s(x)$ is determined by minimizing the internal work of the beam (in the work expression the work of the transverse normal stresses σ_y being disregarded, which amounts to the assumption that the sheet is rigid transversely). In this way, as has been shown in reference 2, a differential equation and boundary conditions for s are found. The differential equation for $s(x)$ is of the form

$$m \frac{d}{dx}\left[\frac{1}{t}\frac{d}{dx}(ts)\right] - \frac{21m - 15}{35m - 21} w^2 \frac{d}{dx}\left[\frac{1}{t}\frac{d}{dx}\left(\frac{ts}{w^2}\right)\right] - \frac{6G}{E}\frac{s}{w^2} = 3\frac{d}{dx}\left[\frac{1}{t}\frac{d}{dx}(t\sigma_b)\right] \qquad (5)$$

where t is the sheet thickness, w is one-half the sheet width, and G/E is the ratio of effective shear modulus and Young's modulus for the material.

For flat unstiffened and unwrinkled sheets the value of G/E will be $3/8$. For flat unstiffened sheets, wrinkled because of shear, the value of G/E is generally assumed to be somewhat smaller than that for the unwrinkled

sheet. The same is true for corrugated sheets where $G/E = (3/8)(w/w_d)$ if w_d is the developed half width for flat sheet-corrugated sheet combinations, and for sheets stiffener by n (say $n \geq 5$), equally spaced longitudinals of area A where $(G/E) = (3/8)\, 2wt/(2wt + nA)$.

The boundary conditions for $s(x)$ are of the following form:

At the free end of the beam,

$$ts = 0 \tag{6}$$

At the fixed end of the beam,

$$\frac{d}{dx}(ts) - \frac{21m - 15}{35m - 21} w^2 \frac{d}{dx}\left(\frac{ts}{w^2}\right) = 3 \frac{d}{dx}(t\sigma_b) \tag{7}$$

In addition, it is useful to have conditions for the case when at some section of the beam a discontinuous change of section properties take place, with or without simultaneous application of a concentrated load at this section. If the values of quantities immediately to the left or right of the section are indicated by subscripts l and r, the following transition conditions are found:

$$t_l s_l = t_r s_r \tag{8}$$

$$\frac{m_l}{t_l}\frac{d}{dx}(t_l s_l) - \frac{21m_l - 15}{35m_l - 21} w^2 \frac{1}{t_l}\frac{d}{dx}\left(\frac{t_l s_l}{w^2}\right) - \frac{3}{t_l}\frac{d}{dx}(t_l \sigma_{b,l})$$

$$= \frac{m_r}{l_r}\frac{d}{dx}(t_r s_r) - \frac{21m_r - 15}{35m_r - 21}\frac{w^2}{t_r}\frac{d}{dx}\left(\frac{t_r s_r}{w^2}\right) - \frac{3}{t_r}\frac{d}{dx}(t_r \sigma_{b,r}) \tag{9}$$

Equation (8) expresses the condition of continuity of the sheet normal-stress resultants and equation (9) is the condition of continuity of the spanwise displacement component, in the form required by the least-work method. Equation (9) corrects and generalizes a corresponding equation mentioned in a footnote in reference 2.

The shear-lag problem is now reduced to the solution of equations (5) to (9) and to the substitution of the results in equation (1).

From equation (1) an expression for the effective sheet width w_{eff} is obtained in the form

$$\frac{w_{eff}}{w} = \frac{\int_0^w \sigma_x(x,y)\,dy}{w\,\sigma_x(x,w)} = \frac{1}{3} + \frac{2\sigma_x(x,o)}{3\,\sigma_x(x,w)} \tag{10}$$

which is valid at those sections where $\sigma_x(x,w) > \sigma_x(x,o)$. Equation (10) can also be written in the form

$$\frac{w_{eff}}{w} = \frac{1 - \frac{m-1}{3}\frac{s(x)}{\sigma_b(x)}}{1 + \left(1 - \frac{m}{3}\right)\frac{s(x)}{\sigma_b(x)}} \tag{10a}$$

For the edge and center sheet stresses in equation (10), follows from equation (1)

$$\frac{\sigma_x(x,o)}{\sigma_b(l)} = \frac{\sigma_b(x)}{\sigma_b(l)} - \frac{m}{3}\frac{s(x)}{\sigma_b(l)} \tag{11}$$

$$\frac{\sigma_x(x,w)}{\sigma_b(l)} = \frac{\sigma_b(x)}{\sigma_b(l)} - \left(1 - \frac{m}{3}\right)\frac{s(x)}{\sigma_b(l)} \tag{12}$$

The application of the preceding set of basic equations to a series of representative cases and the conclusions drawn from these applications form the body of the following developments.

Before proceeding to examples, it has been found helpful to introduce dimensionless variables of a kind explained in the following paragraph.

DIMENSIONLESS FORM OF THE BASIC EQUATIONS

Write

$$\xi = \frac{x}{l_e} \tag{13}$$

$$H(\xi) = \frac{h}{h_R} \tag{14}$$

$$T(\xi) = \frac{t}{t_R} \tag{15}$$

$$W(\xi) = \frac{w}{w_R} \tag{16}$$

$$F(\xi) = \frac{\sigma_b(x)}{\sigma_o} \tag{17}$$

$$f(\xi) = \frac{s(x)}{\sigma_o} \tag{18}$$

$$\sigma_o = (\sigma_b)_R \tag{19}$$

In equations (13) to (19) it is understood that l_e represents the span l of the beam, if its cross section is uniform, and that in the case of tapering cross section l_e is the "extended" span, that is, the distance from the origin of the coordinate system to the root of the beam of length l, and the origin is chosen according to the simplicity of the analytical expressions for W or T or both. σ_o is the value of the elementary bending stress at the root section.

It is convenient to represent $F(\xi)$ in equation (17) in the following way. From

$$\sigma_b(x) = \frac{M}{I}\frac{h}{2},\quad I = I_s + I_w,\quad I_s = h^2tw,\quad m = (3I_w + I_s)/I$$

follows

$$\sigma_b(x) = \frac{3 - m}{4}\frac{M(x)}{htw}$$

and consequently

$$F(\xi) = \frac{M(\xi)}{M_R}\frac{1}{H(\xi)\ T(\xi)\ W(\xi)}\frac{3 - m}{3 - m_R} \tag{20}$$

where $M(\xi)$ is the moment distribution as function of the dimensionless span coordinate.

Introduction of the dimensionless variables into the differential equation (5) leads to

$$m \frac{d}{d\xi}\left[\frac{1}{T}\frac{d}{d\xi}(Tf)\right] - \frac{21m - 15}{42m - 21} W^2 \frac{d}{d\xi}\left[\frac{1}{T}\frac{d}{d\xi}\left(\frac{Tf}{W^2}\right)\right]$$

$$- \frac{6G}{E}\left(\frac{l_e}{w_R}\right)^2 \frac{f}{W^2} = 3 \frac{d}{d\xi}\left[\frac{1}{T}\frac{d}{d\xi}(TF)\right] \qquad (21)$$

The boundary and transition conditions become, if $\xi = \xi_o$ is the coordinate of the free end and $\xi = 1$ is the coordinate of the fixed end,

$$T(\xi_o)\, f(\xi_o) = 0 \qquad (22)$$

$$\left[m \frac{d}{d\xi}(Tf) - \frac{21m-15}{42m-21} W^2 \frac{d}{d\xi}\left(\frac{Tf}{W^2}\right) - 3 \frac{d}{d\xi}(TF)\right]_{\xi=1} = 0 \qquad (23)$$

$$T_l f_l = T_r f_r \qquad (24)$$

$$\frac{m_l}{T_l}\frac{d}{d\xi}(T_l f_l) - \frac{21m_l-15}{42m_l-21}\frac{W^2}{T_l}\frac{d}{d\xi}\left(\frac{T_l f_l}{W^2}\right) - \frac{3}{T_l}\frac{d}{d\xi}(T_l F_l)$$

$$= \frac{m_r}{T_r}\frac{d}{d\xi}(T_r f_r) - \frac{21m_r-15}{42m_r-21}\frac{W^2}{T_r}\frac{d}{d\xi}\left(\frac{T_r f_r}{W^2}\right) - \frac{3}{T_r}\frac{d}{d\xi}(T_r F_r) \qquad (25)$$

The stresses of equations (11) and (12) and the effective width as given by equation (10) now have the form

$$\frac{\sigma_x(x,o)}{\sigma_o} = F(\xi) - \frac{m}{3} f(\xi) \qquad (26)$$

$$\frac{\sigma_x(x,w)}{\sigma_o} = F(\xi) + \left(1 - \frac{m}{3}\right) f(\xi)$$

and

$$\frac{w_{eff}}{w} = \frac{1}{3} + \frac{2\sigma_x(x,o)}{3\sigma_x(x,w)} = \frac{1 - \frac{m-1}{3}\frac{f(\xi)}{F(\xi)}}{1 + \left(1 - \frac{m}{3}\right)\frac{f(\xi)}{F(\xi)}} \qquad (27)$$

It is useful to have the following simple result with regard to the superposition of shear-lag solutions. To

superimpose the stresses due to a moment distribution $M_n(\xi)$ and a moment distribution $M_m(\xi)$ for which F_n, F_m and f_n, f_m are known, F corresponding to $M_n + M_m$ is written as

$$F_{m,n}(\xi) = \frac{M_m(1)\ F_m(\xi) + M_n(1)\ F_n(\xi)}{M_m(1) + M_n(1)} \tag{28}$$

Because of the linearity of the problem, there follows also

$$f_{m,n}(\xi) = \frac{M_m(1)\ f_m(\xi) + M_n(1)\ f_n(\xi)}{M_m(1) + M_n(1)} \tag{29}$$

BEAMS WITH UNIFORM CROSS SECTION

EFFECTS OF LOAD DISTRIBUTION, OF WIDTH-SPAN RATIO, AND OF CROSS-SECTIONAL CHARACTERISTICS

Development of Equations

With

$$H = W = T = 1, \quad l = l_e \tag{30}$$

the differential equation and boundary conditions reduce to

$$\frac{d^2f}{d\xi^2} - \kappa^2 f = 3\lambda^2 \frac{d^2F}{d\xi^2} \tag{31}$$

$$f(0) = 0 \tag{32}$$

$$\left(\frac{df}{d\xi} - 3\lambda^2 \frac{dF}{d\xi}\right)_{\xi=1} = 0 \tag{33}$$

where

$$\lambda^2 = \frac{35m - 21}{35m^2 - 42m + 15}, \quad \kappa^2 = 6\,\frac{G}{E}\left(\frac{l_e}{w_R}\right)^2 \lambda^2 \tag{34}$$

The transition conditions while still utilizable to obtain

the solution for concentrated loads are not essential in this case since concentrated loads can conveniently be considered as limiting cases of distributed loads. The general solution of the system of equations (31) to (33) has the form

$$f(\xi) = \frac{3\lambda^2}{\kappa}\left\{\frac{\sinh \kappa \xi}{\cosh \kappa}\left[F'(1) - \int_0^1 \cosh \kappa(1-\eta)\, F''(\eta)\, d\eta\right] + \int_0^{\xi} \sinh \kappa(\xi-\eta)\, F''(\eta)\, d\eta\right\} \tag{35}$$

and in particular, if $F'(o) = 0$,

$$f(1) = \frac{3\lambda^2}{\kappa}\int_0^1 \frac{\sinh \kappa - \sinh \kappa \eta}{\cosh \kappa}\, F''(\eta)\, d\eta \tag{36}$$

In extension and partial recapitulation of the work in reference 2, the shear-lag functions f corresponding to the following basic loading conditions may be given.

1. Uniform loading

$$F_1(\xi) = \xi^2 \tag{37}$$

2. Loading increasing linearly from tip to root

$$F_2(\xi) = \xi^3 \tag{38}$$

3. Concentrated load at a point ξ_c,

$$F_3(\xi) = \begin{cases} 0, & 0 \leqslant \xi < \xi_c \\ \dfrac{\xi-\xi_c}{1-\xi_c}, & \xi_c \leqslant \xi \leqslant 1 \end{cases} \tag{39}$$

Subscripts are used here and throughout the present paper to identify cases treated explicitly.

By evaluation of equation (35),

$$f_1(\xi) = \frac{6\lambda^2}{\kappa^2}\left[\frac{\cosh \kappa(1-\xi) + \kappa \sinh \kappa \xi}{\cosh \kappa} - 1\right] \tag{40}$$

$$f_2(\xi) = \frac{18\lambda^2}{\kappa^2}\left[\left(\frac{1}{\kappa} + \frac{\kappa}{2}\right)\frac{\sinh \kappa\,\xi}{\cosh \kappa} - \xi\right] \tag{41}$$

$$f_3(\xi) = \begin{cases} -\dfrac{3\lambda^2}{\kappa}\dfrac{\cosh \kappa(1-\xi_c) - 1}{(1-\xi_c)\cosh \kappa}\sinh \kappa\,\xi, & \xi \leqslant \xi_c \\ \dfrac{3\lambda^2}{\kappa}\dfrac{1}{1-\xi_c}\left[\sinh \kappa(\xi - \xi_c) - \dfrac{\cosh \kappa(1-\xi_c)-1}{\cosh \kappa}\sinh \kappa\,\xi\right], & \xi_c \leqslant \xi \end{cases} \tag{42}$$

In particular, at the fixed end where, as has been stated in reference 2, the effective width is in general smallest,

$$f_1(1) = \frac{6\lambda^2}{\kappa}\left[\tanh \kappa - \frac{1}{\kappa} + \frac{1}{\cosh \kappa}\right] \tag{40a}$$

$$f_2(1) = \frac{9\lambda^2}{\kappa}\left[\left(1 + \frac{2}{\kappa^2}\right)\tanh \kappa - \frac{2}{\kappa}\right] \tag{41a}$$

$$f_3(1) = \frac{3\lambda^2}{\kappa}\frac{1}{1 - \xi_c}\left[\tanh \kappa - \frac{\sinh \kappa\,\xi_c}{\cosh \kappa}\right] \tag{42a}$$

In reference 2 an approximate expression was given for $f(1)$ which led to the theorem that, for beams of uniform cross section, the ratio $\left(\frac{w_{eff}}{w}\right)_R$ is approximately proportional to $\frac{w}{L}$ where L is the distance of the center of gravity of the $F''(\xi)$-curve, which for beams of uniform cross section coincides with the load curve, from the fixed end of the beam. This approximate result is also obtained by putting the contents of the brackets in equations (40a) to (42a) equal to 1. While this result is sufficiently accurate for large values of κ (say $\kappa > 12$) it leads for smaller values of κ to an underestimation of the effective width. The general result referred to appears to be the first statement of the fact that the amount of shear lag depends on w/L rather than on w/l.

The general formula, which may be quoted here for completeness, was

$$\left(\frac{w_{eff}}{w}\right)_R = \frac{1 - (m-1)\lambda\sqrt{\frac{E}{6G}}\frac{w}{L}}{1 + (3-m)\lambda\sqrt{\frac{E}{6G}}\frac{w}{L}} \tag{43}$$

Evidence will be presented later that, in the general case of tapering beams, an equivalent result can be stated with the same degree of approximation if L refers to the $(TF)''$-curve and w becomes w_R.

Numerical Examples

In order to obtain a quantitative idea of the results, a beam has been taken for which $(6G/E)^{1/3}(l/w) = 7.5$; so that, when $G/E = 3/8$, the beam is two and one-half times as long as wide. It is further assumed that the side webs and cover sheets contribute equally to the total stiffness, so that $m = 2$. On the basis of these data, the stress distribution has been calculated for

(1) a uniformly distributed load

(2) a linearly distributed load

(3a) a concentrated tip load

(3b) a concentrated load at midspan

Diagrammatical sketches of these and of all other problems treated numerically in this work are given in figure 2.

Throughout the rest of the present paper, individual stress diagrams will be described only by the case number of the problem designated beneath each sketch of figure 2. In all the stress diagrams, B refers to the stress of the elementary theory of bending, E to the actual edge stress, and M to the actual stress along the middle line of the sheet.

In order to obtain the results the values of the auxiliary parameters λ and κ, which are defined by equation (34), $\lambda^2 = 0.690$, $\kappa = 6.231$, are first calculated; the function $f(\xi)$ is then calculated according to equations (40) to (42). If these values are introduced with the simple expressions for $F(\xi)$ into equation (26), the values of the normal stresses along the edge and along the center line of the cover sheets are obtained. The results are given numerically in table I and as diagrams in figure 3. These diagrams show clearly how shear lag depends greatly on the shape of the load curves, since the maximum stresses in the four different cases are 11, 18, 24, and 21 percent higher than those given by elementary beam theory.

Concerning the effect of $m = (3I_w + I_s)/I$, an average value in the practical range $(I_w = I_s)$ has been chosen for the calculation of the curves. Calculations in reference 2 indicate that shear lag decreases with increasing m and vice versa; in other words, the more appreciable the contribution of the cover sheet to the total stiffness of the beam, the more appreciable is the shear lag. The magnitude of this effect in the range $1.5 < m < 2.5$, $(0.25 < (I_s/I_w) < 0.75)$ is, however, sufficiently small to permit working with the average value $m = 2$.

In table II values are given of the effective width at the built-in end for the three loading cases, concentrated tip load, uniform load, and linearly increasing load, as functions of the ratio $\sqrt{\frac{27E}{32G}\frac{w}{l}}$ and also as functions of the ratio $\sqrt{\frac{27E}{32G}\frac{w}{L}}$. In this comparison it is assumed that $m = 2$. The quantitative effect of a variation of the stiffness parameter m is investigated by calculating $\left(\frac{w_{eff}}{w}\right)_R$ for the concentrated tip-load case with $m = 1.5$ and $m = 2.5$. The results are plotted in figure 4 as functions of $\frac{w}{L}$. They show that in fact $\left(\frac{w_{eff}}{w}\right)_R$ for the case of a concentrated tip load gives a slightly conservative estimate of $\left(\frac{w_{eff}}{w}\right)_R$ for other load conditions and that the effect of a variation of m is small.

Case of a Sine Moment Curve

As a further example of a shear-lag problem for a beam with uniform cross section, a case considered by Younger (reference 5) is taken and analyzed within the frame of this theory. The dimensionless elementary bending-stress function is given by

$$F_4(\xi) = \sin \frac{\pi}{2} \xi \qquad (44)$$

From

$$F'(\xi) = \frac{\pi}{2} \cos \frac{\pi}{2} \xi, \quad F''(\xi) = -\left(\frac{\pi}{2}\right)^2 \sin \frac{\pi}{2} \xi \qquad (45)$$

it follows that the loading in this case consists of a concentrated load at the free end and of a distributed load

having a resultant of equal magnitude and opposite direction as the concentrated load. (That the two load systems balance each other follows from the fact that $F_4'(1) = 0$).

Since it had been shown that shear lag is quite sensitive with regard to changes in load distribution, this load case may behave with regard to shear lag rather differently from the three typical cases considered previously.

The solution of the shear-lag equations (31) to (33) is obtained for F_4 in an especially simple form. By substituting $3\lambda^2 F_4''$ in equation (31), a particular solution is found in the form

$$f_4(\xi) = \frac{3\lambda^2}{1 + \left(\frac{2\kappa}{\pi}\right)^2} \sin \frac{\pi}{2} \xi \tag{46}$$

and it so happens that this particular solution satisfies already the boundary conditions given in equations (32) and (33) and therefore represents the complete solution.

The stresses of equation (26) become here

$$\frac{\sigma_x(x,o)}{\sigma_o} = \left(1 - \frac{m\lambda^2}{1 + \left(\frac{2\kappa}{\pi}\right)^2}\right) \sin \frac{\pi}{2} \xi \tag{47}$$

$$\frac{\sigma_x(x,w)}{\sigma_o} = \left(1 + \frac{(3 - m)\lambda^2}{1 + \left(\frac{2\kappa}{\pi}\right)^2}\right) \sin \frac{\pi}{2} \xi \tag{48}$$

A comparison of this solution numerically with the corresponding solutions for the other loading cases shows, with $m = 2$, $\lambda^2 = 0.690$, $\kappa = 6.231$, $\frac{\lambda^2}{1 + \left(\frac{2\kappa}{\pi}\right)^2} = 0.041$ that the increase in maximum stress as given by equation (48) amounts to only 4 percent as compared with increases between 11 and 24 percent for the other loading conditions.

Case of a Sine Series Moment Curve

A more general load condition, that is, one which can be made to represent all load conditions, is obtained by assuming

$$F_5(\xi) = \sum_{n=0}^{\infty} A_n \sin (2n+1) \frac{\pi}{2} \xi \tag{49}$$

The introduction of equation (49) into the differential equation (31) gives

$$f_5(\xi) = 3\lambda^2 \sum_{n=0}^{\infty} \frac{A_n}{1 + \left(\frac{2\kappa}{(2n+1)\pi}\right)^2} \sin (2n+1) \frac{\pi}{2} \xi \tag{50}$$

The convergence of the series of equation (50) is, however, slow; whereas one of the advantages of the least-work method is that it permits avoidance of such series developments, which in an exact theory are the only known means of representing the solution.

As an example for the determination of the coefficients, the case of a concentrated tip load may be considered where $F(\xi) = \xi$ and where convergence is still better than, for instance, in the uniform or linear load case. The Fourier development of $F(\xi) = \xi$ is obtained from

$$\int_0^1 \xi \sin (2m+1) \frac{\pi}{2} \xi \, d\xi = \sum A_n \int_0^1 \sin (2m+1) \frac{\pi}{2} \xi \sin (2m+1) \frac{\pi}{2} \xi \, d\xi$$

$$\frac{\sin (2m+1) \frac{\pi}{2}}{\left[(2m+1) \frac{\pi}{2}\right]^2} = \frac{1}{2} A_m \tag{51}$$

in the form

$$\xi = \sum_{0}^{\infty} \frac{2 \sin (2n+1) \frac{\pi}{2}}{\left[(2n+1) \frac{\pi}{2}\right]^2} \sin (2n+1) \frac{\pi}{2} \xi \tag{52}$$

and, consequently,

$$f(\xi) = \sum_{0}^{\infty} \frac{6\lambda^2 \sin (2n+1) \frac{\pi}{2}}{\left[(2n+1) \frac{\pi}{2}\right]^2 + \kappa^2} \sin (2n+1) \frac{\pi}{2} \xi \tag{53}$$

The convergence of equation (53), while rapid for small values of ξ, becomes slower when ξ approaches unity. In order to show that the solution actually represents the concentrated load case, it is necessary to show that

$$\lim_{\xi \to 0} F'(\xi) = 1, \qquad \lim_{\xi \to 1} F'(\xi) = 1$$

where

$$F'(\xi) = \sum_{0}^{\infty} \frac{2 \sin (2n+1) \frac{\pi}{2}}{(2n+1) \frac{\pi}{2}} \cos (2n+1) \frac{\pi}{2} \xi \tag{54}$$

This series, every term of which vanishes when $\xi = 1$, has the required properties when it is recognized that the series, representing the function $F'(\xi) = 1$ in the interval $0 < \xi < 1$, jumps at the point $\xi = 1$ and represents $F'(\xi) = -1$ in the interval $1 < \xi < 2$.

Example of the Application of the Superposition Principle

The application of the superposition equations (28) and (29) is shown by considering a beam with uniform load p_o and a concentrated load $-P_o$ at the section $x = x_c$. The moment functions are

$$M_1(\xi) = \frac{1}{2} p_o x^2 = \frac{p_o l^2}{2} \xi^2 \tag{55}$$

$$M_3(\xi) = \begin{cases} 0, & x < x_c \\ -P_o (x - x_c) = -P_o l (\xi - \xi_c), & x_c < x \end{cases} \tag{56}$$

and it follows in accordance with equation (28) that

$$F_{1,3}(\xi) = \frac{\frac{p_o l^2}{2} F_1(\xi) - P_o l (1-\xi_c) F_3(\xi)}{\frac{p_o l^2}{2} - P_o l (1-\xi_c)}$$

$$= \frac{F_1(\xi) - \frac{P_o (1-\xi_c)}{p_o l/2} F_3(\xi)}{1 - \frac{P_o (1-\xi_c)}{p_o l/2}} \tag{57}$$

where F_1 and F_3 are defined by equations (37) and (39). In accordance with equation (29),

$$f_{1,3}(\xi) = \frac{f_1(\xi) - \frac{P_o\ (1-\xi_c)}{p_o l/2} f_3(\xi)}{1 - \frac{P_o\ (1-\xi_c)}{p_o l/2}} \qquad (58)$$

If, for a numerical example, as before,

$$m = 2, \qquad \kappa = 6.23l$$

and

$$\xi_c = 0.5, \qquad \frac{P_o}{p_o l} = 0.5$$

then, with the case 3b for a concentrated load at midspan,

$$\left.\begin{aligned} F_{1,3b} &= 2F_1 - F_{3b} \\ f_{1,3b} &= 2f_1 - f_{1,3b} \end{aligned}\right\} \qquad (59)$$

From table I, the values of F and of f are obtained and, by introducing these values into equations (26) for the stresses, a stress pattern is obtained as given in figure 5.

EFFECTS OF TAPER IN HEIGHT FOR OTHERWISE UNIFORM CROSS SECTION

The only difference between the case of beams with taper in height and the case of beams without taper is that, in equations (5) and (7), σ_b is modified and, in equation (20), the variability of $H(\xi)$ has to be taken into account. Thus, for given $F(\xi)$ and $H(\xi)$, the moment function is given by

$$\frac{M(\xi)}{M_R} = H(\xi)\ F(\xi) \qquad (60)$$

Otherwise the entire theory for the beam with uniform cross section can be directly applied.

In addition to the results of the preceding section, which can be interpreted in this place by equation (60), the case has been calculated in which the height tapers linearly according to the law

$$H(\xi) = \frac{1}{2}(1 + \xi) \tag{61}$$

so that the tip height is one-half the root height. Concentrated tip load and uniformly distributed load have been assumed. Then, according to equation (60)

$$F_6(\xi) = \frac{2\xi}{1 + \xi} \tag{62}$$

and

$$F_7(\xi) = \frac{2\xi^2}{1 + \xi} \tag{63}$$

The shear-lag functions $f(\xi)$ as given by equation (35) become

$$f_6 = \frac{3\lambda^2}{\kappa}\left\{\frac{\sinh \kappa \xi}{\cosh \kappa}\left[\frac{1}{2} + 4\int_0^1 \frac{\cosh \kappa (1-\eta)}{(1 + \eta)^3}\, d\eta\right] - 4\int_0^\xi \frac{\sinh \kappa (\xi-\eta)}{(1 + \eta)^3}\, d\eta\right\} \tag{64}$$

and

$$f_7 = \frac{3\lambda^2}{\kappa}\left\{\frac{\sinh \kappa \xi}{\cosh \kappa}\left[\frac{3}{2} - 4\int_0^1 \frac{\cosh \kappa (1-\eta)}{(1 + \eta)^3}\, d\eta\right] + 4\int_0^\xi \frac{\sinh \kappa (\xi-\eta)}{(1 + \eta)^3}\, d\eta\right\} \tag{65}$$

The functions f_6 and f_7 have been determined again with the following values of the parameters

$$\sqrt{\frac{6G}{E}}\frac{l}{w} = 7.5, \quad m = 2, \quad \kappa = 6.231$$

The integrals occurring in equations (64) and (65) have been evaluated by means of Simpson's rule. The resultant

stress distribution is given in table III and in figure 6.

A comparison of these results with the results for a beam with the same load distribution but with no taper in height (figs. 3(a) and 3(c)) shows that the maximum stress increases are reduced from 11 to $6\frac{1}{2}$ percent and from 18 to 15 percent owing to the variability of $H(\xi)$ and the subsequent change of shape of the F-curve.

EFFECTS OF DISCONTINUOUS CHANGES IN COVER-SHEET THICKNESS

Beams with constant width and piecewise constant cover-sheet thickness and web stiffness are considered in this section. For every bay with constant T and m the differential equation (31) applies and for the tip and root sections the boundary conditions of equations (32) and (33) apply. At a section where T and m change the transition conditions of equations (24) and (25) occur, and equation (25) simplifies to

$$\frac{d}{d\xi}\left(f_l - 3\lambda_l^2 F_l\right) = \frac{d}{d\xi}\left(f_r - 3\lambda_r^2 F_r\right) \tag{66}$$

The procedure for obtaining the explicit solution may be exemplified for beams consisting of two bays, one tip bay of length l_1 and sheet thickness t_1 and one root bay of length l_2 and sheet thickness t_2. We assume that the stiffness parameter m and therewith λ and κ have the same values in both bays.

The thickness function is

$$T(\xi) = \begin{cases} \dfrac{t_1}{t_2}, & 0 \leqslant \xi \leqslant \xi_1 \\ 1, & \xi_1 \leqslant \xi \leqslant 1 \end{cases} \tag{67}$$

and, according to equation (20),

$$F(\xi) = \frac{M(\xi)}{M_R}\,\frac{1}{T(\xi)} \tag{68}$$

If

$$\frac{t_2}{t_1} = \delta \tag{69}$$

the system of equations to be solved becomes

$$\frac{d^2 f_l}{d\xi^2} - \kappa^2 f_l = 3\lambda^2 \frac{M''(\xi)}{M_R} \delta, \quad 0 \leqslant \xi \leqslant \xi_1 \tag{70}$$

$$\frac{d^2 f_r}{d\xi^2} - \kappa^2 f_r = 3\lambda^2 \frac{M''(\xi)}{M_R}, \quad \xi_1 \leqslant \xi \leqslant 1 \tag{71}$$

$$f_l(0) = 0, \quad f_r'(1) = 3\lambda^2 \frac{M'(1)}{M_R} \tag{72,73}$$

$$f_l(\xi_1) = \delta f_r(\xi_1) \tag{74}$$

$$f_l'(\xi_1) - 3\lambda^2 \delta \frac{M'(\xi_1)}{M_R} = f_r'(\xi_1) - 3\lambda^2 \frac{M'(\xi_1)}{M_R} \tag{75}$$

For the solution of the system of equations (70) to (75), the general solutions of the differential equations (70) and (71) should be first written in the form

$$f_l = 3\delta \frac{\lambda^2}{\kappa} \left(A_l \sinh \kappa \xi + B_l \cosh \kappa \xi + p(\xi) \right) \tag{76}$$

$$f_r = 3 \frac{\lambda^2}{\kappa} \left(A_r \sinh \kappa \xi + B_r \cosh \kappa \xi + p(\xi) \right) \tag{77}$$

According to equations (72), (73), (74), and (75), the following conditions serve to determine the constants of integration;

$$B_l + p(o) = 0 \tag{78}$$

$$\lambda^2 \left(A_r \cosh \kappa + B_r \sinh \kappa + \frac{p'(1)}{\kappa} \right) = \lambda^2 \frac{M'(1)}{M_R} \tag{79}$$

$$A_l \sinh \kappa \xi_1 + B_l \cosh \kappa \xi_1 = A_r \sinh \kappa \xi_1 + B_r \cosh \kappa \xi_1 \tag{80}$$

$$\delta \left\{ \left[A_l \cosh \kappa \xi \; B_l \sinh \kappa \xi + \frac{p'(\xi_1)}{\kappa} \right] - \frac{M'(\xi_1)}{M_R} \right\}$$

$$= \left\{ \left[A_r \cosh \kappa \xi_1 + B_r \sinh \kappa \xi_1 + \frac{p'(\xi_1)}{\kappa} \right] - \frac{M'(\xi_1)}{M_R} \right\} \tag{81}$$

Equations (76) to (81) are evaluated for three cases of concentrated tip load and of uniformly distributed load as follows:

Case	m	κ	δ	$\frac{l_1}{l}$	$p(\xi)$	$\frac{M(\xi)}{M_R}$
8	2	6.231	2	0.5	0	ξ
9	2	6.231	2	.5	$-\frac{6\lambda^2}{\kappa}$	ξ^2
10	2	6.231	2	.9	$\frac{6\lambda^2}{\kappa}$	ξ^2

For the shear-lag functions f there is obtained

$$f_8 = \begin{cases} 0.02141 \sinh 6.231\xi, & 0 \leqslant \xi \leqslant 0.5 \\ 2.37789 \cosh 6.231\xi - 2.37657 \sinh 6.231\xi, & 0.5 \leqslant \xi \leqslant 1 \end{cases} \tag{76}$$

$$f_9 = \begin{cases} -0.18990 \sinh 6.231\xi + 0.21334 \cosh 6.231\xi \\ \qquad -0.21333, \quad 0 \leqslant \xi \leqslant 0.5 \\ -2.40681 \sinh 6.231\xi + 2.40944 \cosh 6.231\xi \\ \qquad -0.10667, \quad 0.5 \leqslant \xi \leqslant 1 \end{cases} \tag{77}$$

$$f_{10} = \begin{cases} -0.20671 \sinh 6.231\xi + 0.21333 \cosh 6.231\xi \\ \qquad -0.21333, \quad 0 \leqslant \xi \leqslant 0.9 \\ -20.15981 \sinh 6.231\xi + 20.16258 \cosh 6.231\xi \\ \qquad -0.10667, \quad 0.9 \leqslant \xi \leqslant 1 \end{cases} \tag{78}$$

The functions f corresponding to equations (76) to (78) have been calculated for various values of ξ and from equations (26) the corresponding stresses have been calculated. Table IV and figure 7 contain the results. It should be noted that, instead of the stresses themselves, the stress resultants $T\frac{\sigma}{\sigma_0}$ have been plotted. Thus, in order to obtain the stresses from figures 7(a), 7(b), and 7(c) the parts of the curves in the first bay have to be magnified by a factor $\frac{t_2}{t_1} = 2$. It is seen that, in the cases of equal bay length, the thickness change has almost no effect on the stresses at the fixed end; while, in the extreme case of the very much shorter root bay, there is a noticeable effect with an increase of 21 instead of

18 percent for the corresponding beam with uniform cross section (fig. 3(a)). As is to be expected, an appreciable shear-lag effect occurs near the transition section and it is seen that the percentage of stress increase is as high as the corresponding increase at the root section.

EFFECTS OF LINEAR TAPER IN WIDTH

Development of Equations

The theory is developed in this section for beams in which the width varies linearly while the cover-sheet thickness is assumed to be uniform. The theory can be applied to problems in which the sheet thickness is piecewise uniform by means of the transition conditions of equations (24) and (25).

The more general taper law

$$w = \xi^q \tag{71}$$

is first introduced into differential equation (21) with

$$T = \text{constant} \tag{80}$$

There is then obtained the differential equation

$$f'' + 4\gamma^2 q \frac{f'}{\xi} - 2\gamma^2 q (2q+1) \frac{f}{\xi^2} - \kappa^2 \frac{f}{\xi^{2q}} = 3\lambda^2 F'' \tag{81}$$

which, for any value of q, can be integrated in terms of Bessel functions. Of the constants occurring in equation (81), λ and κ are defined in equation (34) and

$$\gamma^2 = m\lambda^2 - 1 \tag{82}$$

The conditions at the free end and at the fixed end follow from equations (22) and (23) in the form

$$f(\xi_0) = 0 \tag{83}$$

$$f'(1) + 2q\gamma^2 f(1) = 3\lambda^2 F'(1) \tag{84}$$

For the transition conditions, there follows from

equations (24) and (25)

$$T_l f_l = T_r f_r \tag{24}$$

and

$$f_l' + 2q\gamma_l^2 f_l - 3\lambda_l^2 F_l' = f_r' + 2q\gamma_r^2 f_r - 3\lambda_r^2 F_r \tag{85}$$

In the case of linearly tapering width for which

$$q = 1$$

the differential equation (81) takes a form which can be integrated by an expression of the type

$$f(\xi) = 3\lambda^2 \left[c_1 \xi^{n_1} - c_2 \xi^{n_2} + p(\xi) \right] \tag{86}$$

where $3\lambda^2 p(\xi)$ is a particular integral and the remainder the general solution of the homogeneous equation. The substitution of equation (86) in (81) gives the exponents

$$n_1 = \frac{1}{2} - 2\gamma^2 + \sqrt{\frac{1}{4} + 4m\gamma^2\lambda^2 + \kappa^2} \tag{87a}$$

$$n_2 = \frac{1}{2} - 2\gamma^2 - \sqrt{\frac{1}{4} + 4m\gamma^2\lambda^2 + \kappa^2} \tag{87b}$$

and the function

$$p(\xi) = \frac{1}{n_1 - n_2} \left\{ \xi^{n_1} \int^{\xi} \frac{F''(\eta)\, d\eta}{\eta^{n_1 - 1}} - \xi^{n_2} \int^{\xi} \frac{F''(\eta)\, d\eta}{\eta^{n_2 - 1}} \right\} \tag{88}$$

In particular, if F can be expressed in the form

$$F(\xi) = \sum a_\nu \xi^\nu \tag{89}$$

then

$$p(\xi) = \sum \frac{\nu(\nu - 1)}{(n_1 - \nu)(n_2 - \nu)} a_\nu \xi^\nu \tag{90}$$

By the introduction of the solution (86) into the

boundary conditions of equations (83) and (84), the following equations that determine the constants c_1 and c_2 are obtained

$$c_1 \xi_o^{n_1} - c_2 \xi_o^{n_2} = - p(\xi_o) \tag{91}$$

$$(n_1+2\gamma^2)c_1-(n_2+2\gamma^2)c_2 = F'(1)-\left[p'(1) + 2\gamma^2 p(1)\right] \tag{92}$$

In the case in which a concentrated load is applied at a section $\xi = \xi_c$, it is convenient to proceed as follows: Let

$$f(\xi) = \begin{cases} 3\lambda^2 \left[p_l(\xi) + c_1 \xi^{n_1} - c_2 \xi^{n_2}\right], & \xi_o \leqslant \xi \leqslant \xi_c \\ 3\lambda^2 \left[p_r(\xi) + d_1 \xi^{n_1} - d_2 \xi^{n_2}\right], & \xi_c \leqslant \xi \leqslant 1 \end{cases} \tag{93}$$

Equations (83), (84), (24), and (85) then take the form

$$c_1 \xi_o^{n_1} - c_2 \xi_o^{n_2} = - p_l(\xi_o) \tag{94}$$

$$(d_1-c_1) \xi_c^{n_1} - (d_2-c_2) \xi^{n_2} = \left[p_r(\xi_c) - p_l(\xi_c)\right] \tag{95}$$

$$(d_1-c_1)n_1\xi_c^{n_1} -(d_2-c_2)n_2\xi^{n_2} = - \xi_c \left[F_l'(\xi_c)-F_r'(\xi_c)\right] + \xi_c \left[p_l'(\xi_c) - p_r'(\xi_c)\right] \tag{96}$$

$$(n_1+2\gamma^2)d_1-(n_2+2\gamma^2)d_2 = F'(1) - \left[p_r'(1) + 2\gamma^2 p_r(1)\right] \tag{97}$$

The evaluation of equations (94) to (97) is best accomplished by first solving equations (95) and (96) for $d_1 - c_1$ and $d_2 - c_2$ and then determining the constants themselves from equations (94) and (97).

Numerical Examples

Beams with concentrated tip load (cases 11 to 14).- The following values of the parameters are chosen for cases 11 to 14:

$$m = 2, \quad \sqrt{\frac{6G}{E}}\frac{l_e}{w_R} = 15; \quad \frac{h}{l_e} = \xi_o = 0.5 \tag{98}$$

From equations (34) and (82),

$$\lambda^2 = 0.6901, \quad \gamma^2 = 0.3803, \quad \kappa^2 = 155.2817 \tag{99}$$

and from equation (87)

$$n_1 = 12.2946, \quad n_2 = -12.8157 \tag{100}$$

Also, since

$$\frac{M(\xi)}{M_R} = \frac{\xi - \xi_o}{1 - \xi_o} = 2\xi - 1, \quad W = \xi, \quad T = 1 \tag{101}$$

it follows from equation (20) that

$$F(\xi) = \frac{2\xi - 1}{\xi\, H(\xi)} \tag{102}$$

The following height functions, which are listed with the corresponding F, are chosen

$$H = 1, \qquad F_{11} = 2 - \xi^{-1} \tag{103}$$

$$H = \xi, \qquad F_{12} = 2\xi^{-1} - \xi^{-2} \tag{104}$$

$$H = 2\xi - 1, \qquad F_{13} = \xi^{-1} \tag{105}$$

$$H = \frac{2\xi - 1}{\xi}, \qquad F_{14} = 1 \tag{106}$$

From equations (90) and (87), for the corresponding particular integrals,

$$p_{11} = 0.01273\ \xi^{-1} \tag{107}$$

$$p_{12} = -0.02546\ \xi^{-1} + 0.03881\ \xi^{-2} \tag{108}$$

$$p_{13} = -0.01273\ \xi^{-1} \tag{109}$$

$$p_{14} = 0 \tag{110}$$

The coefficients c_1 and d_1 are next determined from

equations (91) and (92). This process is carried out in detail for case 11 to illustrate the procedure, while for the other cases only the results are listed.

By substituting first in equation (91),

$$2^{-n_1} c_1 - 2^{-n_2} c_2 = -0.02546$$

and then, by substituting in equation (92)

$$F_{11}'(1) = 1, \quad p_{11}'(1) + 2\gamma^2 p_{11}(1) = -0.0030485$$

$$(n_1 + 2\gamma^2) c_1 - (n_2 + 2\gamma^2) c_2 = 1.0030485$$

For the constants occurring in the two equations,

$$2^{-n_1} = 0.00019905, \quad 2^{-n_2} = 7209.515, \quad n_1 + 2\gamma^2 = 13.05513, \quad n_2 + 2\gamma^2 = -12.05513$$

so that altogether

$$0.00019905\, c_1 - 7209.515\, c_2 = -0.02546 \qquad (111)$$

$$13.05513\, c_1 + 12.05513\, c_2 = 1.0030485 \qquad (112)$$

The relative magnitude of the coefficients in equation (111) makes it numerically most convenient to solve by successive approximations of which the first is found sufficiently accurate in this and in most of the following analogous cases. Thus, as first approximation,

$$c_2 = \frac{0.02546}{7209.515} = 0.0000035320 \qquad (113)$$

and, with this value of c_2 substituted in equation (112)

$$c_1 = \frac{1}{13.05513}(0.0030485 - 12.05513 \times 0.0000035320)$$

$$= 0.076828 \qquad (114)$$

A resubstitution of this value of c_1 in equation (111) gives as second approximation

$$c_2 = \frac{1}{7209.515}(0.02546 - 0.00019905 \times 0.076828)$$

$$= 0.0000035321$$

showing that the first approximation for c_2 was exact to four significant figures. It is convenient to use, instead of c_2, the value of

$$2^{-n_2} c_2 = 0.025479 \qquad (115)$$

With the introduction of equations (114) and (115) into equation (86) with p_{11} from equation (107), there results

$$f_{11} = 0.0246\ \xi^{-1} + 0.1591\ \xi^{12.295} - 0.0528(2\xi)^{-12.816} \qquad (116)$$

In exactly the same manner the solutions in the other three cases are found as

$$f_{12} = -0.0527\xi^{-1} + 0.0803\xi^{-2} + 0.0067\xi^{12.295} - 0.2160(2\xi)^{-12.816} \qquad (117)$$

$$f_{13} = -f_{11} \qquad (118)$$

$$f_{14} = 0 \qquad (119)$$

Expressions for the stresses are obtained by again substituting $f(\xi)$ in equations (26). The numerical results are contained in table V and in figure 8. If these results are compared with the corresponding results for a beam with concentrated tip load and no width taper (fig. 3(c)), it is seen that shear lag is substantially less pronounced in cases 11 and 12. In case 13, for which the beam dimensions are such that $F(\xi)$ (and thus the stress σ_b) decreases from tip to root, a condition occurs which might be called negative shear lag, in that instead of an increase of edge stress due to shear lag a decrease of this stress takes place with a corresponding increase of stress in the interior of the sheet. In case 14 (for which no diagram is given) the variation of beam height h is so chosen that the stress according to the

elementary theory does not vary along the span and no shear lag occurs in this case. This is in accordance with the general result of reference 2 that no shear lag occurs when the product of sheet thickness t and bending stress σ_b does not vary along the span. With regard to case 12, it is noted that shear lag is quite appreciable in the tip half of the beam while it decreases almost to zero toward the fixed end, a behavior which is in contrast with the results obtained in the cases of uniform width.

Beams with uniformly distributed load (cases 15 to 18).- The same dimensions are assumed and the procedure for obtaining the solutions is the same for cases 15 to 18 as for cases 11 to 14. The moment function now takes the form

$$\frac{M(\xi)}{M_R} = (2\xi - 1)^2 \tag{120}$$

and thus

$$F(\xi) = \frac{(2\xi - 1)^2}{\xi\, H(\xi)} \tag{121}$$

The following choices are made for the height function and with that for F

$$H = 1, \qquad F_{15} = 4\xi - 4 + \xi^{-1} \tag{122}$$

$$H = \xi, \qquad F_{16} = 4 - 4\xi^{-1} + \xi^{-2} \tag{123}$$

$$H = 2\xi - 1, \qquad F_{17} = 2 - \xi^{-1} = F_{11} \tag{124}$$

$$H = 2 - \xi^{-1}, \qquad F_{18} = 2\xi - 1 \tag{125}$$

From equation (90)

$$p_{15} = 0.01273\ \xi^{-1} = -p_{11} \tag{126}$$

$$p_{16} = 0.05093\ \xi^{-1} - 0.03881\ \xi^{-2} \tag{127}$$

$$p_{17} = p_{11} \tag{128}$$

$$p_{18} = 0 \tag{129}$$

and for the shear-lag functions f

$$f_{15} = -0.0264\xi^{-1}+0.4753\xi^{12.295}+0.0526(2\xi)^{-12.816} \quad (130)$$

$$f_{16} = 0.1054\xi^{-1}-0.0803\xi^{-2}+0.3115\xi^{12.295}+0.1105(2\xi)^{-12.816} \quad (131)$$

$$f_{17} = f_{11} \quad (132)$$

$$f_{18} = 0.31718\xi^{12.295} - 0.00006(2\xi)^{-12.816} \quad (133)$$

Introducing f into equation (26) again gives the stresses as in table VI and in figure 9. It is seen that, in case 15 in which the F-curve is most similar to the corresponding curve for the beam of uniform cross section (fig. 3(a)), the stress pattern as modified by shear lag is also most similar but that the taper in width reduces the maximum-stress increase from 18 to 15 percent. In cases 16 and 18, the F-curve approximates that of the beam with uniform cross section and concentrated tip load and a corresponding similarity is observed in the stress patterns. In case 17, the curve is concave upward and shear lag is further reduced. In general, it can be said that these examples do not permit the conclusion that width taper materially affects shear lag beyond a modification of the F-curves.

Beams with linearly increasing load (cases 19 to 22).- The beam dimensions are again assumed to be the same and the procedure for obtaining the solutions is also the same as in previous cases.

The moment function is now

$$\frac{M(\xi)}{M_R} = (2\xi - 1)^3 \quad (134)$$

so that

$$F(\xi) = \frac{(2\xi - 1)^3}{\xi\, H(\xi)} \quad (135)$$

The following choices are made for the height function H and with that for F

$$H = 1, \qquad F_{19} = 8\xi^2 - 12\xi + 6 - \xi^{-1} \quad (136)$$

$$H = \xi, \qquad F_{20} = 8\xi - 12 + 6\xi^{-1} - \xi^{-2} \quad (137)$$

$$H = 2\xi-1, \qquad F_{21} = 4\xi - 4 + \xi^{-1} = F_{15} \quad (138)$$

$$H = 2-\xi^{-1}, \quad F_{22} = 4\xi^2 - 4\xi + 1 \tag{139}$$

The corresponding functions f are obtained exactly as in the preceding paragraphs

$$f_{19} = -0.2172\xi^2+0.0246\xi^{-1}+0.8394\xi^{12.295}+0.0014(2\xi)^{-12.816} \tag{140}$$

$$f_{20} = -0.1582\xi^{-1}+0.0803\xi^{-2}+0.6391\xi^{12.295}-0.0052(2\xi)^{-12.816} \tag{141}$$

$$f_{21} = f_{15} \tag{142}$$

$$f_{22} = -0.1086\xi^2+0.6573\xi^{12.295}+0.0270(2\xi)^{-12.816} \tag{143}$$

Numerical values of the functions f and of the corresponding stresses are given in table VII and in figure 10. It is again seen to what extent taper reduces the magnitude of the shear lag that would occur for a beam with uniform cross section.

Beams with concentrated load at midspan (cases 23 and 24).- The same values of the parameters are assumed as in the preceding cases. The moment function is now

$$\frac{M(\xi)}{M_R} = \begin{cases} 0, & 0.5 \leq \xi \leq 0.75 \\ 4\xi-3, & 0.75 \leq \xi \leq 1.0 \end{cases} \tag{144}$$

so that

$$F(\xi) = \begin{cases} 0 = F_l, & 0.5 \leq \xi \leq 0.75 \\ \dfrac{4\xi-3}{H(\xi)} = F_r, & 0.75 \leq \xi \leq 1.0 \end{cases} \tag{145}$$

For the height function H is chosen

$$H = 1, \quad F_{23} = \begin{cases} 0, & 0.5 \leq \xi \leq 0.75 \\ 4-3\xi^{-1}, & 0.75 \leq \xi \leq 1.0 \end{cases} \tag{146}$$

$$H = \xi, \quad F_{24} = \begin{cases} 0, & 0.5 \leq \xi \leq 0.75 \\ 4\xi^{-1}-3\xi^{-2}, & 0.75 \leq \xi \leq 1.0 \end{cases} \tag{147}$$

The method of solution by means of equations (94) to (97) is given explicitly for case 23, while the corresponding results for case 24 are listed.

First, from equations (146) and (90),

$$p_{l,23} = 0, \quad p_{r,23} = 0.038196\ \xi^{-1} \tag{148}$$

Equations (94) and (97) become

$$0.00019905\ c_1 - 7209.515\ c_2 = 0 \tag{149}$$

$$13.05513\ d_1 + 12.05513\ d_2 = 3.00915 \tag{150}$$

and the transition conditions of equations (95) and (96) become

$$(4/3)^{-n_1}\ (d_1-c_1)\ \ (4/3)^{-n_2}\ (d_2-c_2) = -0.050928 \tag{151}$$

$$12.29457(4/3)^{-n_1}(d_1-c_1)+12.81569(4/3)^{-n_2}(d_2-c_2)=4.05093 \tag{152}$$

Solving equations (151) and (152) gives

$$\left(\frac{4}{3}\right)^{-n_1}\ (d_1-c_1) = 0.13533, \quad d_1 - c_1 = 4.65020 \tag{153}$$

$$\left(\frac{4}{3}\right)^{-n_2}\ (d_2-c_2) = 0.18628, \quad d_2 - c_2 = 0.004660 \tag{154}$$

From equation (149) follows that, in first approximation

$$c_2 \approx 0 \tag{155}$$

and hence, from equation (154)

$$d_2 \approx 0.004660 \tag{156}$$

Then, from equation (150),

$$d_1 \approx 0.22619 \tag{157}$$

and, from equation (153),

$$c_1 \approx -4.42401 \tag{158}$$

From substituting this c_1 in equation (149) a second ap-

proximation follows:

$$c_2 \approx - 0.00000012 \tag{159}$$

and, from equation (154),

$$d_2 \approx 0.0046659 \tag{160}$$

and, from equation (150),

$$d_1 \approx 0.22619 \tag{161}$$

and, from equation (153),

$$c_1 \approx - 4.42401 \tag{162}$$

It is seen that the second approximations agree sufficiently well with the first approximations to permit discontinuing the process.

In this way the following final results are obtained for cases 23 and 24:

$$f_{23} = \begin{cases} -9.1600\xi^{12.295} + 0.0012(2\xi)^{-12.816}, & 0.5 \leq \xi \leq 0.75 \\ 0.0791\xi^{-1} + 0.4683\xi^{12.295} - 0.0097\xi^{-12.816}, & 0.75 \leq \xi \leq 1 \end{cases} \tag{163}$$

$$f_{24} = \begin{cases} -10.7170\xi^{12.295} + 0.0021(2\xi)^{-12.816}, & 0.5 \leq \xi \leq 0.75 \\ -0.1054\xi^{-1} + 0.2410\xi^{-2} + 0.3240\xi^{12.295} - 0.0153\xi^{-12.816}, & \\ 0.75 \leq \xi \leq 1 \end{cases} \tag{164}$$

Numerical values of the functions f and of the corresponding stresses are given in table VIII and in figure 11. It is again observed that the effect of taper is a reduction of the maximum percentage increase of stress due to shear lag in the beam of untapered cross section with corresponding load (fig. 3(a)).

Beams with uniformly distributed load and increased taper (cases 25 to 28).- In order to observe the effect of increasing the rate of taper, beams with uniform load distribution are assumed to taper in the following ways:

$$\frac{l_e}{w_R} = \frac{20}{3}, \quad \frac{l}{l_e} = \frac{3}{4}, \quad H = 1 \tag{165}$$

$$\frac{l_e}{w_R} = \frac{20}{3}, \quad \frac{l}{l_e} = \frac{3}{4}, \quad H = \xi \tag{166}$$

$$\frac{l_e}{w_R} = 5, \quad \frac{l}{l_e} = 1, \quad H = 1 \tag{167}$$

$$\frac{l_e}{w_R} = 5, \quad \frac{l}{l_e} = 1, \quad H = \xi \tag{168}$$

for cases 25, 26, 27, and 28, respectively. As before, if $m = 2$,

$$\lambda^2 = 0.6901, \quad \gamma^2 = 0.3803 \tag{99}$$

while, from equation (34), for cases 25 and 26,

$$\kappa^2 = 69.01409 \tag{169}$$

and, for cases 27 and 28,

$$\kappa^2 = 38.82042 \tag{170}$$

The exponents of equation (87) in the solution of equation (86) are now, for cases 25 and 26,

$$n_1 = 8.18714, \quad n_2 = -8.70826 \tag{171}$$

and for cases 27 and 28,

$$n_1 = 6.15582, \quad n_2 = -6.67695 \tag{172}$$

The calculations carried out in exactly the same way as has been indicated for the sample case 11 show that

$$F_{25} = \frac{(4\xi - 1)^2}{9\xi} = \frac{16}{9}\xi - \frac{8}{9} + \frac{1}{9}\xi^{-1} \tag{173}$$

$$f_{25} = -0.0065\xi^{-1} + 0.3855\xi^{8.127} + 0.0260(4\xi)^{-8.708} \tag{174}$$

$$F_{26} = \frac{(4\xi - 1)^2}{9\xi^2} = \frac{16}{9} - \frac{8}{9}\xi^{-1} + \frac{1}{9}\xi^{-2} \tag{175}$$

$$f_{26}=0.0520\xi^{-1}-0.0202\xi^{-2}+0.1529\xi^{8.187}+0.1153(4\xi)^{-8.708} \quad (176)$$

$$F_{27} = \xi \quad (177)$$

$$f_{27} = 0.2994\ \xi^{6.156} \quad (178)$$

$$F_{28} = 1 \quad (179)$$

$$f_{28} = 0 \quad (180)$$

Numerical values of the functions $f(\xi)$ and of the corresponding stresses are given in table IX and in figure 12. The increased taper has reduced the maximum percentage stress increase still further. An indication that width taper is most significant inasmuch as it modifies the F-curves is given by case 27, for which the F-curve is identical with the F-curve of the beam with uniform cross section and concentrated tip load (fig. 3(c)), with the result that the effects of shear lag are of almost identical nature. Case 28 is again a case for which $TF = 1$ so that no shear lag occurs.

Beams with uniformly distributed load and different stiffness parameters (cases 29 to 32).- Beams with uniform load distribution are taken with the same taper law as in cases 11 to 24. The results are to be compared with the corresponding results for cases 15 and 16, which are identical with cases 29 to 32 except for the value of the stiffness parameter m.

By determining first the values of the auxiliary parameters for $m = 1.1$ and $m = 3$ it is found, from equations (34) and (82), that

$$m = 1.1 : \lambda^2=1.5695,\ \gamma^2=0.7265,\ \kappa^2=883.13901 \quad (181)$$

$$m = 3 : \lambda^2=0.4118,\ \gamma^2=0.2353,\ \kappa^2=92.64706 \quad (182)$$

and from equation (87), that for the values of the exponents,

$$m = 1.1 : n_1 = 17.9787,\ n_2 = -19.8845 \quad (183)$$

$$m = 3 : n_1 = 9.7278,\ n_2 = -9.6690 \quad (184)$$

By carrying out the remaining calculations as detailed in

case 11, it is found that

$$m=1.1 : H = 1, \quad F_{29} = 4\xi - 4 + \xi^{-1} = F_{15} \tag{185}$$

$$f_{29}= -0.0263\xi^{-1}+0.7275\xi^{17.979}+0.0525(2\xi)^{-19.885} \tag{186}$$

$$m=1.1 : H = \xi, \quad F_{30} = 4 - 4\xi^{-1} + \xi^{-2} = F_{16} \tag{187}$$

$$f_{30}=0.1051\xi^{-1}-0.0791\xi^{-2}+0.4799\xi^{17.979} +0.1016(2\xi)^{-19.885} \tag{188}$$

$$m = 3 : H = 1, \quad F_{31} = F_{29} \tag{189}$$

$$f_{31}= -0.0266\xi^{-1}+0.3621\xi^{9.728}+0.0527(2\xi)^{-9.669} \tag{190}$$

$$m = 3 : H = \xi, \quad F_{32} = F_{30} \tag{191}$$

$$f_{32}=0.1063\xi^{-1}-0.0824\xi^{-2}+0.2355\xi^{9.728} +0.1168(2\xi)^{-9.669} \tag{192}$$

Numerical values of the functions $f(\xi)$ and of the corresponding stresses are given in table X and in figure 13. A comparison of cases 29 to 32 with cases 15 and 16 shows that decreasing m, that is, making the side webs relatively weaker, tends to increase shear lag and vice versa. It is noted, however, that by choosing values for m as extreme as the present ones a larger effect is observed than is likely to occur in practice for which, as has been previously stated, the value of m is larger than 1.5 and smaller than 2.5. The fact that, for the limiting case, $m = 3$, the actual edge-stress distribution coincides with that given by the elementary theory is explained by the vanishing contribution of the cover sheets to the total beam stiffness.

EFFECTS OF SIMULTANEOUS TAPER IN WIDTH AND COVER-SHEET THICKNESS

In this section, beams are considered that are tapered

according to the laws

$$W = \xi^q, \quad T = \xi^r, \quad m = \text{constant} \tag{193}$$

Introducing equation (193) into the differential equation (21) gives

$$f'' + (r+4\gamma^2 q)\frac{f'}{\xi} - \left[r + 2\gamma^2 q\,(2q - r+1)\right]\frac{f}{\xi^2} - \kappa^2 \frac{f}{\xi^{2q}}$$

$$= 3\lambda^2\left[F'' + \frac{r}{\xi}F' - \frac{r}{\xi^2}F\right] = 3\lambda^2 R \tag{194}$$

and introducing equation (193) into equations (22) and (23) for the boundary conditions gives

$$\xi_o^r\, f(\xi_o) = 0 \tag{195}$$

$$f'(1) + (2q\gamma^2+r)\, f(1) = 3\lambda^2\,[F'(1) + r] \tag{196}$$

if use is made in equation (196) of the fact that $F(1) = 1$. From equations (24) and (25), if for the present purposes it is assumed that W and T are continuous so that only the effect of a concentrated load remains, it follows for the transition conditions that

$$f_l(\xi_c) = f_r(\xi_c) \tag{197}$$

and, if equation (197) is utilized in the evaluation of equation (25),

$$f_l'(\xi_c) - f_r'(\xi_c) = 3\lambda^2\left[F_l'(\xi_c) - F_r'(\xi_c)\right] \tag{198}$$

The Case of Linear Width Taper

As in the preceding section, an especially simple class of solutions is obtained in the case of linear width taper where $q = 1$. The solution of equation (194) is then of the form

$$f(\xi) = 3\lambda^2\left[c_1\,\xi^{n_1} - c_2\,\xi^{n_2} + p(\xi)\right] \tag{199}$$

where now the exponents are given by

$$n_1 = \frac{1-r}{2} - 2\gamma^2 + \sqrt{\frac{(1+r)^2}{4} + 4m\gamma^2\lambda^2 + \kappa^2} \qquad (199a)$$

$$n_2 = \frac{1-r}{2} - 2\gamma^2 - \sqrt{\frac{(1+r)^2}{4} + 4m\gamma^2\lambda^2 + \kappa^2} \qquad (199b)$$

and $p(\xi)$ is defined as before by means of equations (88) to (90), where the first factor ν, in the numerator of equation (90) is to be replaced by $\nu + r$.

Thus it is seen that, in the case of linear width taper and thickness taper according to equation (193), the calculations of individual examples proceed in entirely the same way as in the cases of linear width taper and no thickness taper. Some calculations have been made here for beams with linear sheet thickness taper, that is, $r = 1$.

Beams with uniform load (cases 33 and 34).- In addition to $q = r = 1$, the following values are assumed for the remaining parameters

$$m = 2, \quad \sqrt{\frac{6G}{E}}\frac{l_e}{w_R} = 15, \quad \frac{l}{l_e} = \xi_0 = \frac{1}{2}, \quad \frac{M(\xi)}{M_R} = (2\xi-1)^2 \qquad (200)$$

so that the top view of these beams is identical with most of those treated without thickness taper. The two cases considered distinguish themselves by different height tapers, namely,

$$H = 1, \quad F_{33} = \frac{(2\xi-1)^2}{\xi^2} = 4 - 4\xi^{-1} + \xi^{-2} \qquad (201)$$

$$H = \xi, \quad F_{34} = \frac{(2\xi-1)^2}{\xi^3} = 4\xi^{-1} - 4\xi^{-2} + \xi^{-3} \qquad (202)$$

For the auxiliary parameters,

$$\lambda^2 = 0.6901, \quad \gamma^2 = 0.3801, \quad \kappa^2 = 155.2817$$

and from equation (199), for the exponents

$$n_1 = 11.8244, \quad n_2 = -13.3455 \qquad (203)$$

The remaining calculations carried through as in the preceding section give

$$f_{33}=0.0525-0.0396\xi^{-2}+0.4497\xi^{11.824}+0.1058(2\xi)^{-13.346} \quad (204)$$

$$f_{34}=0.1584\xi^{-2}-0.1080\xi^{-3}+0.2978\xi^{11.824}+0.2303(2\xi)^{-13.346} \quad (205)$$

The distribution of stresses corresponding to these results is contained in table XI and in figure 14.

A comparison of case 33 with case 16, which has the same F-curve, shows that the thickness taper is responsible for increased shear lag and that the percentage increase of the maximum stress has risen from about 11 to about 15 percent, indicating that the neglect of thickness taper is not a conservative procedure.

A comparison of cases 33 and 15, which have the same TF-function, shows that the stress patterns are most similar and that, in both cases, the maximum stress increase amounts to about 15 percent. This result indicates that the shape of the TF-curve rather than the shape of the F-curve determines the shear-lag pattern. Further evidence to support this view is obtained if cases 34 and 16 are compared. For these cases, the TF-curves are identical and again the maximum stress increase is in both cases the same and amounts to 11 percent.

Beams with no spanwise variation of extreme fiber stress according to elementary beam theory (cases 35 and 36).- The effect of thickness taper is further emphasized by considering two cases for which

$$F(\xi) = 1 \quad (206)$$

so that, if T is constant, there would be no shear lag. The two cases considered are distinguished from each other by different degrees of taper in the following way:

For case 35,

$$\sqrt{\frac{6G}{E}}\frac{l_e}{w_R} = 15, \quad \frac{l}{l_e} = \frac{1}{2}, \quad H = 1 \quad (207)$$

and, for case 36,

$$\sqrt{\frac{6G}{E}}\frac{l_e}{w_R} = 7.5, \quad \frac{l}{l_e} = 1, \quad H = 1 \tag{208}$$

It follows, from the definition of $F(\xi)$, that the external moment distribution is given by

$$\frac{M(\xi)}{M_R} = \xi^2 \tag{209}$$

so that in both cases there is a uniform spanwise load distribution; while, for case 35, there is in addition a concentrated tip moment of amount $M(\frac{1}{2})/M_R = 1/4$ and a concentrated tip force of magnitude $M'(\frac{1}{2})/M_R = 1$.

For case 35, all the necessary parameters are given by equation (203). For case 36,

$$\kappa^2 = 38.8204, \quad n_1 = 5.71400, \quad n_2 = -7.23513 \tag{210}$$

and the shear-lag functions $f(\xi)$ take on the form

$$f_{35} = 0.0131 + 0.1507\xi^{11.824} - 0.0132(2\xi)^{-13.34} \tag{211}$$

$$f_{36} = 0.0501 + 0.2652\,\xi^{5.714} \tag{212}$$

The stresses corresponding to equations (211) and (212) are given in table XII and in figure 15. Stress increases of 6 and 11 percent are found owing to the cover-sheet thickness taper, while neglect of the variation of T would have indicated that there was no shear lag. Case 36 is particularly interesting because the TF-curve coincides with the corresponding curves in cases 27 and 3a, in which there is only width taper or no taper at all. In all three of these cases, the stress increase is the same and equals 11 percent. This evidence further supports the contention that the shape of the TF-curves and the value of the aspect-ratio parameter $(E/G)^{1/2}(w/l)$ are of main importance in determining the amount of shear lag.

The Case of Sheet Thickness Taper Only

If constant width is assumed, that is, if

$$q = 0$$

equation (194) reduces to

$$f'' + \frac{r}{\xi} f' - \left(\kappa^2 + \frac{r}{\xi^2}\right) f = 3\lambda^2 \left(F'' + \frac{r}{\xi} F' - \frac{r}{\xi^2} F\right) \tag{213}$$

and can be written in the form

$$\left[\xi^{-r}(\xi^r f)'\right]' - \kappa^2 f = 3\lambda^2 \left[\xi^{-r}(\xi^r F)'\right]' \tag{213a}$$

The solution of this equation is known to be

$$\xi^r f = 3\lambda^2 \xi^{\frac{r+1}{2}} \left[c_1 I_{\frac{r+1}{2}}(\kappa\xi) - c_2 I_{-\frac{r+1}{2}}(\kappa\xi) + p(\xi)\right] \tag{214}$$

where the factor $3\lambda^2$ is inserted for convenience and where $I_{\frac{r+1}{2}}$ is the modified Bessel function of the first kind of order $\frac{r+1}{2}$. If $-\frac{r+1}{2}$ is an integer $I_{-\frac{r+1}{2}}$ would be a constant multiple of $I_{\frac{r+1}{2}}$ and must be replaced by $k_{\frac{r+1}{2}}$ which is the corresponding function of the second kind.

The function $p(\xi)$ is found by the method of variation of parameters in the form

$$p(\xi) = \int^{\xi} \eta^{\frac{r+1}{2}} \left\{I_{\frac{r+1}{2}}(\kappa\xi)\, I_{-\frac{r+1}{2}}(\kappa\eta) - I_{-\frac{r+1}{2}}(\kappa\xi)\, I_{\frac{r+1}{2}}(\kappa\eta)\right\} \cdot \left[\eta^{-r}(\eta^r F)'\right]' d\eta \tag{215}$$

According to equations (195) and (196), the constants of integration are determined by

$$\xi_0^r f(\xi_0) = 0 \tag{195}$$

and

$$\left[\xi^r f\right]'_{\xi=1} = 3\lambda^2 \left[\xi^r F\right]'_{\xi=1} \tag{216}$$

The transition conditions at the place of a concentrated load are as before equations (197) and (198).

In view of the fact that the modified Bessel functions of order $n + \frac{1}{2}$ $(n = 1, 2, \ldots)$ reduce to certain combinations of hyperbolic functions, it follows that when

$$r = 0, 2, 4, \ldots \tag{217}$$

the solution of equation (214) is expressible in terms of hyperbolic functions and reduces, as it should, to the previously derived solution for beams with no taper when $r = 0$.

When $r = 1$, that is, for linear taper, the modified Bessel functions are of the first order and tables for these functions exist. (Tables also exist for the functions corresponding to $r = 3, 5, \ldots$).

It must be said that there still remains the difficulty of evaluating the particular integral of equation (215). In most cases this evaluation will be possible only by numerical methods as exemplified in the section on beams with taper in height and otherwise nonvarying cross section.

In certain instances, however, the particular integral may be obtained in a very simple manner, namely, by choosing the disturbing function F in such a way that either the right-hand side or the first term of the left-hand side of equation (213a) vanishes. Inspection of equation (213a) reveals that

$$F = a_1\xi^3 + a_2\xi^{2-r} + a_3\xi + a_4\xi^{-r}, \quad (a_1+a_2+a_3+a_4=1) \tag{219}$$

is of the nature indicated. Substituting equation (219) in equation (213a) gives the equation

$$\left[\xi^{-r}(\xi^r f)'\right]' - \kappa^2 f = 6\lambda^2\left[(3+r)\, a_1\xi + (1-r)\, a_2\xi^{-r}\right] \tag{220}$$

which is satisfied by

$$f_{part} = -\frac{6\lambda^2}{\kappa^2}\left[(3+r)\, a_1\xi + (1-r)\, a_2\xi^{-r}\right] \tag{221}$$

or, in accordance with equation (214),

$$p(\xi) = -\frac{2}{\kappa^2}\left[(3+r)\ a_1\xi^{\frac{r+1}{2}} + (1-r)\ a_2\xi^{-\frac{r+1}{2}}\right] \qquad (222)$$

From equations (219) and (20) it follows that for the moment distributions which give rise to the simple particular integrals

$$\frac{M(\xi)}{M_R\ H(\xi)} = TF = a_1\xi^{r+3} + a_2\xi^2 + a_3\xi^{r+1} + a_4 \qquad (223)$$

so that for beams of uniform height (H = 1) one of the solutions applies, irrespective of the value of r, to the case of uniform load distribution; while the type of the other load distributions depends on the value of r.

Certain particular cases among the class of solutions included in equation (219) will be investigated further in the following discussion.

Beam with linear thickness taper (case 37).- If uniform height is assumed, from equation (223)

$$\frac{M(\xi)}{M_R} = A_1\frac{\xi^2 - \xi_o^2}{1 - \xi_o^2} + A_2\frac{\xi^4 - \xi_o^4}{1 - \xi_o^4} \qquad (224)$$

where the constants have been so adjusted that the tip section is moment free. From

$$\frac{M'(\xi_o)}{M_R} = -A_1\frac{2\xi_o}{1 - \xi_o^2} + A_2\frac{4\xi_o^3}{1 - \xi_o^4} \qquad (225)$$

it follows that, unless

$$\xi_o = 0 \qquad (226)$$

the load system includes a concentrated tip load. If equation (226) is assumed, it is seen from

$$\frac{M''(\xi)}{M_R} = 2A_1 + 12\ A_2\ \xi^2 \qquad (227)$$

that the effects of a combination of uniform and parabolic load distribution can be analyzed with the solution obtained.

If, in the following development, attention is restricted to the case of a uniform load, that is, if it is assumed that

$$A_1 = a_3 = 1, \quad A_2 = a_1 = a_2 = a_4 = 0 \tag{228}$$

$$F_{37} = \xi \tag{229}$$

$$f_{37} = 3\lambda^2 \left[c_1 I_1(\kappa\xi) - c_2 k_1(\kappa\xi) \right] \tag{230}$$

It seems worth while in this connection to state explicitly that, for linear height taper ($H = \xi$), F_{37} corresponds to the case of linear load distribution.

From the boundary condition of equation (195), which is now

$$T(o)\, f_{37}(o) = 0 \tag{231}$$

it follows that

$$c_2 = 0 \tag{232}$$

and, from the other boundary condition of equation (216), that

$$c_1 \left\{ \frac{d}{d\xi} \left[\xi\, I_1(\kappa\xi) \right] \right\}_{\xi=1} = 2$$

which, in view of the law of differentiation for Bessel functions

$$\frac{d}{dx}\left[x^n I_n(x) \right] = x^n I_{n-1}(x), \quad \frac{d}{dx}\left[x^{-n} I_n(x) \right] = x^{-n} I_{n+1}(x)$$

becomes

$$c_1 = \frac{2}{\kappa\, I_0(\kappa)} \tag{233}$$

so that, finally,

$$f_{37} = \frac{6\lambda^2}{\kappa} \frac{I_1(\kappa\xi)}{I_0(\kappa)} \tag{234}$$

This solution will be discussed with two solutions ob-

tained for quadratic thickness taper in the following paragraph.

Beams with quadratic thickness taper (cases 38 and 39).- When $r = 2$, the moment distribution of equation (223) can be written in the form

$$\frac{M(\xi)}{M_R H(\xi)} = B_1 \frac{\xi^5 - \xi_o^5}{1 - \xi_o^5} + B_2 \frac{\xi^2 - \xi_o^2}{1 - \xi_o^2} + B_3 \frac{\xi^3 - \xi_o^3}{1 - \xi_o^3} \quad (235)$$

If, as before,

$$\xi_o = 0$$

is assumed it is seen that, for uniform height ($H = 1$), the three terms in equation (235) correspond, respectively, to a load increasing according to a cubic law, to a uniform load, and to a linearly increasing load.

For uniform load distribution,

$$F_{38} = 1 \quad (236)$$

and, for linearly increasing load,

$$F_{39} = \xi \quad (237)$$

From equation (222), it follows that

$$p_{38} = \frac{2}{\kappa^2} \xi^{-\frac{3}{2}}, \quad p_{39} = 0 \quad (238)$$

and, in accordance with equation (214),

$$f_{38} = 3\lambda^2 \xi^{-\frac{1}{2}} \left[c_1 I_{\frac{3}{2}}(\kappa\xi) - c_2 I_{-\frac{3}{2}}(\kappa\xi) + \frac{2}{\kappa^2} \xi^{-\frac{3}{2}} \right] \quad (239)$$

$$f_{39} = 3\lambda^2 \xi^{-\frac{1}{2}} \left[c_1 I_{\frac{3}{2}}(\kappa\xi) - c_2 I_{-\frac{3}{2}}(\kappa\xi) \right] \quad (240)$$

The Bessel functions of order $\frac{3}{2}$, may be written

$$I_{\frac{3}{2}} = \sqrt{\frac{2}{\pi}} \frac{1}{\sqrt{x}} \left(\cosh x - \frac{\sinh x}{x} \right),$$

$$I_{-\frac{3}{2}} = \sqrt{\frac{2}{\pi}} \frac{1}{\sqrt{x}} \left(\sinh x - \frac{\cosh x}{x} \right) \quad (241)$$

It follows from the free-end condition of equation (195), for case 38, that

$$\lim_{\xi \to 0} \left[- c_2 \xi^{\frac{3}{2}} I_{-\frac{3}{2}}(\kappa\xi) + \frac{2}{\kappa^2} \right] = 0, \quad c_2 = - \sqrt{\frac{2\pi}{\kappa}} \tag{242}$$

and, for case 39, that

$$c_2 = 0 \tag{243}$$

From the fixed-end condition of equation (216), it follows, for case 38, that

$$\left\{ \frac{d}{d\xi} \left[c_1 \xi^{\frac{3}{2}} I_{\frac{3}{2}}(\kappa\xi) - c_2 \xi^{\frac{3}{2}} I_{-\frac{3}{2}}(\kappa\xi) + \frac{2}{\kappa^2} \right] \right\}_{\xi=1} = 2$$

which can be transformed into

$$c_1 \kappa I_{\frac{1}{2}}(\kappa) - c_2 \kappa I_{-\frac{1}{2}}(\kappa) = 2 \tag{244}$$

and, for case 39,

$$c_1 \left\{ \frac{d}{d\xi} \left[\xi^{\frac{3}{2}} I_{\frac{3}{2}}(\kappa\xi) \right] \right\}_{\xi=1} = 3$$

which can be transformed into

$$c_1 \kappa I_{\frac{1}{2}}(\kappa) = 3 \tag{245}$$

where

$$I_{\frac{1}{2}}(x) = \sqrt{\frac{2}{\pi}} \frac{\sinh x}{x}, \quad I_{-\frac{1}{2}}(x) = \sqrt{\frac{2}{\pi}} \frac{\cosh x}{x} \tag{246}$$

Thus, finally,

$$f_{3s} = \frac{3\lambda^2}{\sqrt{\kappa\xi}} \left\{ \frac{2 - \sqrt{2\pi\kappa}\, I_{-\frac{1}{2}}(\kappa)}{\sqrt{\kappa}\, I_{\frac{1}{2}}(\kappa)} I_{\frac{3}{2}}(\kappa\xi) + \sqrt{2\kappa}\, I_{-\frac{3}{2}}(\kappa\xi) + 2(\kappa\xi)^{-\frac{3}{2}} \right\} \tag{247a}$$

which can be transformed into

$$f_{3s} = \frac{6\lambda^2}{\kappa\xi} \left\{ \frac{1 - \cosh\kappa}{\sinh\kappa} \left(\cosh\kappa\xi - \frac{\sinh\kappa\xi}{\kappa\xi} \right) + \sinh\kappa\xi - \frac{\cosh\kappa\xi}{\kappa\xi} + \frac{1}{\kappa\xi} \right\} \tag{247b}$$

$$f_{39} = \frac{9\lambda^2}{\sqrt{\kappa}\, I_{\frac{1}{2}}(\kappa)} \frac{I_{\frac{3}{2}}(\kappa\xi)}{\sqrt{\kappa\xi}} \tag{248a}$$

which can be transformed into

$$f_{39} = \frac{9\lambda^2}{\kappa\xi \sinh \kappa} \left[\cosh \kappa\xi - \frac{\sinh \kappa\xi}{\kappa\xi}\right] \tag{248b}$$

Discussion of the numerical results for sheet-thickness taper.- Numerical evaluation of the solutions for cases 37 to 39 will further confirm the fact that the shape of the TF-curve is the decisive factor in the effects of shear lag. Since

$$TF_{37} = \xi^2, \quad TF_{38} = \xi^2, \quad TF_{39} = \xi^3$$

this fact will be brought out by a comparison of the results for cases 37 to 39 with the results that were obtained in the section for beams with uniform and linear load distribution, for which

$$TF_1 = F_1 = \xi^2, \quad TF_2 = F_2 = \xi^3$$

If, for a numerical comparison of the states of stress, the same structural data are assumed as were used previously for beams with uniform and linear load distribution, namely,

$$m = 2, \quad \sqrt{\frac{6G}{E}\frac{l}{w}} = 7.5, \quad \kappa = 6.231$$

the stresses along the edge of the sheet and along the middle line of the sheet are calculated by inserting the numerical values of the functions F and of the functions f in equations (26). The results are given in table XIII and in figure 16. A comparison of the stress pattern for cases 37 and 38 with the stress pattern for case 1 (fig. 3(a)) shows that little similarity exists among the three stress patterns, except that the value of the percentage increase of the edge stress at the fixed end is very nearly the same in all three cases. If, however, instead of a comparison of the stress patterns, a comparison of the stress-resultant patterns is made; that is, if the distributions of $T\sigma/\sigma_0$ are compared instead of the distri-

butions of σ/σ_o it is seen that the variation of $T\sigma/\sigma_o$ is very nearly the same in all three cases.

The same results may be observed when the results of case 39 (fig. 16(c)) are compared with the results of case 2 (fig. 3(b)).

It is worth while to note further that, in case 38 (fig. 16(b)), in which according to elementary beam theory the stress does not vary in the spanwise direction, the maximum stress increase does not occur at the fixed end but near the free end of the beam where the sheet thickness decreases to zero. This evidence again indicates that, while the distribution of stress near the fixed end of the beam can be rather closely predicted to be that of a beam with uniform cross section, the same is not always true at other sections of the span.

An additional comparison of the states of stress in beams with and without thickness taper is made by calculating the effective sheet width at the fixed end of the beam as a function of the parameter $\sqrt{\frac{27E}{32G}}\frac{w}{l}$ and of $\sqrt{\frac{27E}{32G}}\frac{w}{L}$ where $\frac{L}{l}$ is again the distance of the center of gravity of the $(TF)^*$-curve from the section $\xi = 1$. For this comparison it is assumed that $m = 2$, so that again

$$\left(\frac{w_{eff}}{w}\right)_R = \frac{1 - \frac{1}{3}f(1)}{1 + \frac{1}{3}f(1)}$$

The numerical results obtained are given in table XIV and in figure 17.

It is noted first that, when the results are compared for corresponding values of $\frac{w}{l}$, there is a pronounced difference between the cases for which $TF = \xi^2$ and the cases for which $TF = \xi^3$. If, however, the results are compared as functions of $\frac{w}{L}$, it is seen that in all cases the agreement is close for not too large values of $\sqrt{\frac{27E}{32G}}\frac{w}{L}$; all curves in fact start out with the same initial slope and a noticeable deviation of the curves from

each other occurs only for rather large values of $\sqrt{\frac{27E}{32G}}\frac{W}{L}$.

As far as calculation of the effective sheet width near the fixed end of the beams is concerned, therefore, all the evidence points to the conclusion that it is permissible, with sufficiently good approximation, to base the calculation for moderately tapered beams on the model of a beam with uniform cross section of which the width equals the root width of the actual beam and the length equals the length of the actual beam; while the effects of taper are incorporated by taking for the model beam with uniform cross section a function $F(\xi)$ identical with the $T(\xi)F(\xi)$-function for the actual beam.

If only an estimate of the effective width is desired the approximation may be carried still further by considering a model beam with uniform cross section, which carries only a concentrated tip load and has a span length the same fraction of the span length of the actual beam as the ratio of the distance of the center of gravity of the $t\sigma_b$ curve from the fixed end of the beam to the span length of the actual beam. Within the accuracy of this estimate it is then possible without any calculation to take the result from the curves in figure 4.

While a very simple general result is deduced for part of the problem, it is also seen from the work of this section and of the preceding section that the percentage of change in the stresses all along the span may be appreciable when there is taper, especially sheet-thickness taper, and that to obtain quantitative results in this respect it appears necessary to base calculations on a beam model rather closely approximating the dimensions of the actual beam.

II - SHEAR LAG IN BEAMS ON TWO SIMPLE SUPPORTS, WITHOUT OR WITH OVERHANGING ENDS

It is possible to use the general results of the least-work method, which are contained in the first two sections of part I, for the analysis of beams supported in any statically determined way, in particular for the analysis of beams on two simple end supports. The only modifications concern the boundary conditions for the shear-lag functions $f(\xi)$. While for cantilever beams $T(\xi)f(\xi)$ vanishes at the free end and a displacement condition is prescribed at the fixed end, beams with two simply supported

or free ends will have T_f vanishing at both ends as a consequence of the condition of vanishing edge bending moments. The examples that follow are intended to show how the method is applied.

BEAMS OF UNIFORM CROSS SECTION ON TWO SIMPLE END SUPPORTS

The differential equation of the problem is as before equation (31). For the bending-moment function $F(\xi)$, it is now more convenient to write

$$F = \frac{M(\xi)}{M_{max}} \tag{249}$$

If the coordinate system is selected so that the ends of the beam have the coordinates $\xi = 1$ and $\xi = -1$ and if l denotes half the span of the beam, the boundary conditions are, instead of equations (22) and (23),

$$f(-1) = 0, \quad f(1) = 0 \tag{250}$$

At the point of application ξ_c of a concentrated load, the transition conditions of equations (24) and (25) occur as before. Explicit solutions will here be obtained for the following load conditions:

(a) A cosine load curve, for which

$$F_{4o} = \cos \frac{\pi}{2} \xi \tag{251}$$

As in case 4, it is seen that

$$f_{4o} = \frac{3\lambda^2}{1 + \left(\frac{2\kappa}{\pi}\right)^2} \cos \frac{\pi}{2} \xi \tag{252}$$

satisfies the differential equation (21) and the boundary conditions of equation (250).

(b) A uniform load distribution, for which

$$F_{41} = 1 - \xi^2 \tag{253}$$

The shear lag function

$$f_{41} = \frac{6\lambda^2}{\kappa^2}\left(1 - \frac{\cosh \kappa\xi}{\cosh \kappa}\right) \tag{254}$$

satisfies the differential equations and the boundary conditions.

(c) A concentrated load at $\xi = \xi_c$, for which

$$F_{40} = \begin{cases} \dfrac{1 + \xi}{1 + \xi_c}, & -1 \leq \xi \leq \xi_c \\ \dfrac{1 - \xi}{1 - \xi_c}, & \xi_c \leq \xi \leq 1 \end{cases} \tag{255}$$

In order to obtain the solution in this case, there may be written

$$f_{42} = \begin{cases} A \sinh \kappa(1+\xi), & -1 \leq \xi \leq \xi_c \\ B \sinh \kappa(1-\xi), & \xi_c \leq \xi \leq 1 \end{cases} \tag{256}$$

which satisfies the differential equation (31) and the boundary conditions of equation (250). The transition conditions of equations (24) and (25) determine the constants A and B as follows:

$$\begin{aligned} A \sinh \kappa(1+\xi_c) - B \sinh \kappa(1-\xi_c) &= 0 \\ A \cosh \kappa(1+\xi_c) + B \cosh \kappa(1-\xi_c) &= \frac{3\lambda^2}{\kappa} \frac{1}{1 - \xi_c^2} \end{aligned} \tag{257}$$

Solving for A and B there is obtained

$$f_{42} = \begin{cases} \dfrac{6\lambda^2 \sinh \kappa(1-\xi_c)}{(1-\xi_c^2) \sinh 2\kappa} \sinh \kappa(1+\xi), & -1 \leq \xi \leq \xi_c \\ \dfrac{6\lambda^2 \sinh \kappa(1+\xi_c)}{\kappa(1-\xi_c^2) \sinh 2\kappa} \sinh \kappa(1-\xi), & \xi_c \leq \xi \leq 1 \end{cases} \tag{258}$$

In particular, when the load acts at midspan,

$$F_{42a} = 1 - |\xi|, \quad f_{42a} = \frac{3\lambda^2}{\kappa} \frac{\sinh \kappa(1-|\xi|)}{\cosh \kappa} \qquad (259)$$

The magnitude of the effective sheet width at the section of greatest bending moment, where $F = 1$, is of particular interest. This quantity is calculated according to equation (27). In what follows values of $\frac{w_{eff}}{w}$ are obtained as function of the parameter $\sqrt{\frac{27E}{32G}} \frac{w}{l}$, if the stiffness parameter m is assumed to have the value 2. The calculations are carried through for cases 40, 41, 42a, and 42b, of which 42b is the case of a concentrated load at the quarter-span point.

The results, which are given in table XV and in figure 18, indicate that, for a load distribution symmetrical about the midspan section, the effective sheet width becomes smaller as the entire load is more nearly concentrated toward the midspan section. It is seen that moving the concentrated load away from midspan reduces still more the effective width.

It should be noted that not only are the results here obtained approximate, much simplified solutions of the effective width problem for beams with isotropic cover sheets such as have been obtained previously by von Kármán, Schnadel, and others, but that the present results go further inasmuch as they permit taking into account the effect of spanwise stiffening of the sheets by assuming an appropriate value of the ratio G/E.

BEAMS ON TWO SUPPORTS WITH OVERHANGING ENDS

The method for obtaining the solution for beams on two supports with overhanging ends may also be indicated here. If it is assumed that the coordinates of the supports are again $\xi = -1$ and $\xi = 1$, the coordinates of the ends of the beam may be denoted by $\xi_1 (\leqslant -1)$ and $\xi_2 (\geqslant 1)$. The bending-moment function F is now defined in the range $\xi_1 \leqslant \xi \leqslant \xi_2$. The differential equation is the same as before and the boundary conditions for the free ends and the transition conditions at the points of

support are

$$f(\xi_1) = 0, \quad f(\xi_2) = 0 \tag{260}$$

$$f_l(\pm 1) = f_r(\pm 1) \tag{261}$$

$$f_l'(\pm 1) - 3\lambda^a F_l'(\pm 1) = f_r(\pm 1) - 3\lambda^a F_r'(\pm 1) \tag{262}$$

No examples of application will be considered here. It may be said, however, that case 3b of a cantilever with concentrated load can be interpreted as the solution of a problem which belongs in this discussion.

III - DETERMINATION OF SHEAR LAG IN STATICALLY UNDETERMINED BEAMS AND ITS EFFECT ON THE DISTRIBUTION OF BENDING MOMENTS

For statically determined beams, that is, for cantilever beams and for beams on two moment-free end supports, the distribution of loads is determined by statics and the aim of any beam theory is only to relate the given moment distribution to the distribution of stresses over the cross section of the beam. When statically indeterminate beams, such as a beam with two clamped ends are considered, the distribution of moments for given load depends on the conditions of support. This condition leads to the question as to whether the distribution of moments as given by the strength-of-materials theory is modified on the basis of a more exact theory of bending; for instance, on the basis of a theory for box beams which takes into account the shear deformation of the cover sheets. The results obtained in the following development show that not only is the distribution of stresses over the cross section affected by modification of the assumptions in the theory of bending but that also their resultant bending moment is in general affected, except when the distribution of bending moments is given by statics.

Since this question has not been previously treated, it was thought worth while to consider it in connection with the related work on statically determined beams even though it seems of less practical interest in aeronautical applications than the corresponding theory for cantilever beams.

The theory will be given here only for beams of uniform cross section, either with both ends clamped or with one end clamped and the other end simply supported. The method of solution is a modification of the least-work method as applied to the problem of the statically supported beam.

For the yet undeterminate distribution of bending moments for given load distribution, there may be assumed

$$M(x) = M_e(x) + M_0 + M_1 \frac{x}{l} \tag{263}$$

where M_e is the moment distribution of elementary beam theory and M_0 and M_1 contain the effect of the shear deformation of the cover sheets.

Corresponding to the distribution of moments of equation (263), the normal stress in the cover sheets is assumed in the form

$$\sigma_x(x,y) = \sigma_b(x) - \left(\frac{m}{3} - \frac{y^2}{w^2}\right) s(x) \tag{264}$$

where

$$\sigma_b(x) = \sigma_e(x) + \sigma_0 + \sigma_1 \frac{x}{l} \tag{265}$$

As has been shown in reference 2, the shear stress in the cover sheets follows from $\frac{\partial \sigma_x}{\partial x} + \frac{\partial \tau}{\partial y} = 0$ in the form

$$\tau(x,y) = y\,\sigma_b'(x) - \frac{y}{3}\left(m - \frac{y^2}{w^2}\right) s'(x) \tag{266}$$

Again, as in the case of the statically determined beam, these expressions for the stresses have to be introduced into the expression for the internal work W of the structure and W has to be made a minimum. Now, however, it is to be taken into consideration that not only the function $s(x)$ but also the constants σ_0 and σ_1 are to be determined by the minimum condition.

If the two ends of the beam are taken at $x = l$ and at $x = -l$, W is given by

$$W = \frac{t}{E}\int_{-l}^{l}\int_{-w}^{w}\left[\sigma_x^2 + \frac{E}{G}\tau^2\right]dy\,dx + \frac{1}{E}\frac{2I_w}{h^2}\int_{-l}^{l}[\sigma_x(x,w)]^2\,dx$$

$$= \frac{t}{E}\int_{-l}^{l}\int_{-w}^{w}\left\{\left[\sigma_e(x) + \sigma_o + \sigma_1\frac{x}{l} - \left(\frac{m}{3} - \frac{y^2}{w^2}\right)s(x)\right]^2 + \frac{E}{G}\left[y\left(\sigma_e'(x) + \frac{\sigma_1}{l} - \frac{y}{3}\left(m - \frac{y^2}{w^2}\right)s'(x)\right]^2\right\}dy\,dx$$

$$+ \frac{2I_w}{Eh^2}\int_{-l}^{l}\left[\sigma_e(x) + \sigma_o + \sigma_1\frac{x}{l} - \left(\frac{m}{3} - 1\right)s(x)\right]^2 dx \qquad (267)$$

From equation (267), it follows that

$$\delta W = \frac{2}{E}\left\{\int_{-l}^{l}\int_{-w}^{w}\left\{\left[\sigma_e+\sigma_o+\sigma_1\frac{x}{l} - \left(\frac{m}{3} - \frac{y^2}{w^2}\right)s(x)\right]\left[\delta\sigma_o + \delta\sigma_1\frac{x}{l} - \left(\frac{m}{3} - \frac{y^2}{w^2}\right)\delta s\right] + \frac{E}{G}\left[y\left(\sigma_e' + \frac{\sigma_1}{l}\right) - \frac{y}{3}\left(m - \frac{y^2}{w^2}\right)s'(x)\right]\left[y\delta\sigma_1\frac{1}{l} - \frac{y}{3}\left(m - \frac{y^2}{w^2}\right)\delta s'\right]\right\}dy\,dx\right.$$

$$\left. + \frac{2I_w}{h^2}\int_{-l}^{l}\left[\sigma_e+\sigma_o+\sigma_1\frac{x}{l} - \left(\frac{m}{3} - 1\right)s\right]\left[\delta\sigma_o + \delta\sigma_1\frac{x}{l} - \left(\frac{m}{3} - 1\right)\delta s\right]dx\right\} \qquad (268)$$

and δW as given by equation (268) has to vanish if W is to be a minimum. It is seen in equation (268) that there are three variations $\delta\sigma_o$, $\delta\sigma_1$, and δs and those are in general arbitrary - except for a relation between $\delta\sigma_o$ and $\delta\sigma_1$ when the moment at one end of the beam is known - so that, for any statically undeterminate problem,

equation (268) implies more conditions than are obtained in the statically determinate case. Evaluation of equation (268) will make this statement evident. If the integration with respect to y is carried out in equation (268), it follows that

$$\delta W = \frac{2}{E}\left\{2wt\int_{-l}^{l}\left\{\left[\left(\delta\sigma_o+\delta\sigma_1\frac{x}{l}\right)\left(\sigma_e+\sigma_o+\sigma_1\frac{x}{l}-\left(\frac{m}{3}-\frac{1}{3}\right)s\right)\right.\right.\right.$$

$$\left.-\delta s\left(\left(\frac{m}{3}-\frac{1}{3}\right)\left(\sigma_e+\sigma_o+\sigma_1\frac{x}{l}\right)-\left(\frac{m^2}{9}-\frac{2m}{9}+\frac{1}{5}\right)s\right)\right]$$

$$+w^2\frac{E}{G}\left[\frac{\delta\sigma_1}{l}\left(\frac{1}{3}\left(\sigma_e'+\frac{\sigma_1}{l}\right)-\frac{1}{3}\left(\frac{m}{3}-\frac{1}{5}\right)s'\right)\right.$$

$$\left.\left.+\delta s'\left(-\frac{1}{3}\left(\frac{m}{3}-\frac{1}{5}\right)\left(\sigma_e'+\frac{\sigma_1}{l}\right)+\frac{1}{9}\left(\frac{m^2}{3}-\frac{2m}{5}+\frac{1}{7}\right)s'\right)\right]\right\}dx$$

$$\left.+\frac{2I_w}{h^2}\int_{-l}^{l}\left[\sigma_e+\sigma_o+\sigma_1\frac{x}{l}-\left(\frac{m}{3}-1\right)s\right]\left[\delta\sigma_o+\delta\sigma_1\frac{x}{l}-\left(\frac{m}{3}-1\right)\delta s\right]dx\right\} \quad (269)$$

If it is observed that

$$I_s = wth^2, \quad m = \frac{3I_w + I_s}{I_w + I_s}$$

if terms with the same variations as factor are combined, and with $\sigma_b = \sigma_e + \sigma_o + \sigma_1\frac{x}{l}$, it follows that

$$0 = \int_{-l}^{l}\left(\delta\sigma_o+\delta\sigma_1\frac{x}{l}\right)\left\{I_s\left[\sigma_b-\frac{1}{3}(m-1)s\right]+I_w\sigma_b-\left(\frac{m}{3}-1\right)s\right]\right\}dx$$

$$+w^2\frac{E}{G}\int_{-l}^{l}I_s\frac{\delta\sigma_1}{l}\left[\frac{1}{3}\sigma_b'-\frac{1}{3}\left(\frac{m}{3}-\frac{1}{5}\right)s'\right]dx$$

(Continued on p. 60)

$$+\int_{-l}^{l} \delta s(x) \left\{ I_s \left[-\frac{1}{3}(m-1)\,\sigma_b + \left(\frac{m^2}{9} - \frac{2m}{9} + \frac{1}{5}\right) s \right] + I_w \left[-\left(\frac{m}{3} - 1\right)\sigma_b + \left(\frac{m}{3} - 1\right)^2 s \right] \right\} dx$$

$$+ w^2 I_s \frac{E}{G} \int_{-l}^{l} \delta s'(x) \left\{ -\frac{1}{3}\left(\frac{m}{3} - \frac{1}{5}\right)\sigma_b' + \frac{1}{9}\left(\frac{m^2}{3} - \frac{2m}{5} + \frac{1}{7}\right) s' \right\} dx \tag{270}$$

The terms containing s in the first integral and the terms containing σ_b in the third integral of equation (270) cancel since

$$I_w\left(1 - \frac{m}{3}\right) + I_s\left(\frac{1}{3} - \frac{m}{3}\right) = \frac{3I_w + I_s}{3} - \frac{m}{3}\left(I_s + I_w\right) = 0$$

If the last integral is integrated by parts, it follows that

$$0 = \int_{-l}^{l} \left(\delta\sigma_o + \delta\sigma_1 \frac{x}{l}\right)\left(I_s\,\sigma_b + I_w\,\sigma_b\right) dx$$

$$+ \frac{E}{3G} w^2 I_s \int_{-l}^{l} \frac{\delta\sigma_1}{l}\left(\sigma_b' - \left(\frac{m}{3} - \frac{1}{5}\right) s'\right) dx$$

$$+ \int_{-l}^{l} \delta s \left\{ \left[I_s\left(\frac{m^2}{9} - \frac{2m}{9} + \frac{1}{5}\right) + I_w\left(\frac{m}{3} - 1\right)^2 \right] s - \frac{E}{3G} w^2 I_s \left[\frac{1}{3}\left(\frac{m^2}{3} - \frac{2m}{5} + \frac{1}{7}\right) s'' - \left(\frac{m}{3} - \frac{1}{5}\right)\sigma_b'' \right] \right\} dx$$

$$+ \frac{E}{3G} w^2 I_s \left\{ \left[\frac{1}{3}\left(\frac{m^2}{3} - \frac{2m}{5} + \frac{1}{7}\right) s' - \left(\frac{m}{3} - \frac{1}{5}\right)\sigma_b' \right] \delta s \right\}_{-l}^{l} \tag{271}$$

With

$$\frac{I_w}{I_s} = \frac{m-1}{3-m}$$

and

$$\frac{m^2}{9} - \frac{2m}{9} + \frac{1}{5} + \frac{m-1}{3-m}\frac{(m-3)^2}{9} = \frac{2}{3}\left(\frac{m}{3} - \frac{1}{5}\right)$$

it follows, finally, that

$$\begin{aligned} 0 = {} & \delta\sigma_0 \int_{-l}^{l} \sigma_b \, dx \\ & + \delta\sigma_1 \int_{-l}^{l} \left\{ \frac{x}{l}\sigma_b + \frac{E}{3G}\frac{I_s}{I}\frac{w^2}{l}\left[\sigma_b' - \left(\frac{m}{3} - \frac{1}{5}\right)s'\right]\right\} dx \\ & + \frac{I_s}{I_w}\int_{-l}^{l} \delta s \left\{ \frac{2}{3}\left(\frac{m}{3} - \frac{1}{5}\right)s - \frac{E}{3G}w^2\left[\frac{1}{3}\left(\frac{m^2}{3} - \frac{2m}{5} + \frac{1}{7}\right)s'' \right.\right. \\ & \qquad \left.\left. - \left(\frac{m}{3} - \frac{1}{5}\right)\sigma_b''\right]\right\} dx \\ & + \frac{E}{3G}w^2\frac{I_s}{I_w}\left\{\left[\frac{1}{3}\left(\frac{m^2}{3} - \frac{2m}{5} + \frac{1}{7}\right)s' - \left(\frac{m}{3} - \frac{1}{5}\right)\sigma_b'\right]\delta s\right\}_{-l}^{l} \end{aligned} \tag{272}$$

If the parameters

$$\lambda^2 = \frac{35m - 21}{35m^2 - 42m + 15}, \qquad \kappa^2 = \frac{6G}{E}\frac{l^2}{w^2}\lambda^2$$

are introduced as before, equation (272) can be written

$$\begin{aligned} 0 = {} & \delta\sigma_0 \int_{-l}^{l} \sigma_b \, dx \\ & + \delta\sigma_1 \int_{-l}^{l} \left\{ \frac{x}{l}\sigma_b + 2\frac{\lambda^2}{\kappa^2}\frac{I_s}{I}l\left[\sigma_b' - \left(\frac{m}{3} - \frac{1}{5}\right)s'\right]\right\} dx \end{aligned}$$

(Equation continued on p. 61)

$$- \frac{I_s}{I} \frac{E}{3G} \frac{w^2}{3} \left(\frac{m^2}{3} - \frac{2m}{5} + \frac{1}{7} \right) \int_{-l}^{l} \delta s \left\{ s'' - \frac{\kappa^2}{l^2} s - 3\lambda^2 \sigma_b'' \right\} dx$$

$$+ \frac{I_s}{I} \frac{E}{3G} \frac{w^2}{3} \left(\frac{m^2}{3} - \frac{2m}{5} + \frac{1}{7} \right) \left\{ \left[s' - 3\lambda^2 \sigma_b' \right] \delta s \right\}_{-l}^{l} \qquad (273)$$

Since s is independent of σ_o and σ_b so far as equilibrium conditions are concerned, the same is true for δs and, in order that equation (12) be true, it is therefore necessary that the integrand of the third integral vanish. Furthermore, because of this independence, the integrated part of equation (273) has to vanish individually. Hence, if for σ_b equation (265) is again introduced, the following set of equations is finally obtained:

$$0 = \delta \sigma_o \int_{-l}^{l} \left[\sigma_e(x) + \sigma_o + \sigma_1 \frac{x}{l} \right] dx$$

$$+ \delta \sigma_1 \int_{-l}^{l} \left\{ \left[\sigma_e(x) + \sigma_o + \sigma_1 \frac{x}{l} \right] \frac{x}{l} + 2 \frac{\lambda^2}{\kappa^2} \frac{I_s}{I} l \left[\sigma_e'(x) + \frac{\sigma_1}{l} - \left(\frac{m}{3} - \frac{1}{5} \right) s'(x) \right] \right\} dx \qquad (274)$$

$$s''(x) - \frac{\kappa^2}{l^2} s(x) = 3\lambda^2 \sigma_b''(x) \qquad (275)$$

$$\left\{ \left[s'(x) - 3\lambda^2 \left(\sigma_e'(x) + \frac{\sigma_1}{l} \right) \right] \delta s(x) \right\}_{-l}^{l} = 0 \qquad (276)$$

As in the statically determinate case, equations (275) and (276) are the differential equations with boundary conditions for the shear-lag function $s(x)$. The new result is contained in equation (274), which represents one or two conditions according to whether σ_o and σ_1 are dependent upon each other and which, therefore, in either case is sufficient to determine σ_o and σ_1.

At this point, it seems best to consider separately the various cases corresponding to a beam with two fixed

ends and a beam with one end fixed and one end simply supported and to consider specific examples showing the effect of the shear deformation of the cover sheets on the stress distribution and, in particular, on the moment distribution.

BEAM WITH BOTH ENDS BUILT IN

No relation between σ_0 and σ_1 follows from equilibrium considerations and consequently equation (274) is equivalent to two separate conditions. The integrals involving $\sigma_e(x)$ vanish because of the conditions of support, since $\sigma_e = \text{constant}\ \frac{d^2w}{dx^2}$, and where in this connection w stands for the deflection of the beam.

$$\int_{-l}^{l} \frac{d^2w}{dx^2}\,dx = \left[\frac{dw}{dx}\right]_{-l}^{l}, \qquad \int_{-l}^{l} x\,\frac{d^2w}{dx^2}\,dx = \left[x\,\frac{dw}{dx} - w\right]_{-l}^{l} = 0$$

The boundary conditions of equation (276) assume their proper form if, for fixed supports, the multipliers of $\delta s(l)$ and of $\delta s(-l)$ vanish. If the integration in equation (274) is carried out, therefore, the complete system of equations (274) to (276) reduces to

$$\sigma_0 = 0 \tag{277}$$

$$\frac{2}{3}\,\sigma_1 + 2\,\frac{\lambda^2}{\kappa^2}\,\frac{I_s}{I}\left[\sigma_e(x) + \sigma_1\,\frac{x}{l} - \left(\frac{m}{3} - \frac{1}{5}\right)s(x)\right]_{-l}^{l} = 0 \tag{278}$$

$$s''(x) - \frac{\kappa^2}{l^2}\,s(x) = 3\lambda^2\,\sigma_e''(x) \tag{275}$$

$$x = \pm l, \qquad s'(x) - 3\lambda^2\left(\sigma_e'(x) + \frac{\sigma_1}{l}\right) = 0 \tag{279}$$

This system of equations indicates immediately that the distribution of bending moments as given by the elementary beam theory remains unchanged if the load and therewith the moment distribution is symmetrical about the middle of the beam because, for this to be the case, σ_1

must vanish while σ_0 vanishes as the consequence of the least-work conditions.

In order for the bending moment distribution of the built-in end beam to be affected by shear lag, it is therefore necessary that the load distribution be asymmetrical about the center of the beam.

The following examples will be solved explicitly:

(1) beam with uniform distribution of load (case 43)

(2) beam with antisymmetrical deflection of both ends (case 44)

(3) beam with antisymmetrical linearly distributed load (case 45)

The first example is taken because it is one for which shear lag is of surprising magnitude. The second example is taken because it illustrates the way in which modification of the moment distribution due to shear lag is connected with a reduction of effective beam stiffness. The third example is taken to illustrate the way in which the effective moment distribution depends on the distribution of load.

The following results are obtained for the three cases:

(a) For the distribution of stress according to elementary beam theory

Case	$\sigma_e(x)/\sigma_e(l)$	$l\sigma_e'(x)/\sigma_e(l)$	$l^2\sigma_e''(x)/\sigma_e(l)$
43	$-\frac{1}{2}\left(1 - 3\frac{x^2}{l^2}\right)$	$3\frac{x}{l}$	3
44	$\frac{x}{l}$	1	0
45	$-\frac{3}{2}\left(\frac{x}{l} - \frac{5}{3}\frac{x^3}{l^3}\right)$	$-\frac{3}{2}\left(1 - 5\frac{x^2}{l^2}\right)$	$15\frac{x}{l}$

(b) For the general form of the shear-lag function s, which follows from equation (275),

$$s(x) = C_1 \cosh \kappa \frac{x}{l} + C_2 \sinh \kappa \frac{x}{l} + s_{part} \qquad (280)$$

If the symmetry conditions are observed and the appropriate values of $\sigma_e''(x)$ are taken, equation (280) takes on the forms

Case	s
43	$C_1 \cosh \kappa \frac{x}{l} - 9 \frac{\lambda^2}{\kappa^2}$
44	$C_2 \sinh \kappa \frac{x}{l}$
45	$C_2 \sinh \kappa \frac{x}{l} - 45 \frac{\lambda^2}{\kappa^2} \frac{x}{l}$

If these expressions are substituted in the boundary conditions of equation (279), there follows for C_n, if in addition $\sigma_e(l) = 1$ is set

Case	C_n
43	$C_1 = \frac{9\lambda^2}{\kappa \sinh \kappa}$
44	$C_2 = \frac{3\lambda^2 (1 + \sigma_1)}{\kappa \cosh \kappa}$
45	$C_2 = \frac{3\lambda^2 (6 + \sigma_1 - 15/\kappa^2)}{\kappa \cosh \kappa}$

The shear-lag function s becomes in the three cases

Case	s(x)	
43	$\frac{9\lambda^2}{\kappa} \left[\frac{\cosh \kappa \frac{x}{l}}{\sinh \kappa} - \frac{1}{\kappa} \right]$	(281)
44	$\frac{3\lambda^2}{\kappa} (1+\sigma_1) \frac{\sinh \kappa \frac{x}{l}}{\cosh \kappa}$	(282)
45	$\frac{3\lambda^2}{\kappa} \left[\left(6+\sigma_1 + \frac{15}{\kappa^2}\right) \frac{\sinh \kappa \frac{x}{l}}{\cosh \kappa} - \frac{15}{\kappa} \frac{x}{l} \right]$	(283)

The values of σ_1 have now to be determined by substituting equations (282) and (283) in equation (278). If $2I_s/I = 3 - m$ is put, there follows

Case	
44	$\sigma_1 = \frac{-\mu}{1+\mu}, \quad \mu = 3\,\frac{\lambda^2(3-m)}{\kappa^2}\left[1-\lambda^2\left(m-\frac{3}{5}\right)\frac{\tanh\kappa}{\kappa}\right]$ (284)
45	$\sigma_1 = -3\,\frac{\lambda^2(3-m)}{\kappa^2}\,\frac{1-3\lambda^2\left(m-\frac{3}{5}\right)\frac{5(\tanh\kappa-\kappa)+2\kappa^2\tanh\kappa}{\kappa^3}}{1+3\,\frac{\lambda^2(3-m)}{\kappa^2}\left[1-\lambda^2\left(m-\frac{3}{5}\right)\frac{\tanh\kappa}{\kappa}\right]}$ (285)

The distribution of normal stress in the cover sheets is again obtained from equations (264) and (265) in the form

$$\frac{\sigma_x(x,y)}{\sigma_e(l)} = \frac{\sigma_e(x) + \sigma_1\frac{x}{l}}{\sigma_e(l)} - \left(\frac{m}{3} - \frac{y^2}{w^2}\right)\frac{s(x)}{\sigma_e(l)} \qquad (286)$$

with $s(x)$ and σ_1 given, for the cases considered, by equations (281) to (283). When σ_e, σ_1, and s are substituted in equation (286), it follows that

Case	$\frac{\sigma_x(x,y)}{\sigma_e(l)}$
43	$\frac{3}{2}\left(\frac{x}{l}\right)^2 - \frac{1}{2} - \left(\frac{m}{3} - \frac{y^2}{w^2}\right)\frac{3\lambda^2}{\kappa}\left[\frac{\cosh\kappa\,\frac{x}{l}}{\sinh\kappa} - \frac{1}{\kappa}\right]$ (287)
44	$(1+\sigma_1)\,\frac{x}{l} - \left(\frac{m}{3} - \frac{y^2}{w^2}\right)\frac{3\lambda^2}{\kappa}(1+\sigma_1)\,\frac{\sinh\kappa\,\frac{x}{l}}{\cosh\kappa}$ (288)
45	$\frac{5}{2}\left(\frac{x}{l}\right)^3 - \frac{3}{2}\left(\frac{x}{l}\right) + \sigma_1\left(\frac{x}{l}\right) - \left(\frac{m}{3} - \frac{y^2}{w^2}\right)\frac{3\lambda^2}{\kappa}\left[\left(6+\sigma_1+\frac{15}{\kappa^2}\right)\frac{\sinh\kappa\,\frac{x}{l}}{\cosh\kappa} - \frac{15}{\kappa}\,\frac{x}{l}\right]$ (289)

The formulas (287) to (289) have been evaluated for a typical beam with $\sqrt{\frac{27E}{32G}}\frac{w}{L} = 0.3$ (span length $2l$ equals five times the width $2w$ for isotropic cover sheet) and with equal contribution of side webs and cover sheets to the stiffness of the beam ($m = 2$). From equation (273), it follows that for the parameters $\lambda^2 = 0.690$ and $\kappa = 6.231$. The values of the end-moment correction σ_1 have been calculated from equations (284) and (285). Table XVI contains the numerical results for the distribution of stress. The data contained in table XVI are given graphically in figure 19.

In order to explain the large amount of shear lag near the fixed ends of the beam in the case of the uniformly distributed load, it may be said that the part of the beam near the fixed ends where the moment curve is positive can be considered approximately as a cantilever beam of correspondingly shorter span l_c. Since $l_c = 0.4\,l$, $w/l_c = (1/5)\,(10/4) = 0.5$. From equations (40) and (26), it follows, for $\sigma_x(l_c,0)/\sigma_b(l_c)$ for a cantilever beam of length l_c and width $2w$ with uniformly distributed load, that

$$\frac{\sigma_x(l_c,0)}{\sigma_b(l_c)} = 1 - m\frac{\lambda^2}{\kappa^2}\left[\kappa\frac{\sinh\kappa}{\cosh\kappa}\right] = 1 - m\frac{\lambda^2}{\kappa}$$

and with

$$\kappa^2 = \frac{6G}{E}\lambda^2\left(\frac{l_c}{w}\right)^2,\quad m = 2,\quad \lambda = 0.83,\quad \frac{w}{l_c} = 0.5,\quad \sqrt{\frac{E}{6G}} = \frac{2}{3}$$

$$\frac{\sigma_x(l_c,0)}{\sigma_b(l_c)} = 1 - 2 \times 0.83 \times 0.666 \times 0.5 = 0.447$$

and this result agrees almost exactly with the corresponding stress ratio obtained for the longer beam with both ends fixed.

In case 44, one-half the beam behaves approximately as the corresponding cantilever with concentrated end load and the amount of shear lag bears out this analogy. (See fig. 19(b).)

For the linearly distributed antisymmetrical distribution of load (case 45), shear lag is even more pronounced than for the uniform, symmetrical distribution of load. The reason for this condition is that the length of the corresponding cantilever is even less, that is, $l_c = 0.2\,l$.

In connection with the modification of the moment distribution, it is seen that shear lag in the two cases considered reduces somewhat the value of the maximum moment, in case 44 by about 4 percent and in case 45 by about 7 percent.

Table XVII contains values of $\sigma_1/\sigma_e(\frac{l}{2})$ as a function of w/l for three values of m in case 44 and for $m = 2$ in case 45, and the data contained in the table are represented in figure 20.

The question arises as to why there is no modification of the moment distribution in the symmetrical case while a modification occurs in the antisymmetrical case. While it is felt that a better physical interpretation of this fact should still be attempted, the following difference between the two cases is evident: In the symmetrical case, the possible superimposed state of stress, due to σ_0, is uniform and involves no shear stress; while in the antisymmetrical case the superimposed state of stress, due to σ_1, is nonuniform, involves shear stress, and is thus affected by shear lag. An explanation should also be given for the fact that, although the effective beam stiffness in the symmetrical case is reduced owing to shear lag near the two supports, this spanwise variation of beam stiffness is not responsible in itself for a modification of the moment distribution of elementary beam theory, according to which the effective beam stiffness does not vary.

BEAM WITH ONE END BUILT IN AND ONE END SIMPLY SUPPORTED

If it is assumed that the end $x = -l$ is simply supported, it follows from equation (265) that

$$\sigma_0 - \sigma_1 = 0 \tag{290}$$

and hence

$$\delta\sigma_0 - \delta\sigma_1 = 0 \tag{291}$$

If equations (290) and (291) are introduced in the main system of equations (274) to (276), it follows from equation (274) that

$$\int_{-l}^{l} \left[\sigma_e(x) + \sigma_1 \left(1 + \frac{x}{l}\right)\right]\left(1 + \frac{x}{l}\right) dx + \frac{2\lambda^2}{\kappa^2} \frac{I_s}{I} l \left\{\sigma_e + \sigma_1 \frac{x}{l} - \left(\frac{m}{3} - \frac{1}{5}\right) s\right\}_{-l}^{l} = 0$$

Equation (275) remains unchanged, and equation (276) separates into the two conditions

$$s(-l) = 0, \quad s'(l) - 3\lambda^2 \sigma_b'(l) = 0 \qquad (292)$$

From equation (292), if it is observed that again

$$\int_{-l}^{l} \sigma_e\left(1 + \frac{x}{l}\right) dx = \text{constant} \int_{-l}^{l} \frac{d^2 w}{dx^2}\left(1 + \frac{x}{l}\right) dx = \text{constant} \left[\left(1 + \frac{x}{l}\right)\frac{dw}{dx} - \frac{w}{l}\right]_{-l}^{l} = 0$$

because of the conditions of support, the equation determining σ_1 can be written as

$$\frac{2}{3}\sigma_1 + 2\frac{\lambda^2}{\kappa^2}\frac{I_s}{I}\left[\sigma_e(l) + 2\sigma_1 - \left(\frac{m}{3} - \frac{1}{5}\right) s(l)\right] = 0 \qquad (293)$$

Since the calculation of examples from this point proceeds exactly as for the beam with two fixed ends and since no basically different results are to be expected, no such calculations have been made here. It should be noted, however, that one of the cases considered for the beam with fixed ends, namely, the case of linear antisymmetrical load distribution, includes the case of a beam with one end fixed and one end simply supported if the portion of the beam to the right or to the left of the center section is considered a separate entity.

CONCLUSIONS

The following conclusions with regard to the problem of shear lag in cantilever box beams may be drawn.

The shear deformation of the cover sheets may be responsible, in actual cases, for stress increases of as much as 20 to 30 percent of the stresses predicted by the elementary beam theory.

The magnitude of the shear-lag effect depends on a variety of factors, of which two are found to be of greatest influence:

1. the product of the span: root-width ratio of the beam and of the square root of the ratio of the effective shear modulus and of Young's modulus of the cover sheets $(l/2w_R)(G/E)^{1/2}$;

2. the shape of the curve representing the product of the spanwise sheet normal stress of elementary beam theory and of the thickness of the cover sheet, $t\sigma_b$.

The magnitude of the shear lag increases with decreasing values of $(l/2w_R)(G/E)^{1/2}$.

Negative curvature of the $t\sigma_b$-curve indicates relatively little shear lag while positive curvature indicates appreciable shear lag.

The present work indicates that taper in beam width is of importance only insofar as it affects the function $t\sigma_b$. Sufficiently accurate results may be obtained by analyzing, instead of the beam with width taper, a substitute beam of uniform width equal to the root width of the tapered beam.

The present work also indicates that taper in cover-sheet thickness is of appreciable importance and should not be neglected in the analysis. Especially noticeable shear-lag effects occur at sections where a discontinuous change of cover-sheet thickness takes place.

The effect of taper in beam height is incorporated entirely in the function $t\sigma_b$.

It is found that within the practical range the effect

of a change of the relative stiffness of the cover sheets and of the side webs including flanges is very small, so that further calculations may be based on the assumption of equal relative stiffnesses.

It is thought that by giving the explicit results for a good many sample cases, an idea is given to the designer of the magnitude of the effect and of its dependence on design data. The results of the calculations should prove useful also for reasonable estimates in those cases where conditions are somewhat different from the ones which were considered here.

No treatment has been given to problems involving beams without symmetry about a spanwise vertical plane. The presence of a slight degree of such unsymmetry is believed to be of little influence on the amount of shear lag present. It would, however, be feasible to extend the analysis to distinctly unsymmetrical beams and to evaluate some typical cases.

A further possible extension of the work would consist in the analysis of beams under combined bending and torsion loads. Such an extension offers no essential difficulty. It is believed, however, that if a loading is separated into a bending component and into a torsional component it will be found that shear lag due to the torsional component is considerably less marked than that due to the bending component.

A further part of the problem which so far has not been investigated is the effect of camber on shear lag. It is possible to extend the work in this direction and to analyze some typical arrangements. A reasonable procedure, which analysis should prove to be correct, is thought to be a modification of the stresses of the elementary theory in the cambered beam by means of the calculated shear-lag effect for the beam without camber.

Department of Mathematics,
Massachusetts Institute of Technology,
Cambridge, Mass., June 1942.

REFERENCES

1. Reissner, Eric: A Method for Solving Shear Lag Problems. Aviation, vol. 40, no. 5, May 1941, pp. 48-49.

2. Reissner, Eric: Least Work Solutions of Shear Lag Problems. Jour. Aero. Sci., vol. 8, no. 7, May 1941, pp. 284-291.

3. Kuhn, Paul, and Chiarito, Patrick: Shear Lag in Box Beams - Methods of Analysis and Experimental Investigations. Rep. No. 739 (to be issued), NACA, 1942.

4. Newell, Joseph S., and Reissner, Eric: Shear Lag in Corrugated Sheets Used for the Chord Member of a Box Beam. T.N. No. 791, NACA, 1941.

5. Younger, John E.: Metal Wing Construction. Part II - Mathematical Investigations. A.C,T.R. ser. no. 3288, Materiel Div., Army Air Corps, 1930.

TABLE I.- NORMAL STRESSES ALONG THE EDGE AND ALONG THE CENTER LINE OF COVER SHEETS FOR BEAMS OF UNIFORM CROSS SECTION.

x/l	F_1	f_1	$\sigma(x,e)/\sigma_e$	$\sigma(x,w)/\sigma_e$
0	0	0	0	0
0.1	.01	-.048	.042	-.006
0.2	.04	-.072	.088	.016
0.3	.09	-.082	.145	.063
0.4	.16	-.082	.215	.133
0.5	.25	-.073	.298	.226
0.6	.36	-.049	.393	.344
0.7	.49	-.003	.492	.489
0.8	.64	.085	.583	.668
0.9	.81	.250	.643	.893
1.0	1.00	.558	.628	1.186

x/l	F_2	f_2	$\sigma(x,0)/\sigma_e$	$\sigma(x,w)/\sigma_e$
0	0	0	0	0
0.125	.002	-.036	.026	-.010
0.250	.016	-.071	.063	-.008
0.375	.053	-.099	.119	.020
0.500	.125	-.114	.201	.087
0.625	.244	-.099	.310	.211
0.750	.422	-.019	.435	.415
0.875	.670	.201	.536	.737
0.950	.857	.464	.548	1.012
0.975	.927	.585	.537	1.122
1.000	1.000	.728	.515	1.243

x/l	F_{3a}	f_{3a}	$\sigma(x,e)/\sigma_e$	$\sigma(x,w)/\sigma_e$
0	0	0	0	0
0.1	.1	.001	.099	.100
0.2	.2	.002	.199	.201
0.3	.3	.004	.297	.301
0.4	.4	.008	.395	.403
0.5	.5	.015	.490	.505
0.6	.6	.027	.582	.609
0.7	.7	.051	.666	.717
0.8	.8	.096	.736	.832
0.9	.9	.178	.781	.959
1.0	1.0	.332	.778	1.111

x/l	F_{3b}	f_{3b}	$\sigma(x,e)/\sigma_e$	$\sigma(x,w)/\sigma_e$
0	0	0	0	0
0.1	0	-.018	.012	-.006
0.2	0	-.043	.029	-.014
0.3	0	-.085	.057	-.028
0.4	0	-.162	.108	-.054
0.45	0	-.221	.148	-.074
0.5	0	-.303	.202	-.101
0.55	.1	-.204	.236	.032
0.6	.2	-.124	.283	.159
0.7	.4	-.005	.397	.402
0.8	.6	.136	.509	.645
0.9	.8	.321	.586	.907
1.0	1.0	.635	.677	1.212

x/l	$F_{1,3b}$	$f_{1,3b}$	$\sigma(x,e)/\sigma_e$	$\sigma(x,w)/\sigma_e$
0	0	0	0	0
0.1	.02	-.078	.072	-.006
0.2	.08	-.101	.147	.046
0.3	.18	-.079	.233	.154
0.4	.32	-.002	.322	.320
0.5	.50	.159	.394	.553
0.6	.52	.026	.503	.529
0.7	.58	-.011	.587	.576
0.8	.68	.034	.657	.691
0.9	.82	.179	.700	.879
1.0	1.00	.481	.679	1.160

TABLE II.- EFFECTIVE WIDTH AT BUILT-IN END OF BEAM OF UNIFORM CROSS SECTION.

$\sqrt{\frac{27E}{32G}}\frac{w}{l}$	K	$m=2$ $f_1(i)$	$\left(\frac{w_{eff}}{w}\right)_R$	$\sqrt{\frac{27E}{32G}}\frac{w}{l_1}$
0		0	1.000	0
0.075	24.922	.160	.899	0.15
0.150	12.461	.306	.815	0.30
0.225	8.307	.439	.745	0.45
0.300	6.231	.561	.685	0.60
0.375	4.984	.675	.632	0.75
0.450	4.154	.788	.584	0.90

$\sqrt{\frac{27E}{32G}}\frac{w}{l}$	K	$m=2$ $f_2(i)$	$\left(\frac{w_{eff}}{w}\right)_R$	$\sqrt{\frac{27E}{32G}}\frac{w}{l_2}$
0		0	1.000	0
0.075	24.922	.230	.858	0.225
0.150	12.461	.425	.752	0.450
0.225	8.307	.589	.672	0.675
0.300	6.231	.728	.609	0.900

$\sqrt{\frac{27E}{32G}}\frac{w}{l}$	K	$m=2$ $f_{3a}(i)$	$\left(\frac{w_{eff}}{w}\right)_R$	$\sqrt{\frac{27E}{32G}}\frac{w}{l_3}$
0		0	1.000	0
0.075	24.922	.083	.946	0.075
0.150	12.461	.166	.895	0.150
0.225	8.307	.249	.847	0.225
0.300	6.231	.332	.801	0.300
0.375	4.984	.415	.757	0.375
0.450	5.154	.498	.715	0.450
0.600	3.115	.662	.638	0.600
0.750	2.492	.819	.571	0.750
0.900	2.077	.966	.513	0.900

$\sqrt{\frac{27E}{32G}}\frac{w}{l}$	K	$m=1.5$ $f_{3a}(i)$	$\left(\frac{w_{eff}}{w}\right)_R$	$\sqrt{\frac{27E}{32G}}\frac{w}{l_3}$
0		0	1.000	0
0.075	30.364	.101	.936	0.075
0.150	15.182	.202	.877	0.150
0.225	10.121	.304	.824	0.225
0.300	7.591	.405	.776	0.300
0.375	6.073	.506	.731	0.375
0.450	5.061	.607	.689	0.450
0.600	3.795	.809	.616	0.600
0.750	3.036	1.007	.553	0.750
0.900	2.530	1.199	.500	0.900

$\sqrt{\frac{27E}{32G}}\frac{w}{l}$	K	$m=2.5$ $f_{3a}(i)$	$\left(\frac{w_{eff}}{w}\right)_R$	$\sqrt{\frac{27E}{32G}}\frac{w}{l_3}$
0		0	1.000	0
0.075	21.560	.072	.953	0.075
0.150	10.780	.144	.906	0.150
0.225	7.187	.216	.861	0.225
0.300	5.390	.287	.817	0.300
0.375	4.312	.359	.774	0.375
0.450	3.593	.431	.732	0.450
0.600	2.695	.570	.653	0.600
0.750	2.165	.700	.582	0.750
0.900	1.797	.816	.521	0.900

TABLE III.- RESULTANT STRESS DISTRIBUTION FOR BEAMS WITH TAPER IN HEIGHT.

x/l	F_6	f_6	$\sigma(x,0)/\sigma_0$	$\sigma(x,w)/\sigma_0$
0	0	0	0	0
0.25	.400	.082	.345	.427
0.50	.667	.071	.619	.690
0.75	.857	.079	.804	.884
0.85	.919	.104	.849	.954
0.90	.947	.127	.863	.990
0.95	.974	.158	.869	1.027
1.00	1.000	.202	.865	1.067

x/l	F_7	f_7	$\sigma(x,0)/\sigma_0$	$\sigma(x,w)/\sigma_0$
0	0	0	0	0
0.25	.100	-.076	.151	.075
0.50	.333	-.042	.361	.319
0.75	.643	.061	.602	.663
0.85	.781	.157	.677	.833
0.90	.853	.230	.699	.929
0.95	.926	.329	.706	1.035
1.00	1.000	.463	.692	1.154

TABLE IV.- STRESS RESULTANTS FOR BEAM WITH DISCONTINUOUS CHANGES IN COVER-SHEET THICKNESS.

x/l	TF_8	Tf_8	$t\sigma(x,0)/t_2\sigma_0$	$t\sigma(x,w)/t_2\sigma_0$
0	0	0	0	0
0.125	.125	.009	.119	.128
0.250	.250	.024	.234	.258
0.375	.375	.055	.338	.393
0.500	.500	.120	.420	.540
0.625	.625	.081	.571	.652
0.750	.750	.093	.688	.781
0.875	.875	.165	.765	.930
1.000	1.000	.342	.772	1.114

x/l	TF_9	Tf_9	$t\sigma(x,0)/t_2\sigma_0$	$t\sigma(x,w)/t_1\sigma_0$
0	0	0	0	0
0.125	.016	-.048	.047	-.0003
0.250	.063	-.058	.101	.043
0.375	.141	-.036	.165	.129
0.500	.250	.030	.230	.260
0.625	.391	.007	.386	.393
0.750	.563	.057	.625	.581
0.875	.766	.211	.625	.836
1.000	1.000	.567	.622	1.189

x/l	TF_{10}	Tf_{10}	$t\sigma(x,0)/t_2\sigma_0$	$t\sigma(x,w)/t_1\sigma_0$
0	0	0	0	0
0.125	.014	-.055	.051	-.004
0.250	.063	-.077	.114	.037
0.500	.250	-.065	.293	.228
0.625	.391	-.023	.406	.383
0.750	.563	.072	.515	.586
0.800	.640	.136	.549	.685
0.825	.681	.177	.563	.740
0.850	.722	.224	.573	.797
0.875	.766	.280	.579	.859
0.900	.810	.345	.580	.925
0.925	.856	.398	.590	.988
0.950	.902	.463	.594	1.057
0.975	.951	.542	.589	1.131
1.000	1.000	.637	.575	1.212

TABLE V.- NORMAL STRESSES FOR BEAMS WITH CONCENTRATED TIP LOAD.

x^*/l	F_{11}	f_{11}	$\sigma(x^*,0)/\sigma_0$	$\sigma(x^*,w)/\sigma_0$
0	0	0	0	0
0.125	.222	.035	.199	.234
0.250	.400	.040	.374	.413
0.375	.545	.039	.519	.558
0.500	.667	.039	.640	.680
0.750	.857	.061	.817	.877
0.875	.933	.100	.867	.967
1.000	1.000	.185	.876	1.062

x^*/l	F_{12}	f_{12}	$\sigma(x^*,0)/\sigma_0$	$\sigma(x^*,w)/\sigma_0$
0	0	0	0	0
0.125	.395	.112	.320	.433
0.250	.640	.109	.567	.676
0.375	.793	.090	.734	.823
0.500	.889	.072	.841	.913
0.750	.980	.046	.949	.995
0.875	.996	.038	.970	1.008
1.000	1.000	.034	.977	1.011

x^*/l	F_{13}	f_{13}	$\sigma(x^*,0)/\sigma_0$	$\sigma(x^*,w)/\sigma_0$
0	2.000	0	2.000	2.000
0.125	1.776	-.035	1.801	1.766
0.250	1.600	-.040	1.626	1.587
0.375	1.455	-.039	1.481	1.442
0.500	1.333	-.039	1.360	1.320
0.750	1.143	-.061	1.183	1.123
0.875	1.067	-.100	1.133	1.033
1.000	1.000	-.185	1.124	.938

TABLE VI.- NORMAL STRESSES FOR BEAMS WITH UNIFORMLY DISTRIBUTED LOAD.

x^*/l	F_{15}	f_{15}	$\sigma(x^*,0)/\sigma_0$	$\sigma(x^*,w)/\sigma_0$
0	0	0	0	0
0.125	.028	-.035	.051	.016
0.250	.100	-.038	.125	.087
0.375	.205	-.033	.226	.194
0.500	.333	-.021	.347	.326
0.750	.643	.062	.602	.664
0.875	.817	.187	.692	.879
1.000	1.000	.449	.701	1.150

x^*/l	F_{16}	f_{16}	$\sigma(x^*,0)/\sigma_0$	$\sigma(x^*,w)/\sigma_0$
0	0	0	0	0
0.125	.049	-.042	.077	.035
0.250	.160	-.030	.180	.150
0.375	.298	-.012	.305	.294
0.500	.444	.007	.439	.447
0.750	.735	.076	.684	.760
0.875	.871	.162	.763	.925
1.000	1.000	.337	.776	1.112

x^*/l	F_{18}	f_{18}	$\sigma(x^*,0)/\sigma_0$	$\sigma(x^*,w)/\sigma_0$
0	0	0	0	0
0.125	.125	.000	.125	.125
0.250	.250	.001	.249	.250
0.375	.375	.003	.373	.376
0.500	.500	.009	.494	.503
0.750	.750	.061	.709	.770
0.875	.875	.143	.779	.923
1.000	1.000	.317	.789	1.106

TABLE VII.- NORMAL STRESSES FOR BEAMS WITH LINEARLY INCREASING LOAD.

x^*/l	F_{13}	f_{13}	$\sigma(x^*,0)/\sigma_0$	$\sigma(x^*,\omega)/\sigma_0$
0	0	0	0	0
0.125	.003	-.021	.017	-.003
0.250	.025	-.040	.052	.012
0.375	.077	-.056	.114	.058
0.500	.167	-.063	.208	.146
0.750	.462	.026	.465	.491
0.875	.715	.217	.570	.787
1.000	1.000	.649	.568	1.216

x^*/l	F_{23}	f_{23}	$\sigma(x^*,0)/\sigma_0$	$\sigma(x^*,\omega)/\sigma_0$
0	0	0	0	0
0.125	.006	-.028	.025	-.003
0.250	.040	-.047	.070	.025
0.375	.112	-.054	.148	.094
0.500	.222	-.049	.255	.206
0.750	.551	.048	.519	.567
0.875	.762	.212	.621	.833
1.000	1.000	.561	.626	1.187

x^*/l	F_{22}	f_{22}	$\sigma(x^*,0)/\sigma_0$	$\sigma(x^*,\omega)/\sigma_0$
0	0	0	0	0
0.125	.016	-.028	.034	.006
0.250	.063	-.039	.088	.050
0.375	.141	-.044	.170	.126
0.500	.250	-.042	.278	.236
0.750	.563	.044	.533	.577
0.875	.766	.202	.631	.833
1.000	1.000	.549	.634	1.183

TABLE VIII.- NORMAL STRESSES FOR BEAMS WITH CONCENTRATED LOAD AT MIDSPAN.

x^*/l	F_{13}	f_{13}	$\sigma(x^*,0)/\sigma_0$	$\sigma(x^*,\omega)/\sigma_0$
0	0	0	0	0
0.125	0	-.007	.005	-.002
0.250	0	-.028	.019	-.009
0.375	0	-.091	.061	-.030
0.500	0	-.267	.178	-.089
0.625	.308	.049	.275	.324
0.750	.571	.128	.486	.614
0.875	.800	.274	.617	.891
1.000	1.000	.538	.642	1.179

x^*/l	F_{24}	f_{24}	$\sigma(x^*,0)/\sigma_0$	$\sigma(x^*,\omega)/\sigma_0$
0	0	0	0	0
0.125	0	-.009	.006	-.003
0.250	0	-.033	.022	-.011
0.375	0	-.107	.071	-.036
0.500	0	-.312	.208	-.104
0.625	.379	.126	.295	.421
0.750	.653	.173	.538	.711
0.875	.853	.273	.671	.944
1.000	1.000	.444	.704	1.148

TABLE IX.- NORMAL STRESSES FOR BEAMS WITH UNIFORMLY DISTRIBUTED LOAD.

x^*/l	F_{25}	f_{25}	$\sigma(x^*,0)/\sigma_0$	$\sigma(x^*,\omega)/\sigma_0$
0	0	0	0	0
.083	.022	-.017	.034	.017
.167	.074	-.016	.085	.069
.250	.143	-.014	.162	.138
.333	.222	-.012	.250	.218
.500	.400	-.002	.401	.399
.667	.593	.028	.674	.602
.750	.690	.062	.648	.710
.833	.794	.122	.712	.834
.917	.896	.220	.749	.970
1.000	1.000	.379	.747	1.126

x^*/l	F_{26}	f_{26}	$\sigma(x^*,0)/\sigma_0$	$\sigma(x^*,\omega)/\sigma_0$
0	0	0	0	0
.083	.071	-.024	.087	.063
.167	.198	-.002	.195	.197
.250	.327	.014	.317	.331
.333	.444	.024	.428	.452
.500	.640	.035	.617	.652
.667	.790	.048	.758	.806
.750	.849	.061	.808	.869
.833	.907	.084	.851	.935
.917	.956	.123	.874	.997
1.000	1.000	.185	.877	1.062

x^*/l	F_{27}	f_{27}	$\sigma(x^*,0)/\sigma_0$	$\sigma(x^*,\omega)/\sigma_0$
0	0	0	0	0
0.125	.125	.0001	.125	.125
0.25	.250	.0007	.250	.250
0.375	.375	.001	.375	.375
0.500	.500	.004	.497	.501
0.625	.625	.017	.614	.631
0.750	.750	.051	.716	.767
0.875	.875	.132	.787	.919
1.000	1.000	.299	.800	1.100

TABLE X.- NORMAL STRESSES FOR BEAMS WITH UNIFORMLY DISTRIBUTED LOAD AND VARYING STIFFNESS PARAMETER.

x^*/l	F_{29}	f_{29}	$\sigma(x^*,0)/\sigma_0$	$\sigma(x^*,\omega)/\sigma_0$
0	0	0	0	0
0.125	.028	-.042	.043	.001
0.250	.100	-.041	.115	.074
0.375	.205	-.037	.218	.181
0.500	.333	-.031	.345	.314
0.625	.481	-.015	.486	.471
0.750	.643	.036	.630	.666
0.875	.817	.200	.743	.943
1.000	1.000	.701	.743	1.444

x^*/l	F_{30}	f_{30}	$\sigma(x^*,0)/\sigma_0$	$\sigma(x^*,\omega)/\sigma_0$
0	0	0	0	0
0.125	.049	-.053	.069	.016
0.250	.160	-.033	.172	.139
0.375	.298	-.014	.303	.289
0.500	.444	.002	.444	.446
0.625	.592	.021	.584	.605
0.750	.735	.060	.715	.773
0.875	.871	.173	.808	.980
1.000	1.000	.506	.814	1.320

x^*/l	F_{31}	f_{31}	$\sigma(x^*,0)/\sigma_0$	$\sigma(x^*,\omega)/\sigma_0$
0	0	0	0	0
0.125	.028	-.029	.057	.028
0.250	.100	-.033	.133	.100
0.375	.205	-.027	.231	.205
0.500	.333	-.012	.346	.333
0.625	.481	.016	.465	.481
0.750	.643	.069	.574	.643
0.875	.817	.165	.652	.817
1.000	1.000	.336	.664	1.000

x^*/l	F_{32}	f_{32}	$\sigma(x^*,0)/\sigma_0$	$\sigma(x^*,\omega)/\sigma_0$
0	0	0	0	0
0.125	.049	-.033	.083	.049
0.250	.160	-.025	.185	.160
0.375	.298	-.008	.306	.298
0.500	.444	.012	.433	.444
0.625	.592	.038	.553	.592
0.750	.735	.079	.656	.735
0.875	.871	.146	.726	.871
1.000	1.000	.260	.740	1.000

TABLE XI.-NORMAL STRESSES FOR BEAMS WITH UNIFORM LOAD.

x^*/l	F_{33}	f_{33}	$\sigma(x^*,0)/\sigma_0$	$\sigma(x^*,w)/\sigma_0$
0	0	0	0	0
0.125	.049	-.050	.083	.033
0.250	.160	-.042	.188	.146
0.375	.298	-.030	.317	.288
0.500	.444	-.002	.446	.444
0.625	.592	.031	.571	.602
0.750	.735	.094	.672	.766
0.875	.871	.217	.726	.943
1.000	1.000	.463	.692	1.154

x^*/l	F_{34}	f_{34}	$\sigma(x^*,0)/\sigma_0$	$\sigma(x^*,w)/\sigma_0$
0	0	0	0	0
0.125	.088	-.058	.127	.068
0.250	.256	-.024	.272	.248
0.375	.433	.010	.426	.436
0.500	.593	.037	.568	.605
0.625	.728	.065	.685	.750
0.750	.840	.107	.768	.875
0.875	.929	.188	.804	.992
1.000	1.000	.348	.768	1.116

TABLE XII.- NORMAL STRESSES FOR BEAMS WITH NO SPANWISE VARIATION OF EXTREME FIBER STRESS.

x^*/l	F_{35}	f_{35}	$\sigma(x^*,0)/\sigma_0$	$\sigma(x^*,w)/\sigma_0$
0	1	0	1	1
0.125	1	.011	.993	1.004
0.250	1	.013	.991	1.004
0.375	1	.015	.990	1.005
0.500	1	.018	.989	1.006
0.625	1	.026	.983	1.009
0.750	1	.044	.971	1.015
0.875	1	.083	.944	1.028
1.000	1	.164	.891	1.055

x^*/l	F_{36}	f_{36}	$\sigma(x^*,0)/\sigma_0$	$\sigma(x^*,w)/\sigma_0$
0	1	.0501	.967	1.017
0.125	1	.0501	.967	1.017
0.250	1	.0502	.967	1.017
0.375	1	.0510	.966	1.017
0.500	1	.0550	.963	1.018
0.625	1	.0680	.955	1.023
0.750	1	.1010	.932	1.034
0.875	1	.1740	.884	1.056
1.000	1	.3150	.790	1.105

TABLE XIII.- NORMAL STRESSES FOR BEAMS WITH LINEAR AND QUADRATIC THICKNESS TAPER.

x^*/l	F_{37}	f_{37}	$\sigma(x^*,0)/\sigma_0$	$\sigma(x^*,w)/\sigma_0$
0	0	0	0	0
0.125	.125	.003	.123	.126
0.250	.250	.008	.244	.253
0.375	.375	.017	.363	.381
0.500	.500	.035	.477	.512
0.625	.625	.071	.578	.649
0.750	.750	.144	.654	.798
0.875	.875	.324	.659	.983
1.000	1.000	.609	.594	1.203

x^*/l	F_{38}	f_{38}	$\sigma(x^*,0)/\sigma_0$	$\sigma(x^*,w)/\sigma_0$
0	1	2.070	-.380	1.690
0.125	1	1.258	.161	1.419
0.250	1	.799	.468	1.266
0.375	1	.535	.643	1.178
0.500	1	.389	.741	1.130
0.625	1	.322	.785	1.107
0.750	1	.298	.801	1.099
0.875	1	.377	.749	1.126
1.000	1	.662	.559	1.221

x^*/l	F_{39}	f_{39}	$\sigma(x^*,0)/\sigma_0$	$\sigma(x^*,w)/\sigma_0$
0	0	0	0	0
0.125	.125	.007	.121	.127
0.250	.250	.016	.239	.255
0.375	.375	.032	.354	.388
0.500	.500	.060	.460	.520
0.625	.625	.115	.549	.663
0.750	.750	.220	.603	.823
0.875	.875	.427	.590	1.017
1.000	1.000	.837	.442	1.279

TABLE XIV.- EFFECTIVE SHEET WIDTH AT THE FIXED END OF A BEAM WITH SHEET-THICKNESS TAPER.

$\sqrt{\frac{27E}{32G}}\frac{w}{l}$	K	$f_{31}(1)$ [m = 2]	$\left(\frac{w_{eff}}{w}\right)_R$	$\sqrt{\frac{27E}{32G}}\frac{w}{L}$
0	---	0	1	0
0.075	24.922	.163	.897	0.15
0.150	12.461	.319	.809	0.30
0.225	8.307	.467	.729	0.45
0.300	6.231	.609	.662	0.60
0.375	4.984	.742	.604	0.75
0.450	4.154	.867	.553	0.90

$\sqrt{\frac{27E}{32G}}\frac{w}{l}$	K	$f_{38}(1)$ [m = 2]	$\left(\frac{w_{eff}}{w}\right)_R$	$\sqrt{\frac{27E}{32G}}\frac{w}{L}$
0	---	0	1	0
0.075	24.922	.166	.895	0.15
0.150	12.461	.332	.801	0.30
0.225	8.307	.498	.715	0.45
0.300	6.231	.662	.638	0.60
0.375	4.984	.806	.576	0.75
0.450	4.154	.948	.519	0.90

$\sqrt{\frac{27E}{32G}}\frac{w}{l}$	K	$f_{39}(1)$ [m = 2]	$\left(\frac{w_{eff}}{w}\right)_R$	$\sqrt{\frac{27E}{32G}}\frac{w}{L}$
0	---	0	1	0
0.075	24.922	.239	.852	0.225
0.150	12.461	.458	.735	0.450
0.225	8.307	.658	.640	0.675
0.300	6.231	.837	.564	0.900

TABLE XV.- EFFECTIVE WIDTH AT THE SECTION OF MAXIMUM BENDING MOMENT FOR BEAMS ON TWO SINGLE SUPPORTS.

$\sqrt{\frac{27E}{32G}}\frac{w}{l}$	$(w_{eff}/w)_{m=m_{max.}}$ $m=2$			
	Case 40	Case 41	Case 42a	Case 42b
0	1	1	1	1
0.15	.979	.982	.895	.863
0.30	.921	.932	.801	.743
0.45	.841	.856	.715	.642
0.60	.755	.771	.638	.560
0.75	.672	.687	.571	.494
0.90	.599	.612	.513	.442

TABLE XVI.- NORMAL STRESSES FOR A BEAM WITH BOTH ENDS BUILT IN.

x/l	F_{43}	$\sigma(x,0)/\sigma_0$	$\sigma(x,w)/\sigma_0$
0	-.50	-.40	-.55
0.2	-.44	-.34	-.49
0.4	-.26	-.17	-.31
0.6	.04	.09	.02
0.8	.46	.38	.60
0.9	.71	.46	.84
1.0	1.00	.44	1.28

x/l	F_{44}	$\sigma(x,0)/\sigma_0$	$\sigma(x,w)/\sigma_0$
0	0	0	0
0.2	.192	.192	.192
0.4	.384	.382	.385
0.6	.575	.559	.583
0.8	.766	.705	.796
1.0	.957	.745	1.062

x/l	$(F_{45})_{el.}$	F_{45}	$\sigma(x,0)/\sigma_0$	$\sigma(x,w)/\sigma_0$
0	0	0	0	0
0.2	-.28	-.294	-.196	-.343
0.4	-.50	-.529	-.347	-.620
0.6	-.36	-.403	-.197	-.506
0.8	.08	.024	.053	.010
0.9	.47	.405	.135	.535
1.0	1.00	.928	.063	1.360

TABLE XVII.- RELATIVE DECREASE IN EDGE MOMENT-$\sigma_1/(\sigma_b)_{elem}$ DUE TO SHEAR LAG.

	$-\sigma_1/(\sigma_b)_{elem.}$			
	Case 44			Case 45
w/l	m=1	m=2	m=2.5	m=2
0	0	0	0	0
0.2	.09	.04	.02	.07
0.4	.27	.13	.06	.24
0.6	.43	.21	.10	.42
0.8	.55	.27	.14	.57
1.0	.64	.32	.17	.66

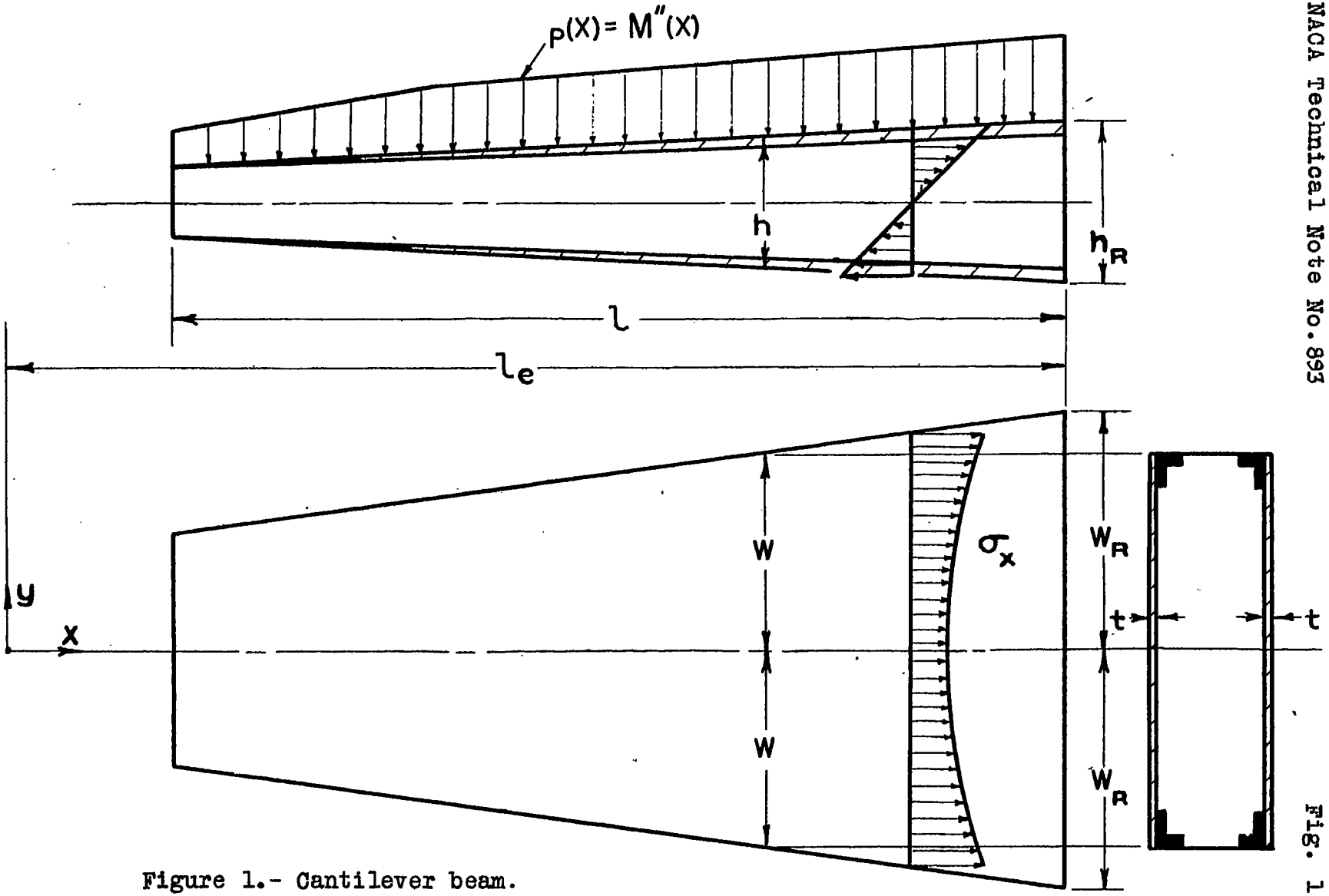

Figure 1.- Cantilever beam.

Fig. 1

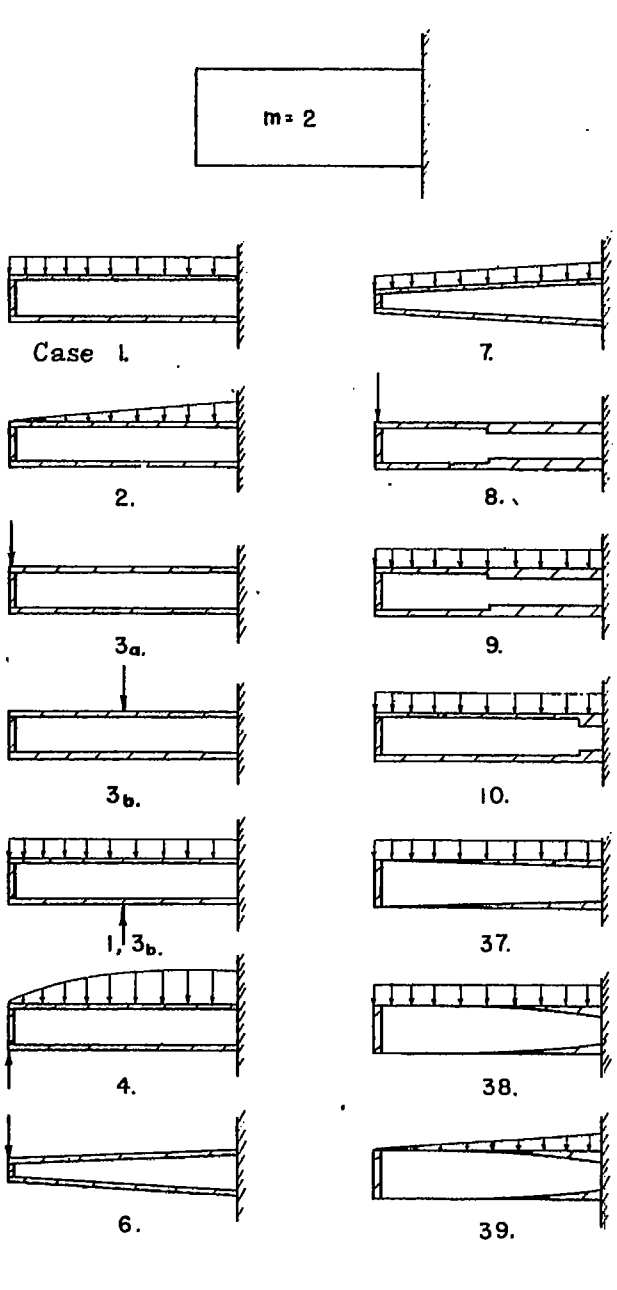

(Continued on next page)

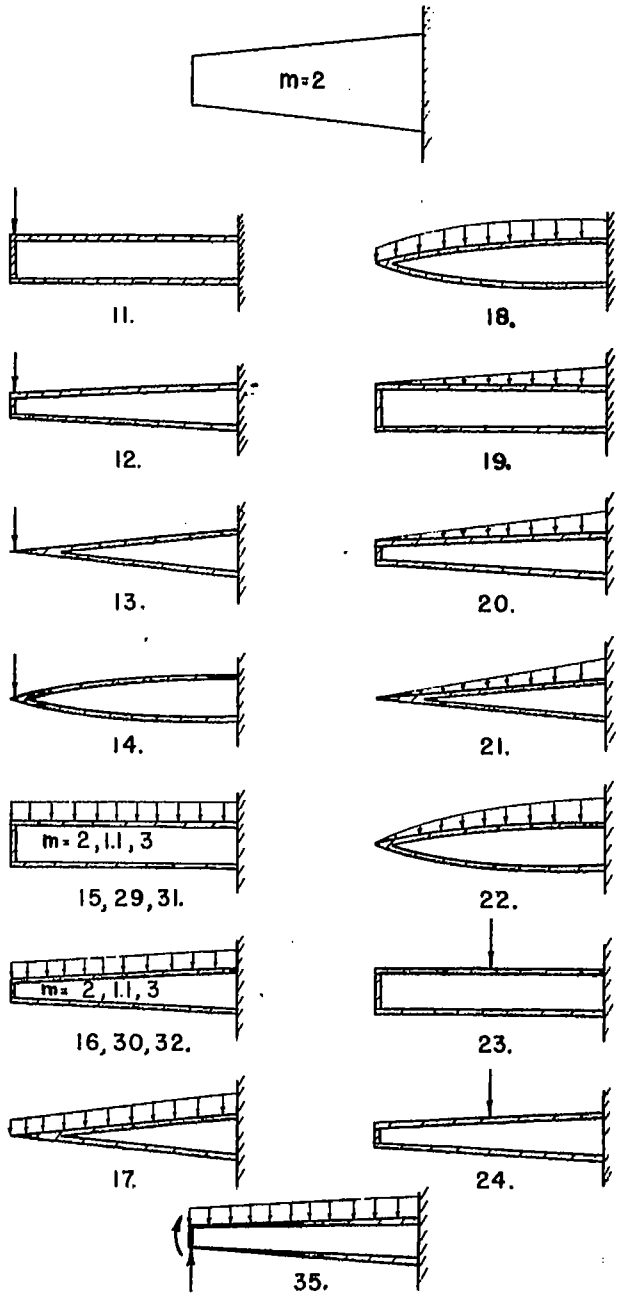

Figure 2a

Fig. 2a

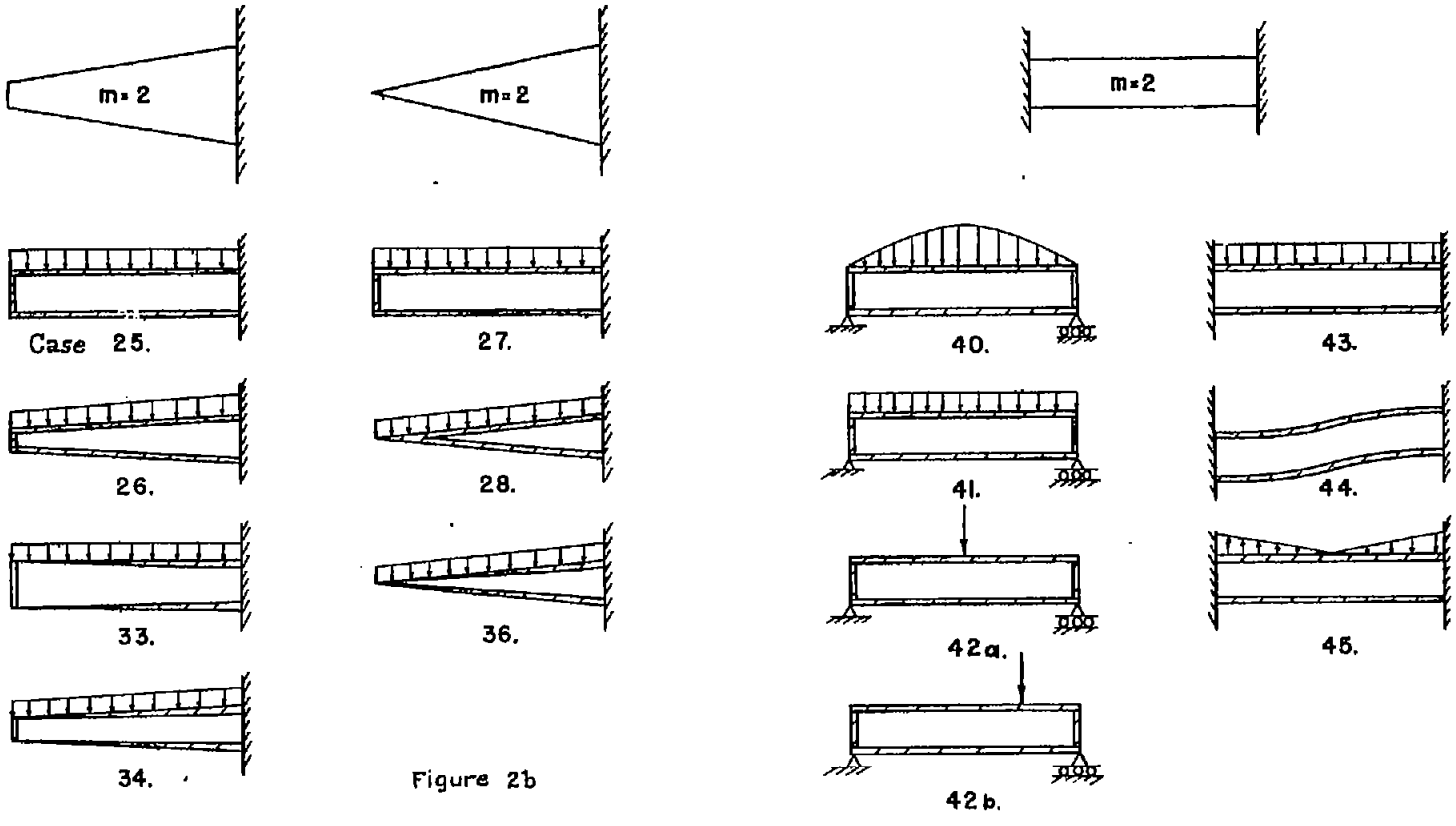

Figure 2b

Figure 2(a,b).- Diagrammatic sketches of beams analyzed, showing assumed loading conditions and laws of taper.

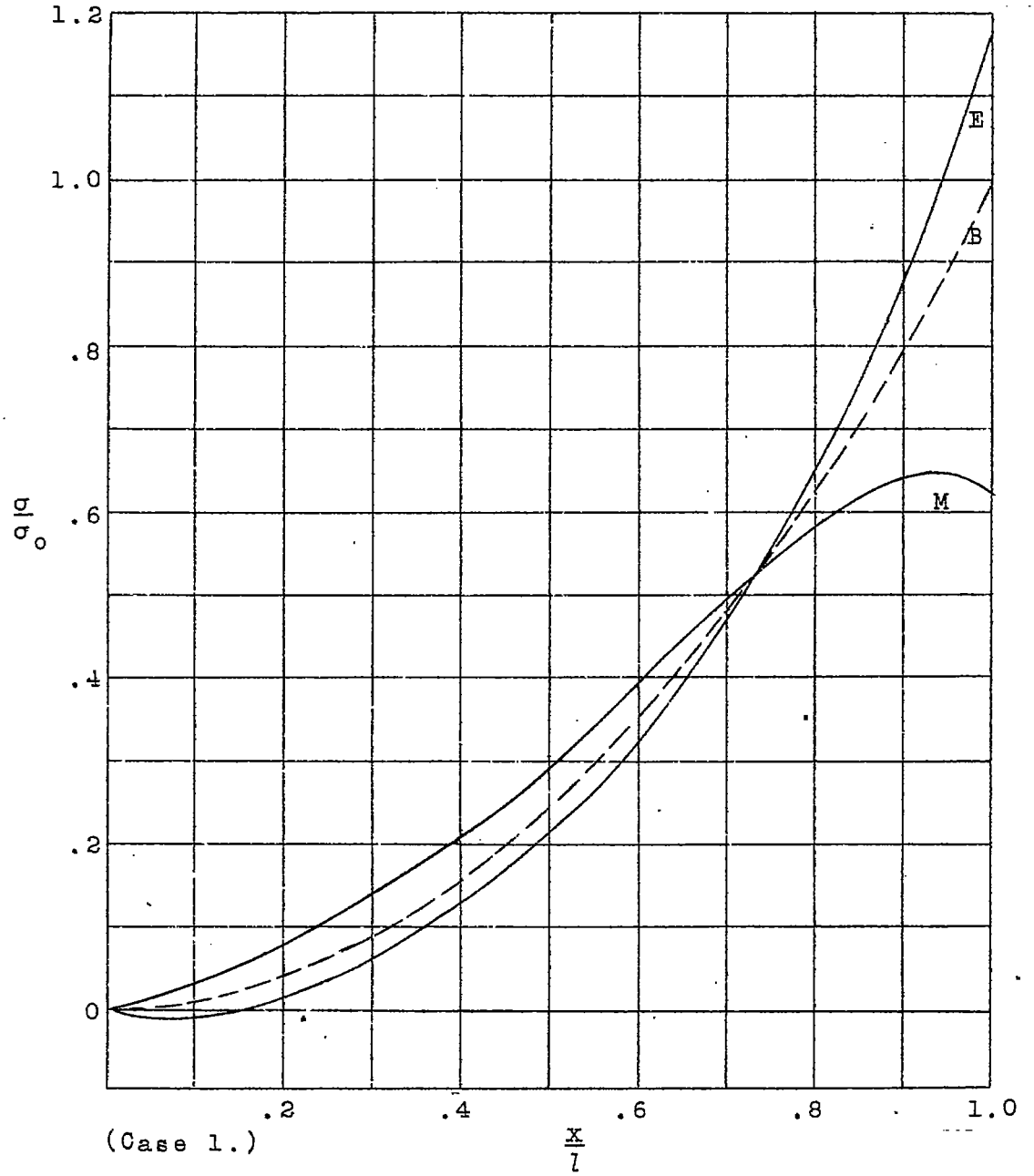

Figure 3 (a to d).- Stress diagrams showing effect of load distribution for a beam of uniform cross section. $\left[(l/w)(6\ G/E)^{1/2} = 7.5;\ m = 2.\right]$

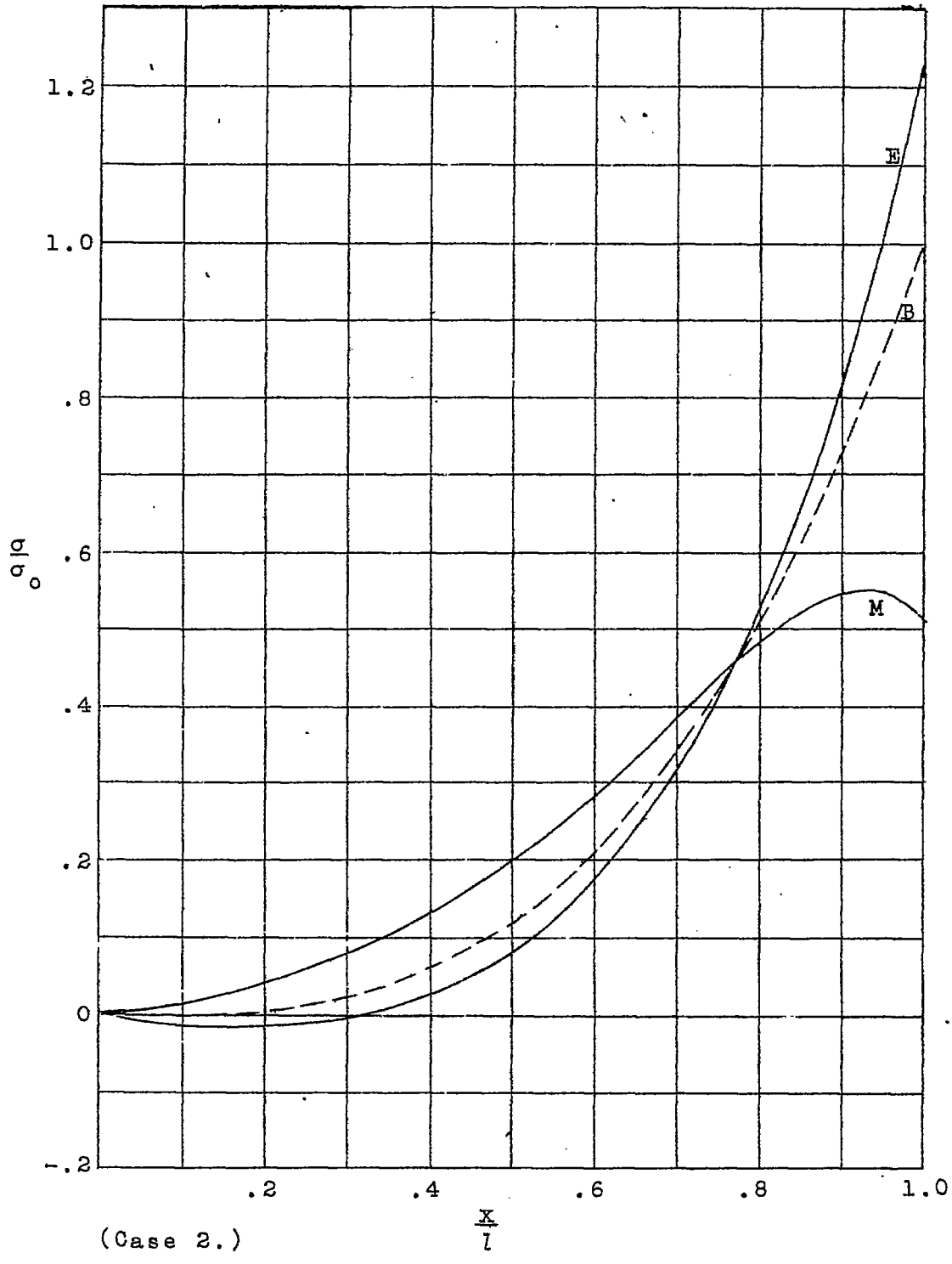

Figure 3.- Continued.

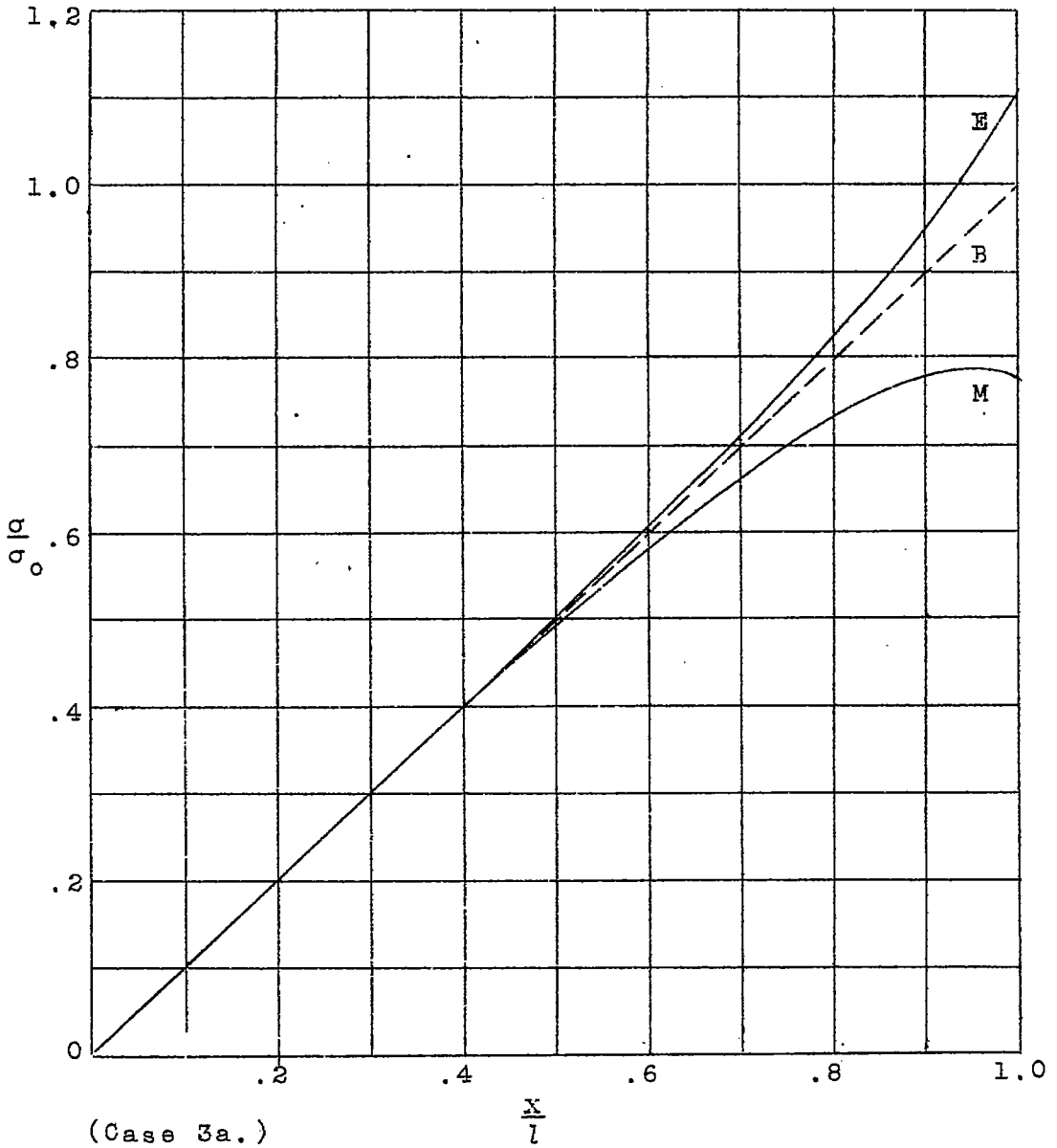

Figure 3.- Continued.

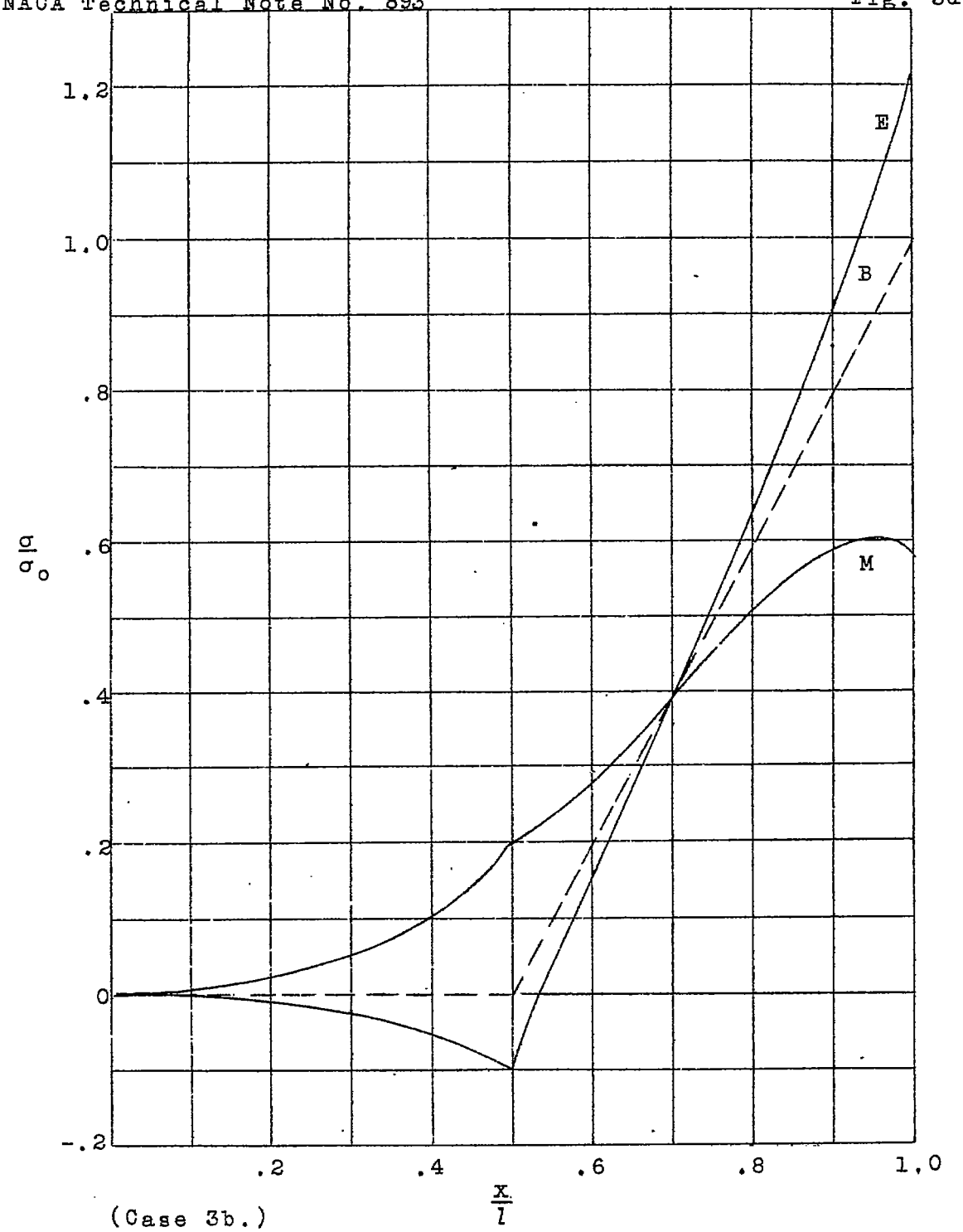

(Case 3b.)

Figure 3.- Concluded.

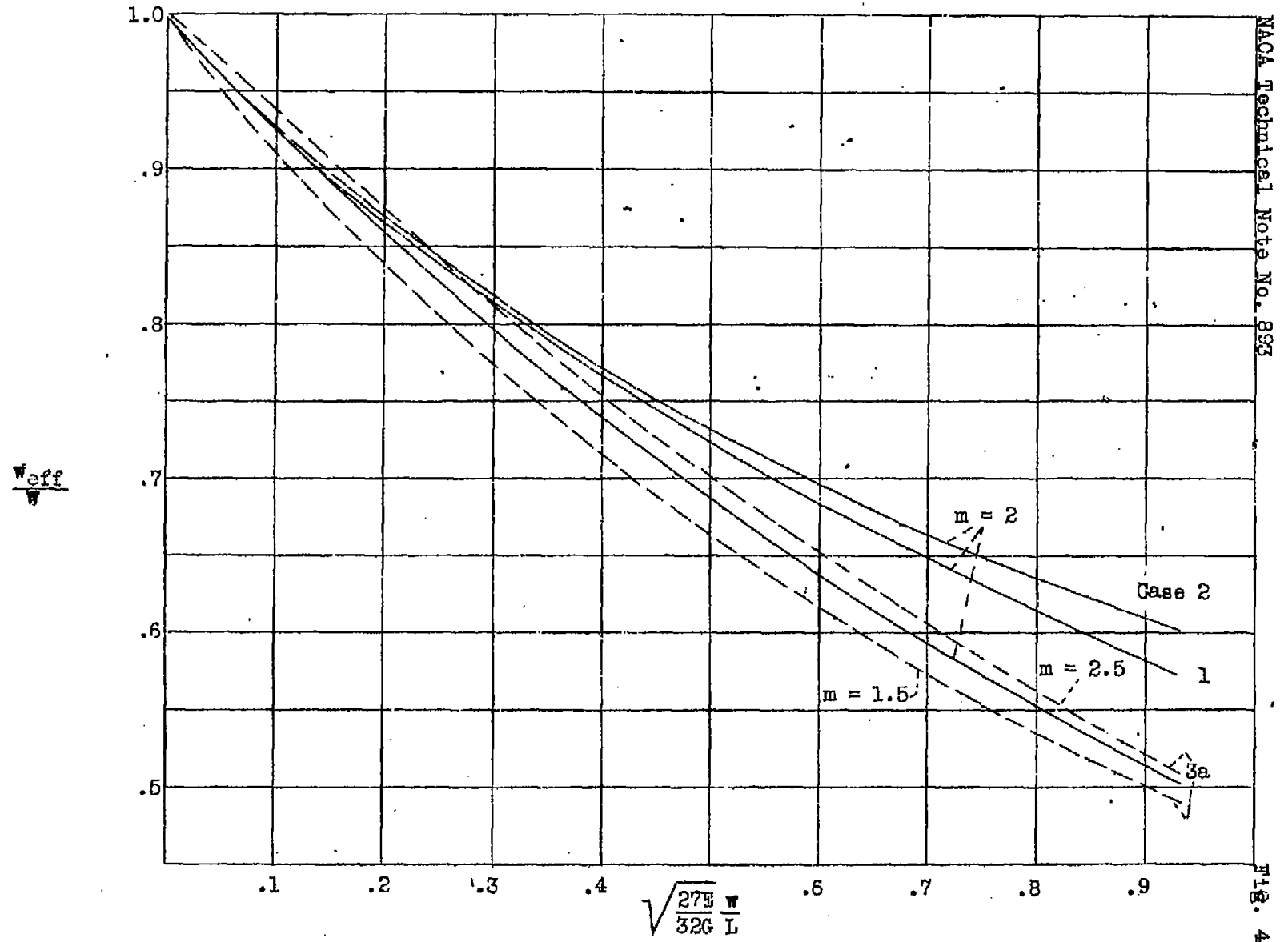

Fig. 4

Figure 4.- Effective width at root sections of beams with uniform cross section for different load conditions. (w/L is ratio of half width of beam to distance of center of gravity of load curve from root section)

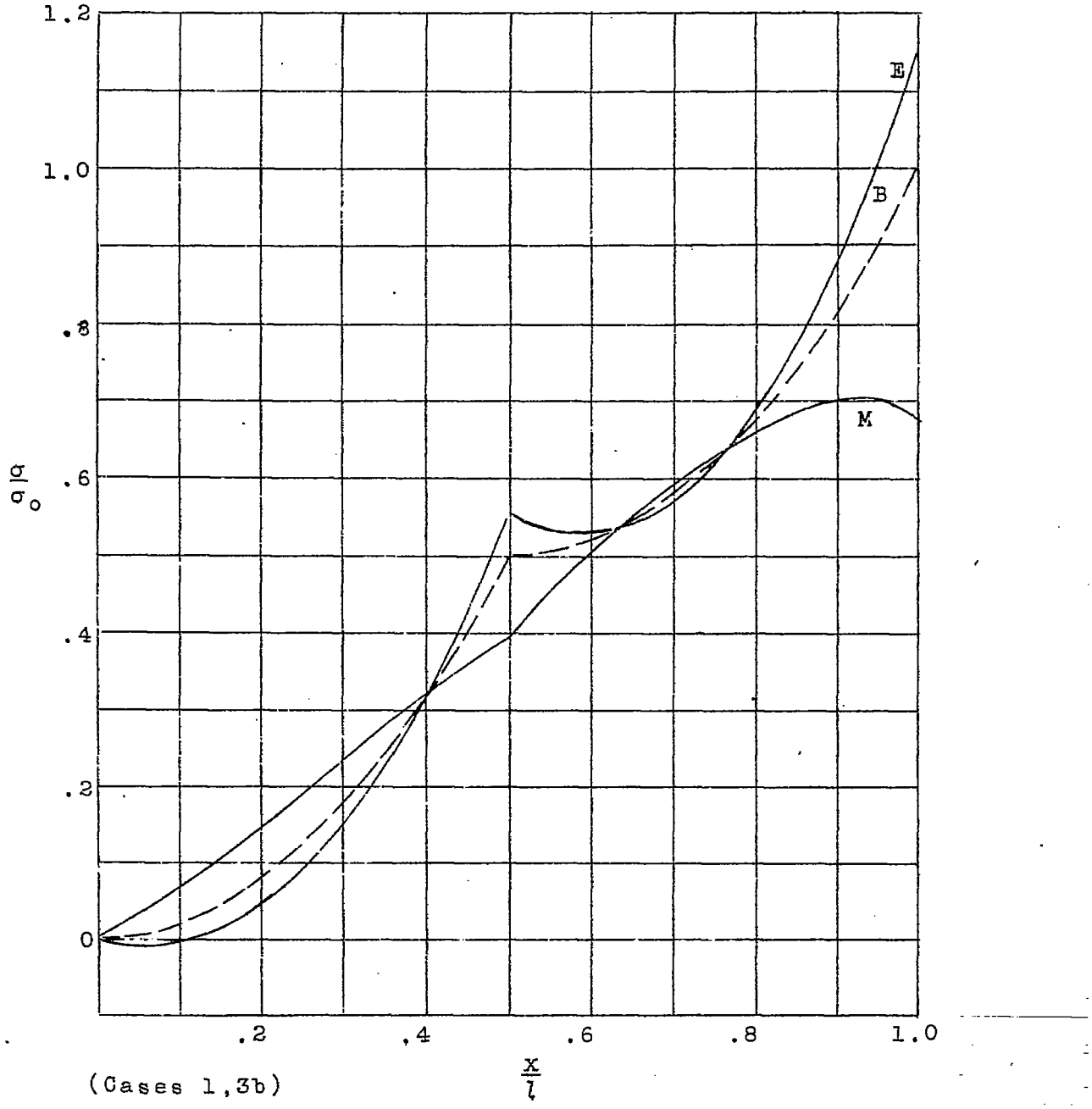

Figure 5.- Stress diagram for a beam with uniform cross section carrying a combination of uniformly distributed load and concentrated load at midspan. $[(l/w)(6\ G/E)^{1/3}=7.5;\ m = 2.]$

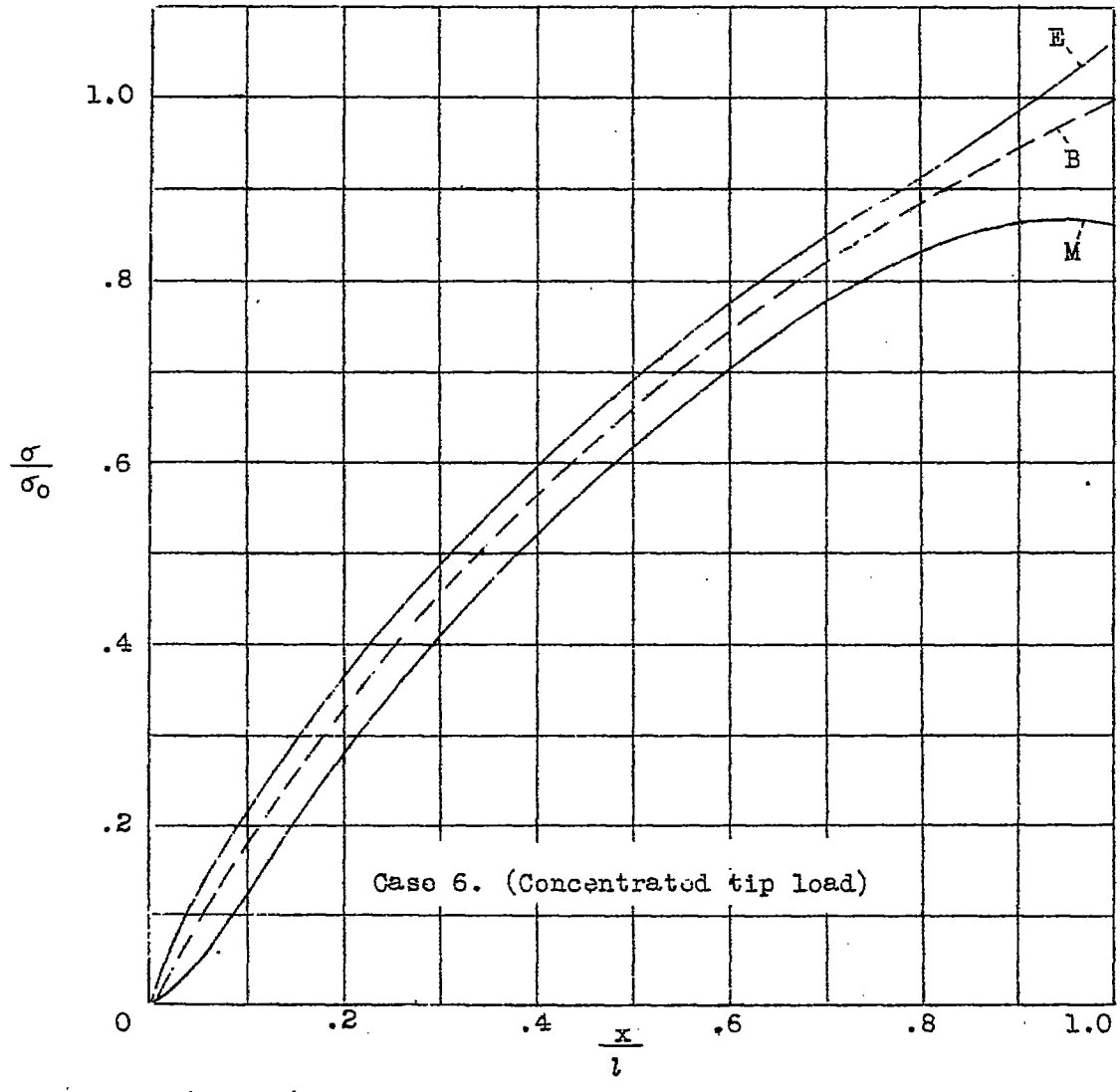

Figure 6(a to b).—Stress diagrams showing effect of taper in height of beam. $\left[(l/w)(6G/E)^{1/2}=7.5;\ m = 2\right]$

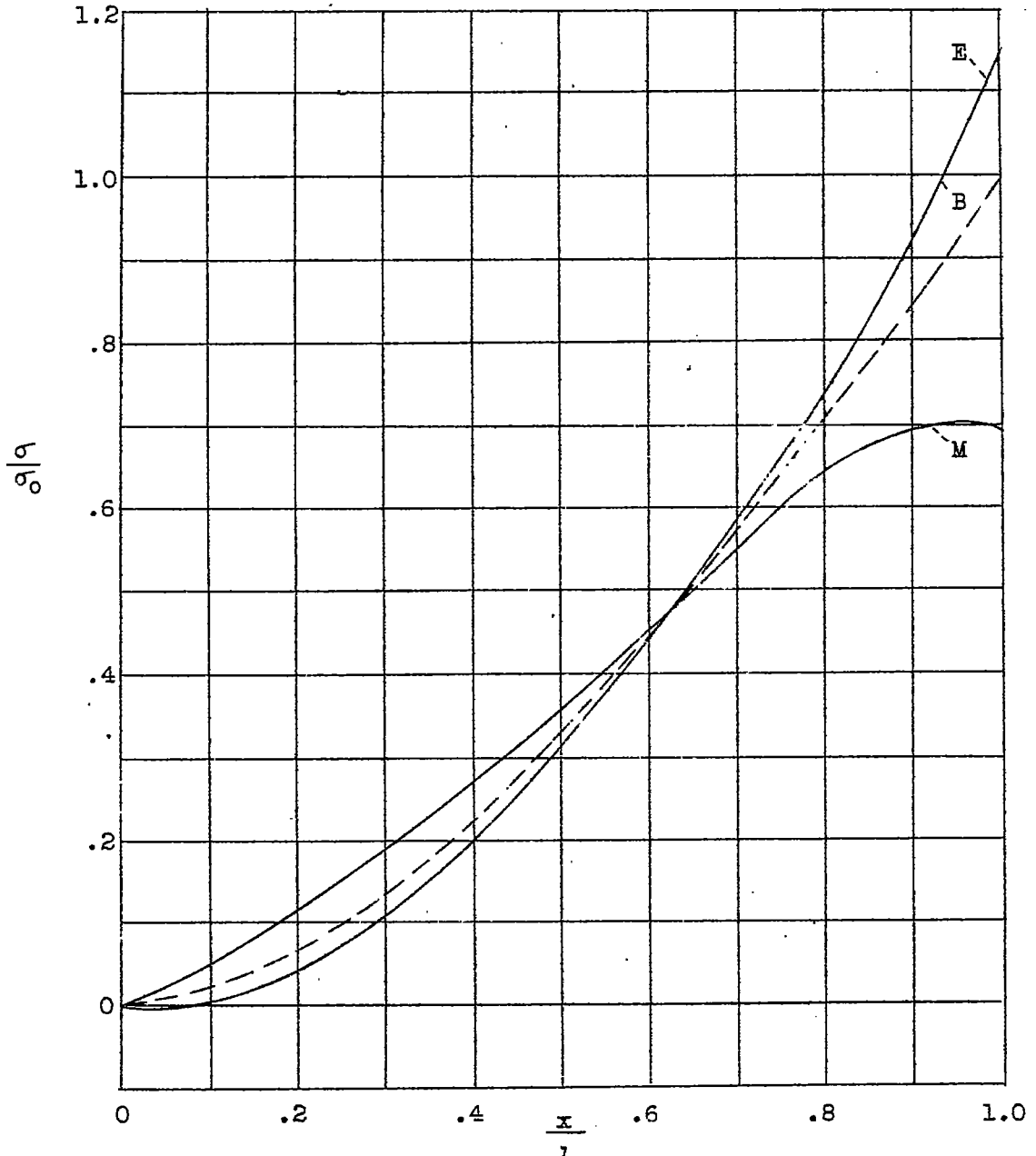

Case 7. (Uniformly distributed load)

Figure 6.5 Concluded.

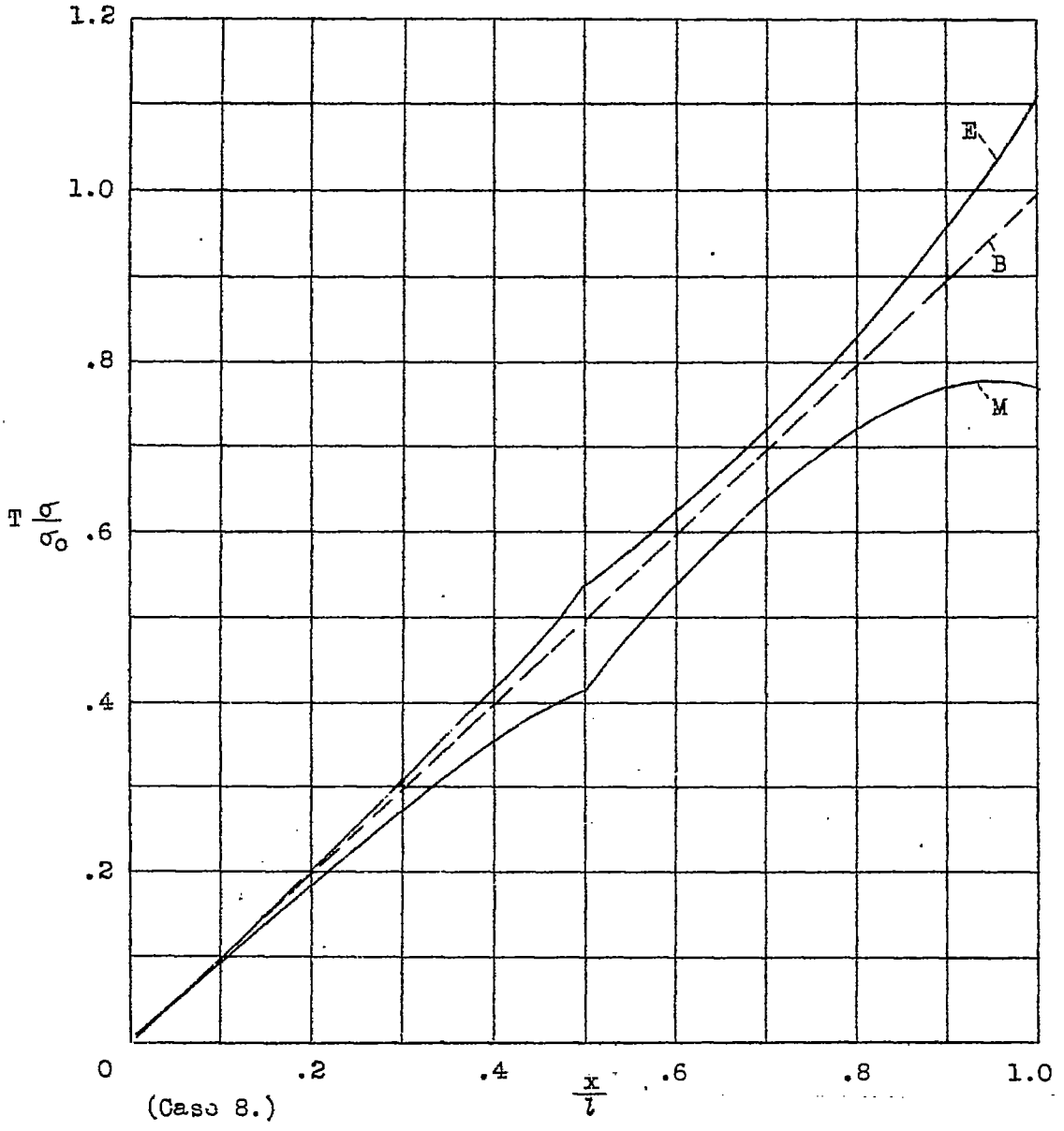

Figure 7(a to c).-- Stress diagrams showing effect of discontinuous cover sheet thickness taper. $\left[(l/w)(6G/E)^{1/2}a = 7.5;\ m = 2;\ t_2/t_1 = 2\right]$

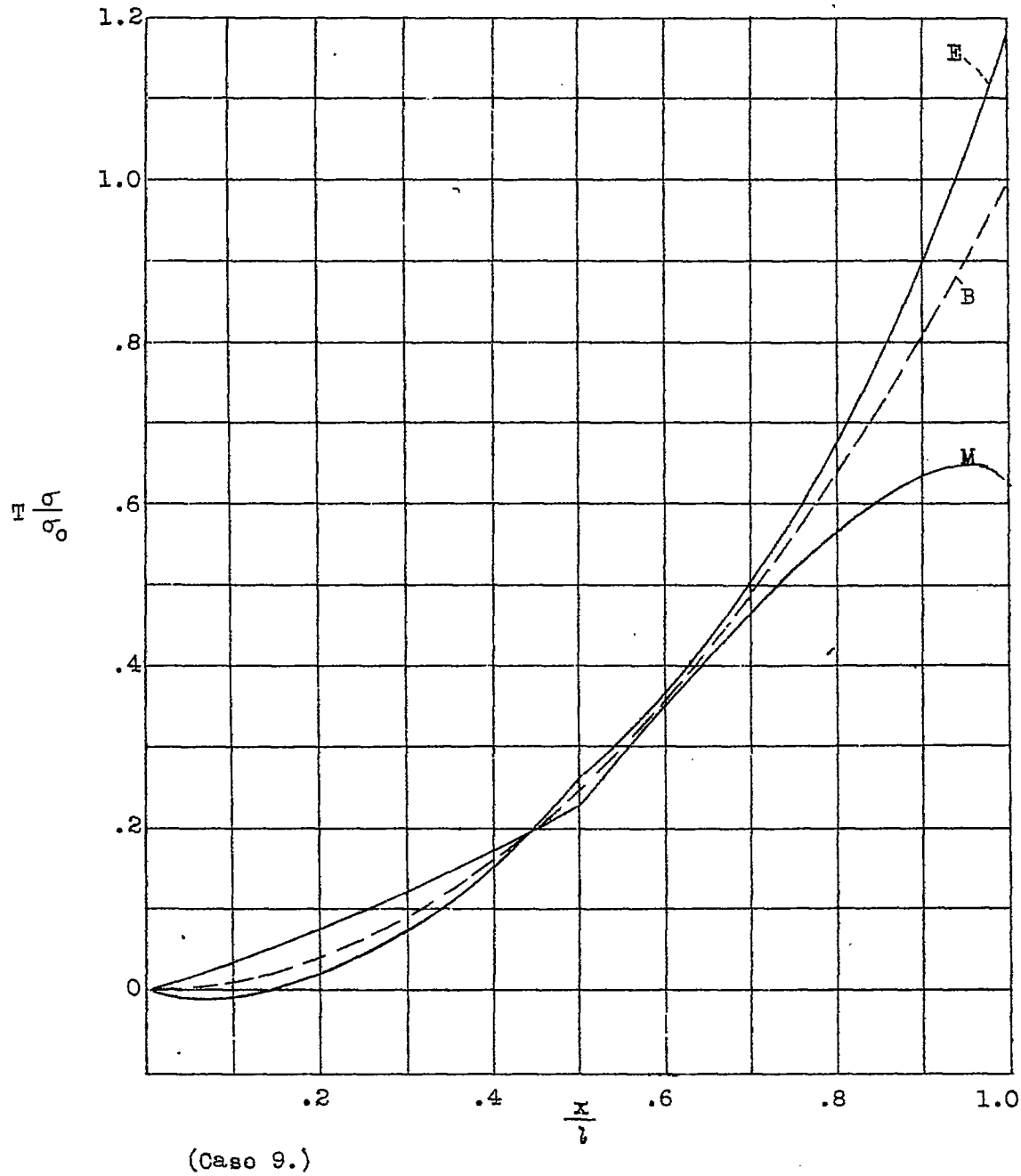

(Case 9.)

Figure 7.- Continued.

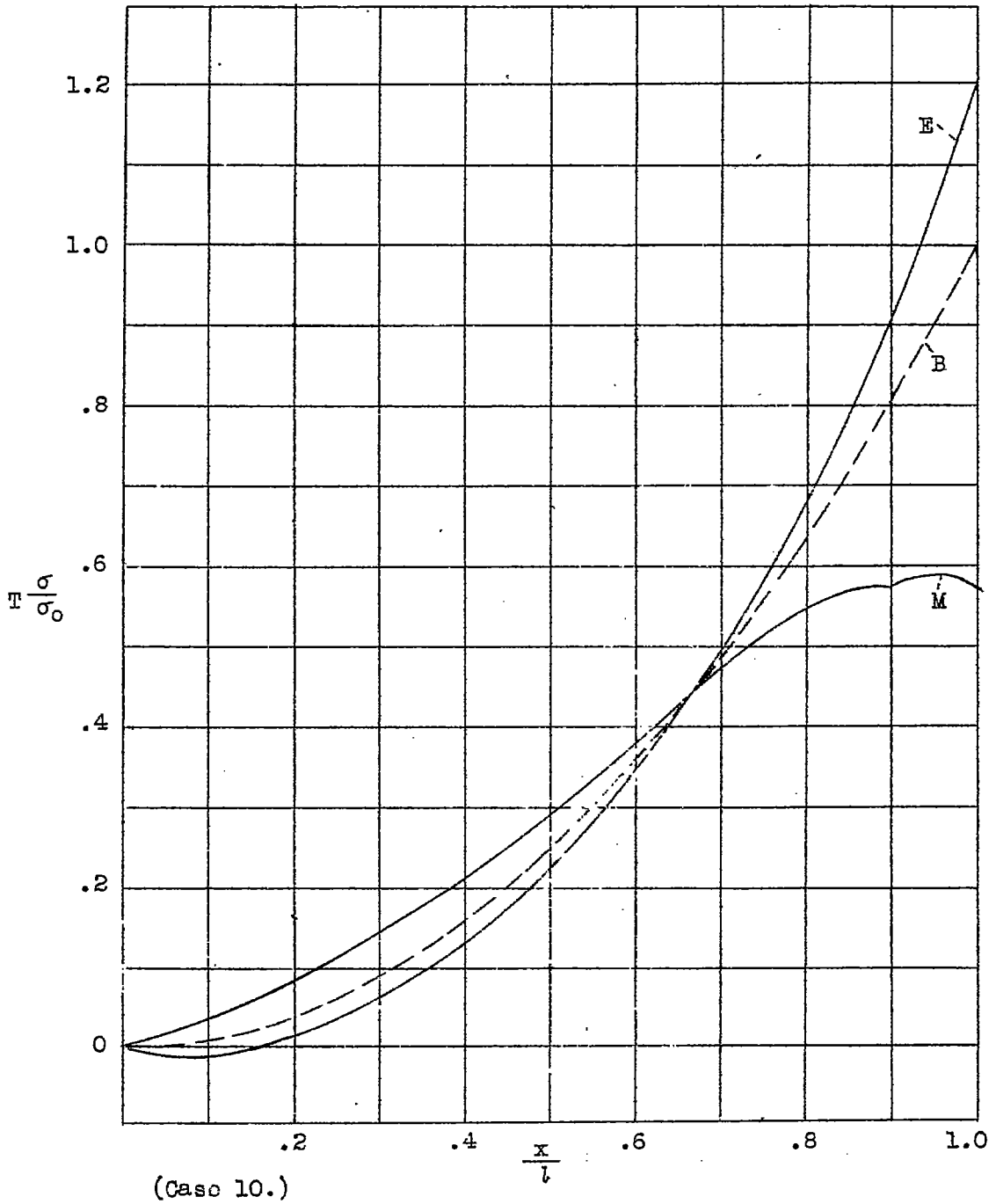

(Case 10.)

Figure 7.- Concluded.

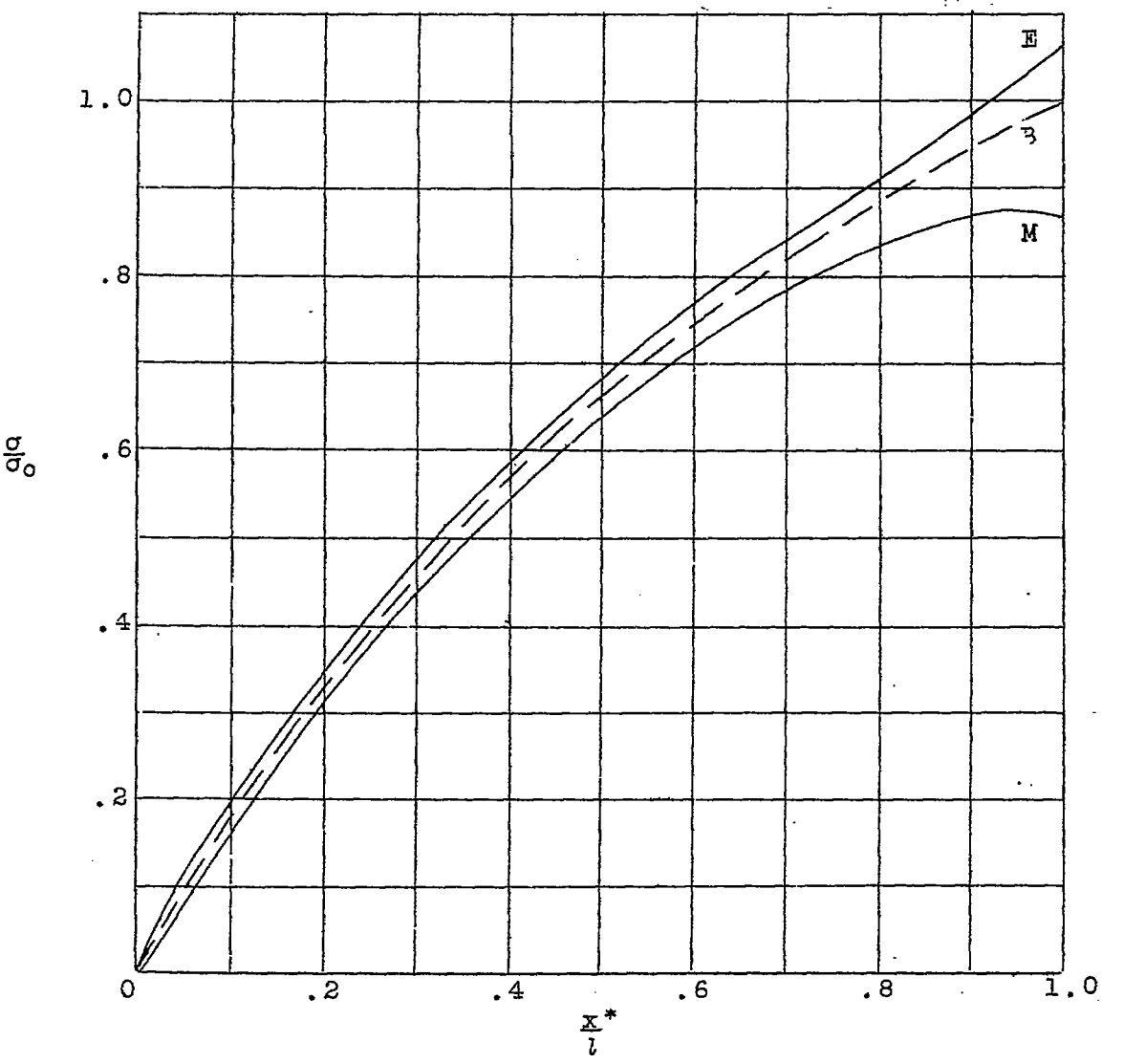

Cases 11 and 17.

Figure 8(a to c).- Stress diagrams showing effect of taper in beam width and beam height. (Concentrated tip load.) $(l/w_R)(6G/E)^{1/2}=7.5$; $w_T/w_R = 0.5$; $m = 2$

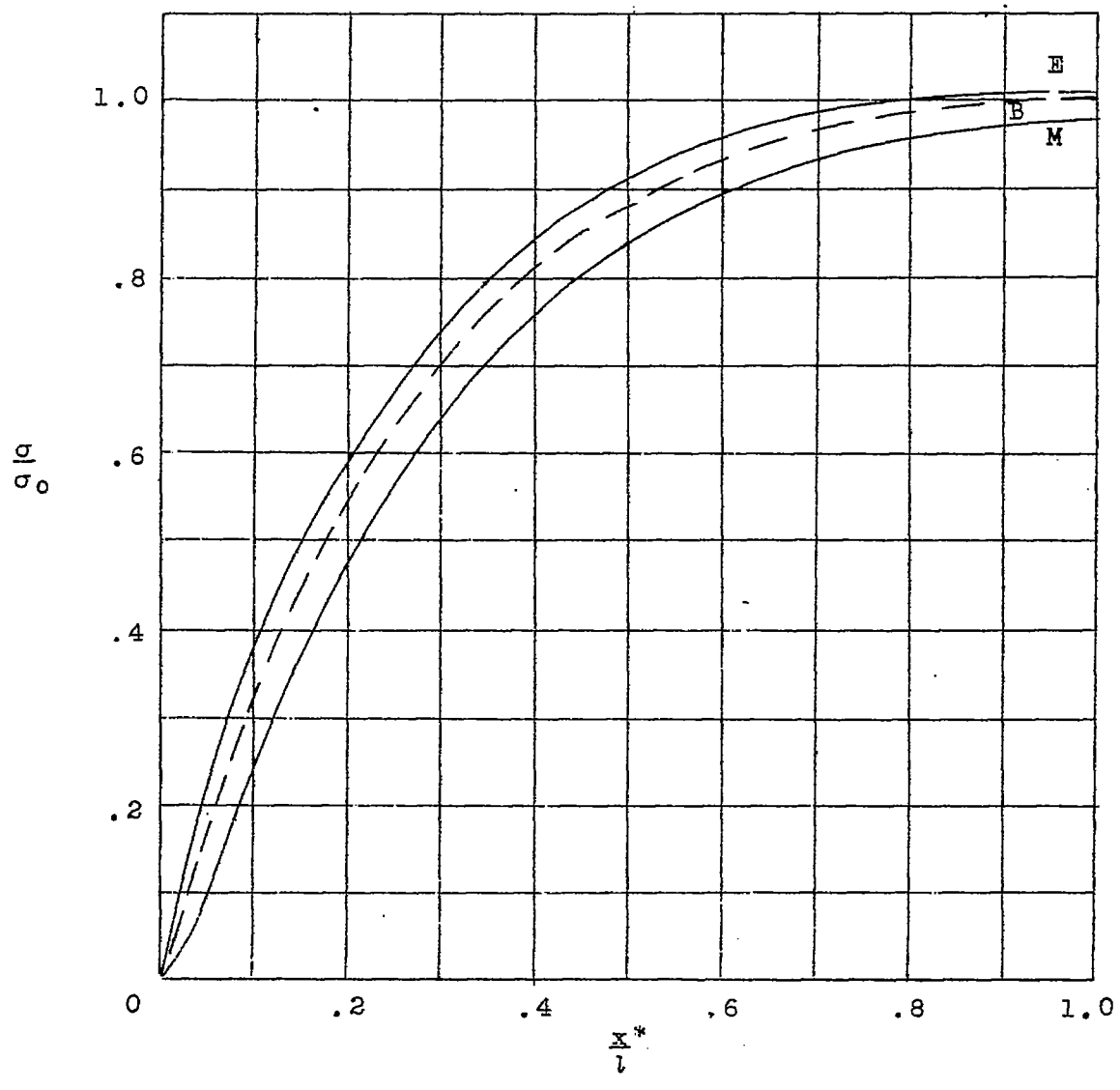

Case 12.

Figure 8.- Continued.

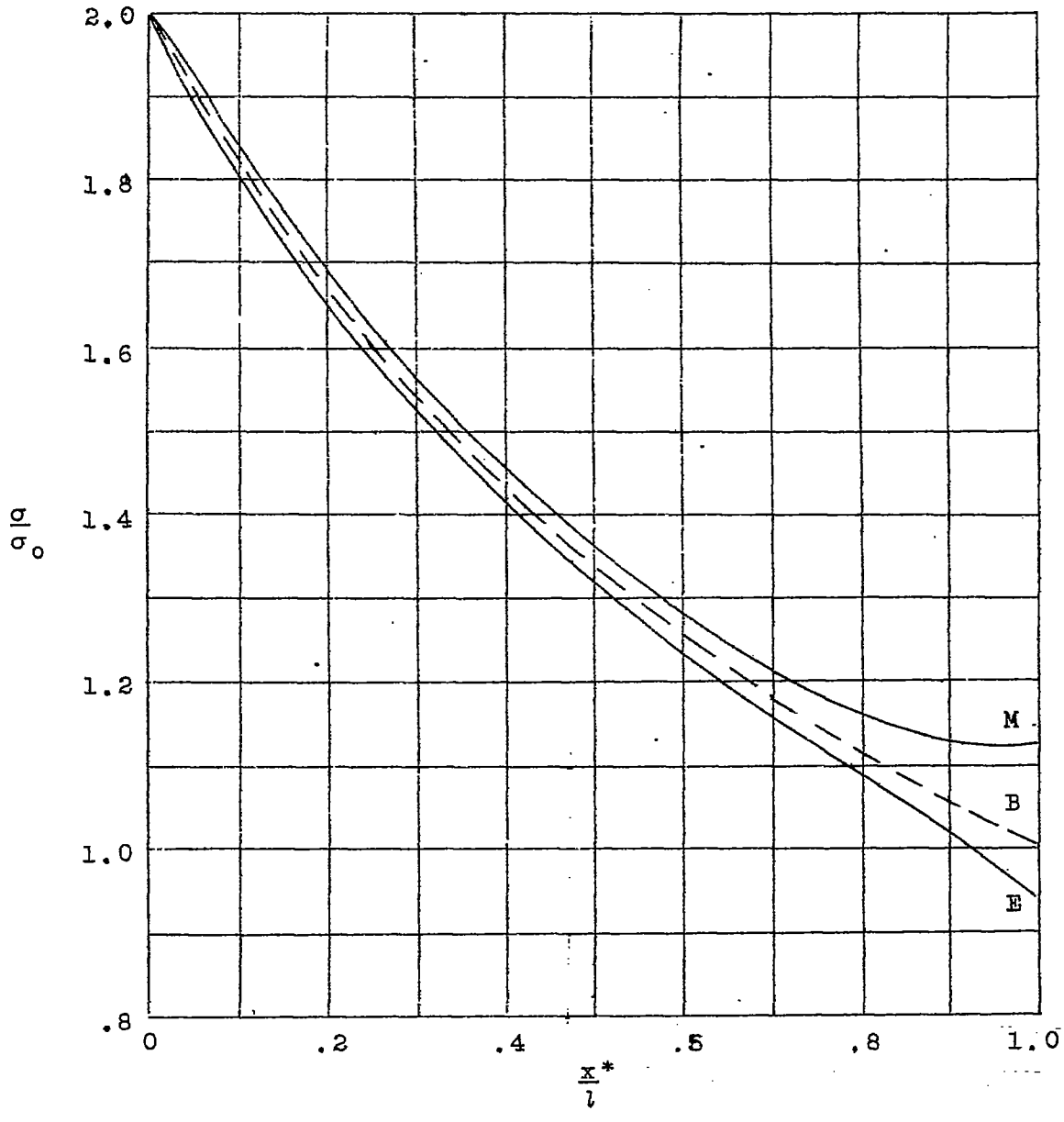

Case 13.

Figure 8.- Concluded.

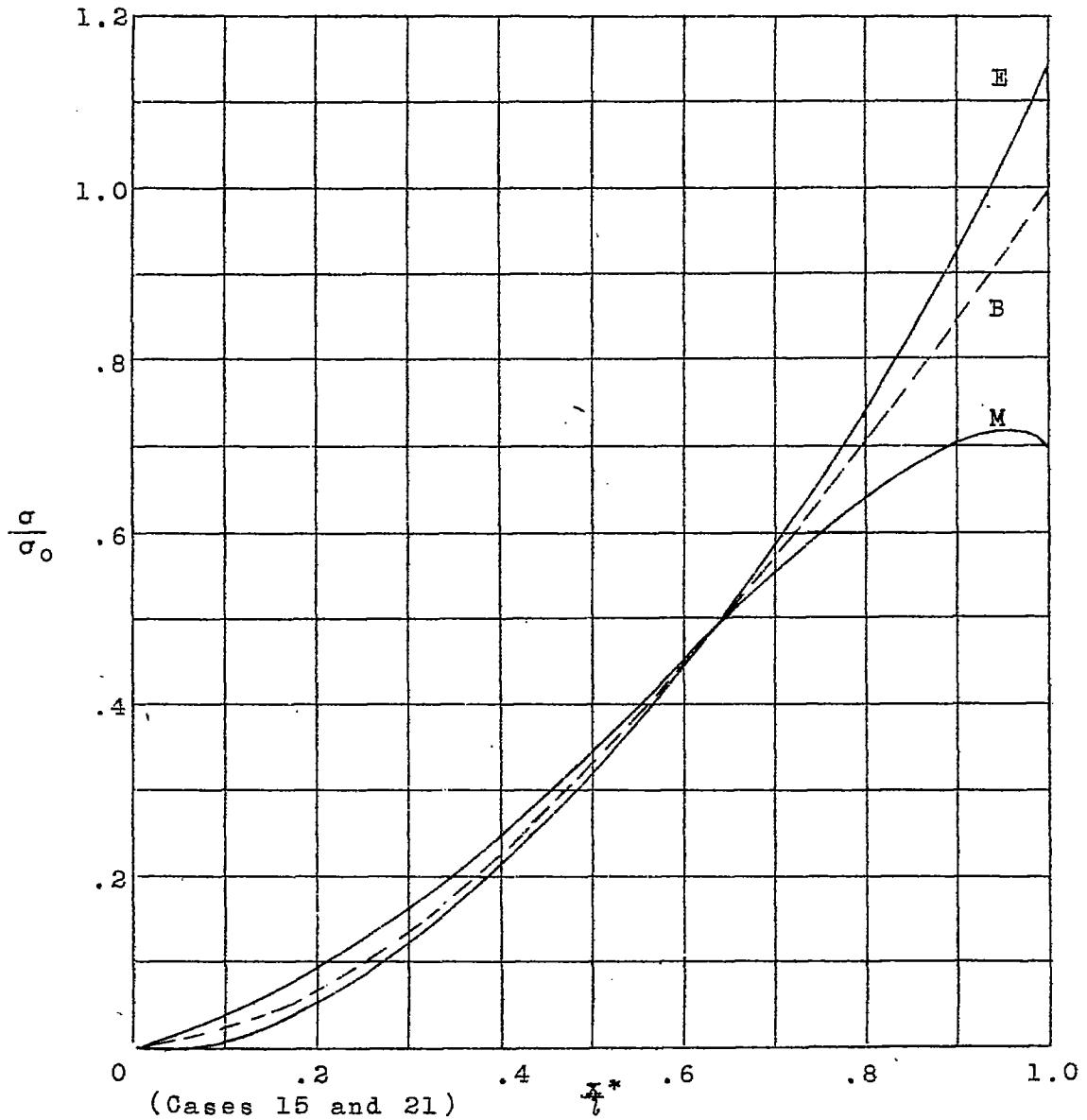

Figure 9(a to c). - Stress diagrams showing effect of taper in beam width and beam height. (Uniformly distributed load). $[(l/w_R)(6G/E)^{1/2} = 7.5;\ w_T/w_R = 0.5;\ m = 2]$

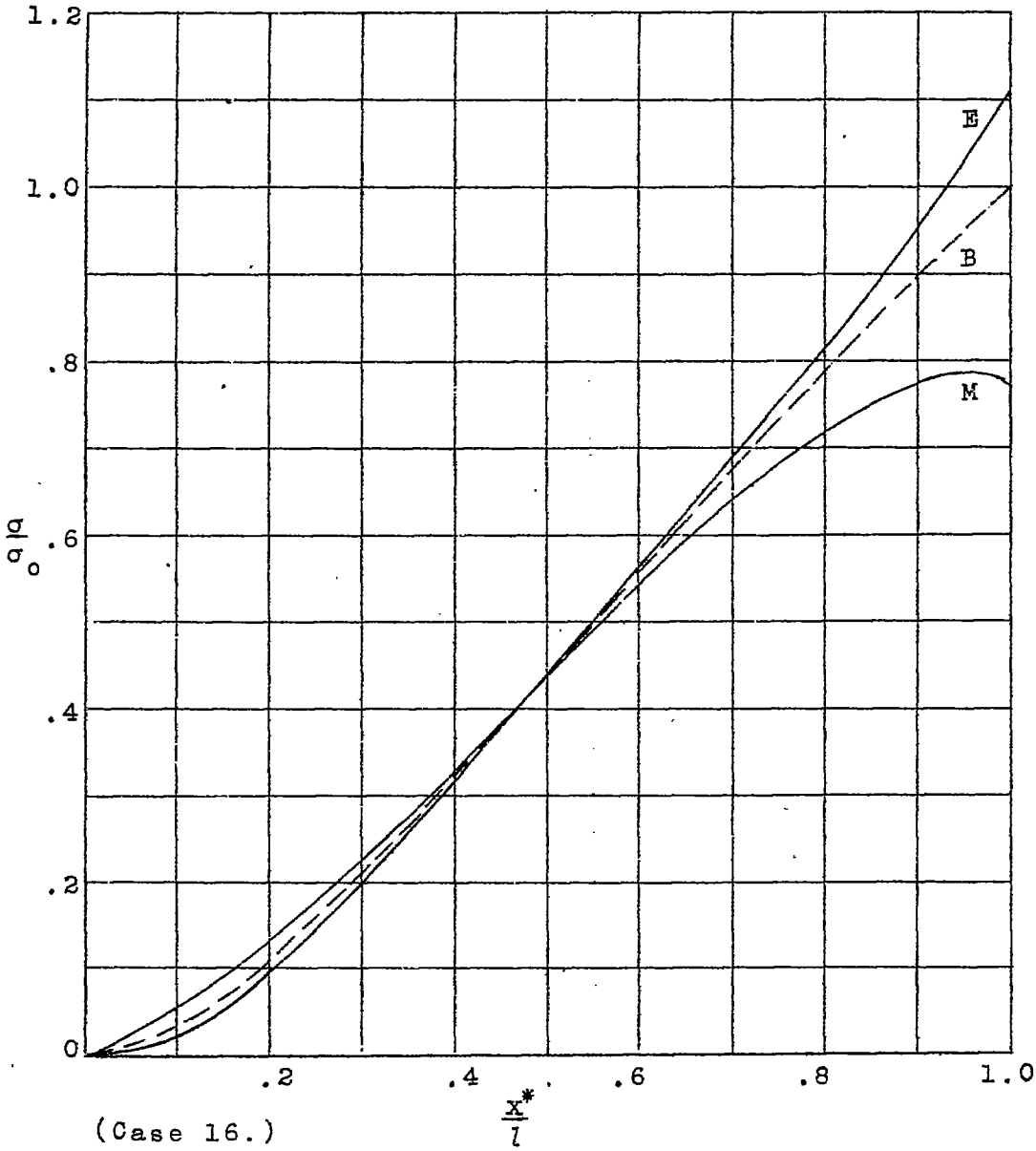

Figure 9.- Continued.

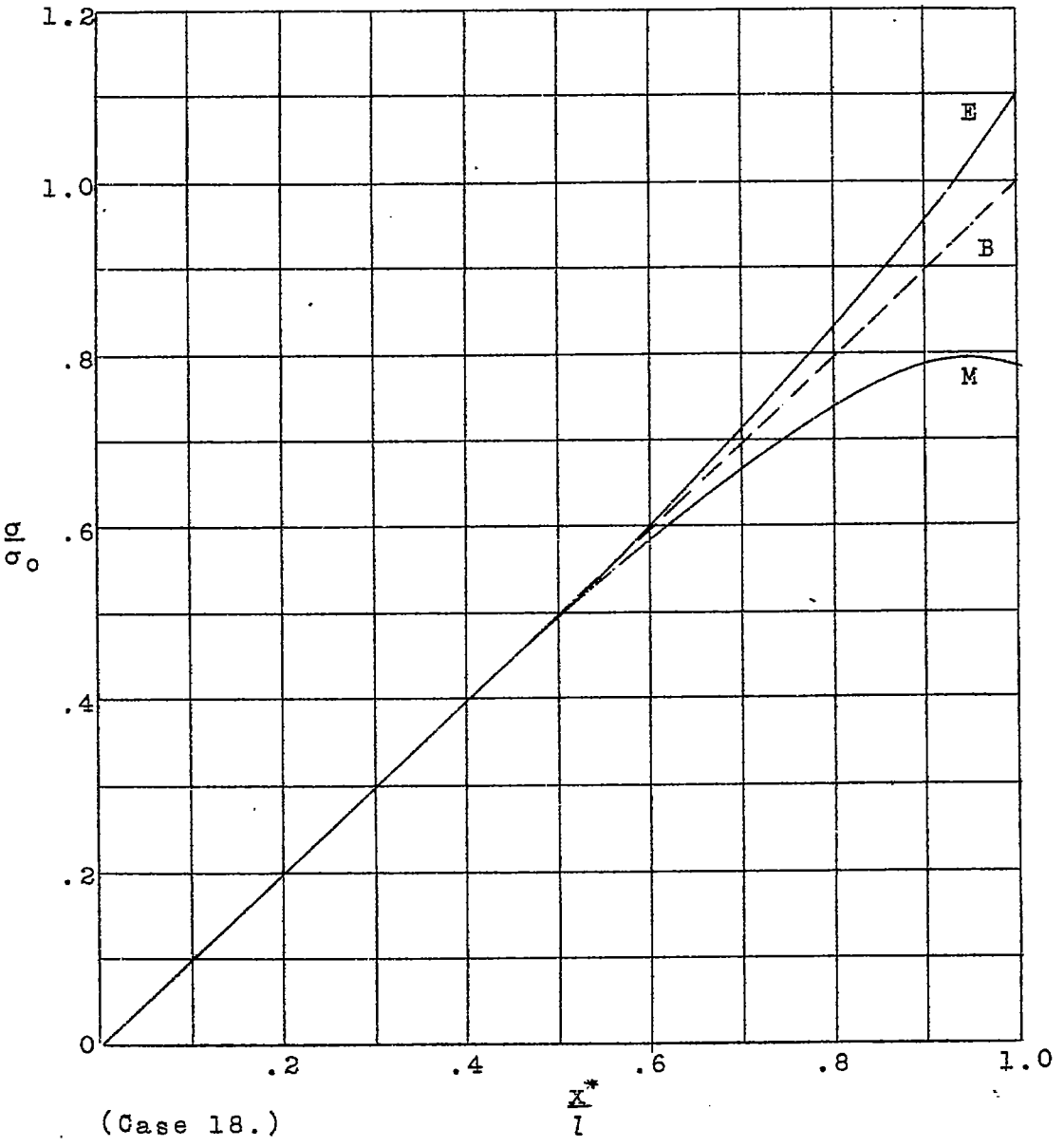

(Case 18.)

Figure 9.- Concluded.

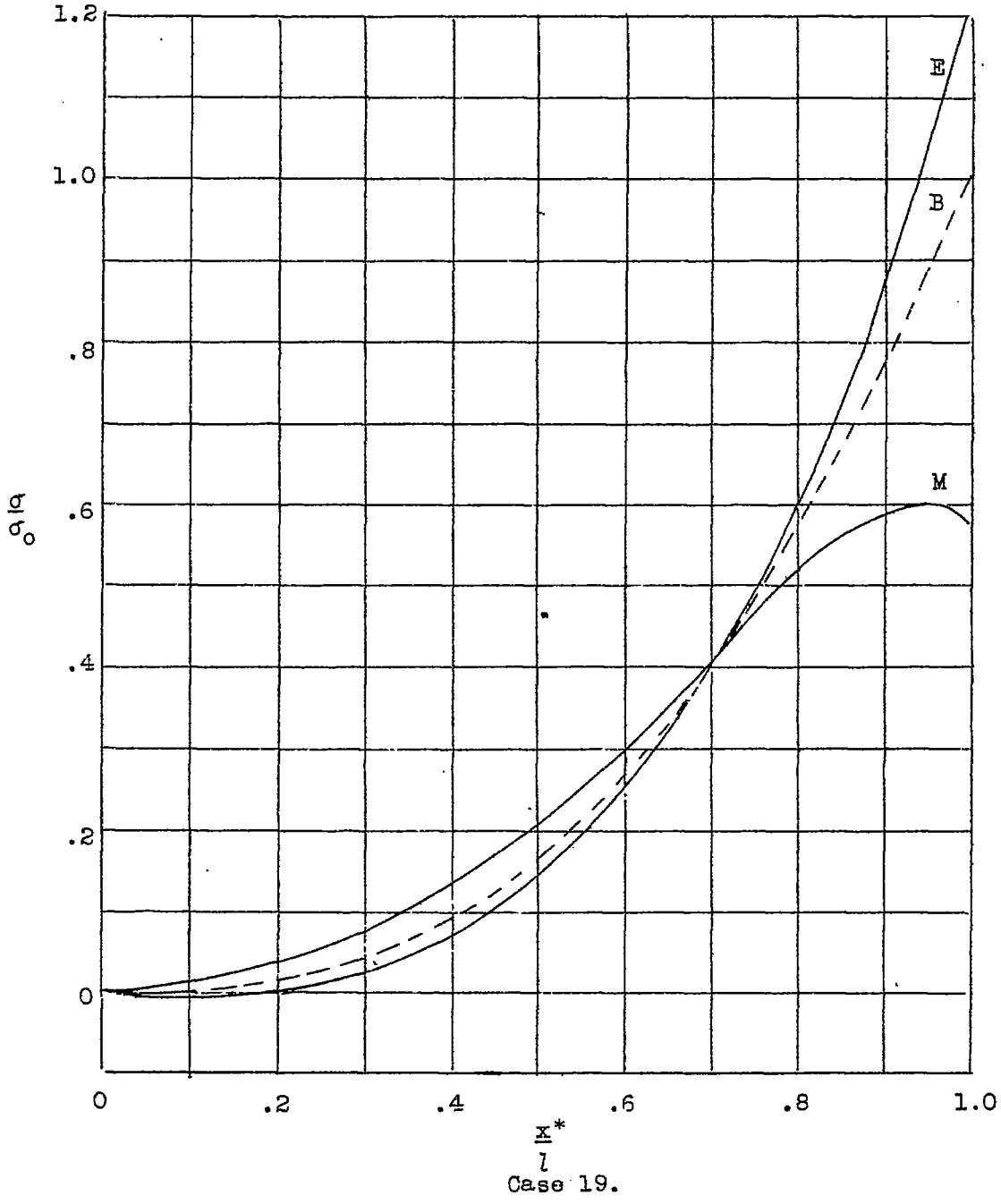

Case 19.

Figure 10(a to c).- Stress diagrams showing effects of taper in beam width and height (linearly increasing load).

[$(l/w_R)(6G/E)^{\frac{1}{2}} = 7.5$; $w_T/w_R = 0.5$; m = 2]

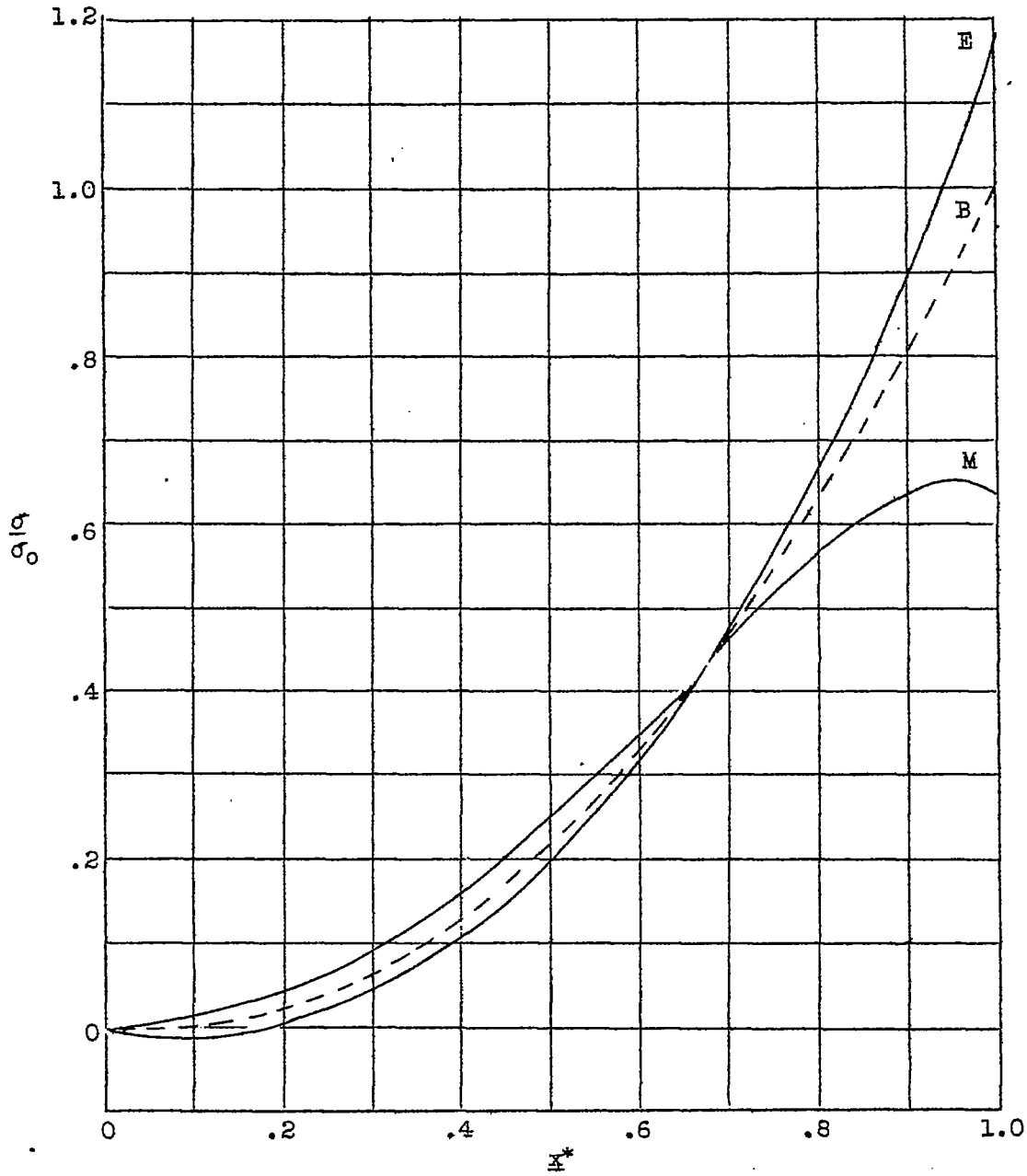

Case 20.

Figure 10.- Continued.

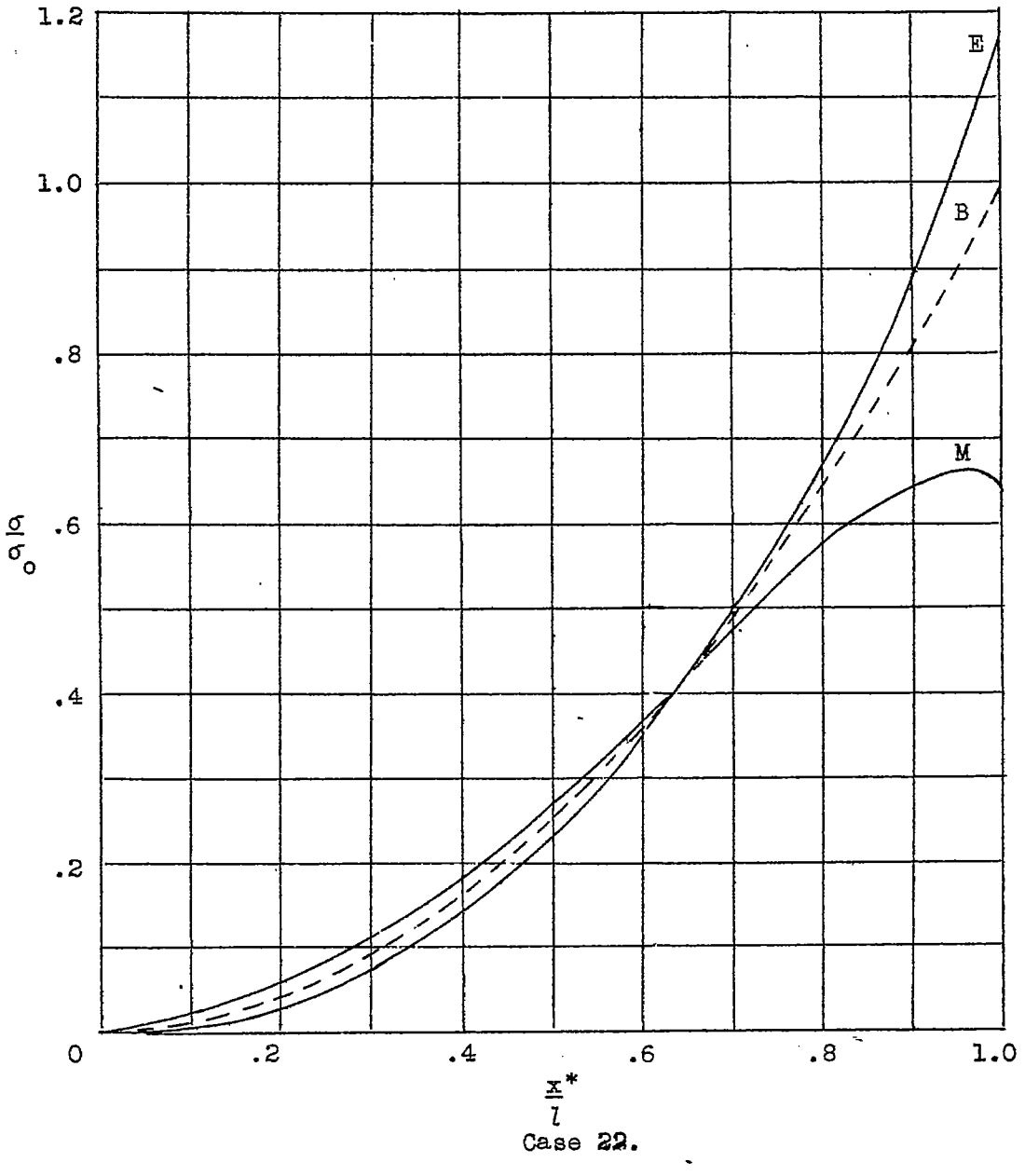

Case 22.

Figure 10.- Concluded.

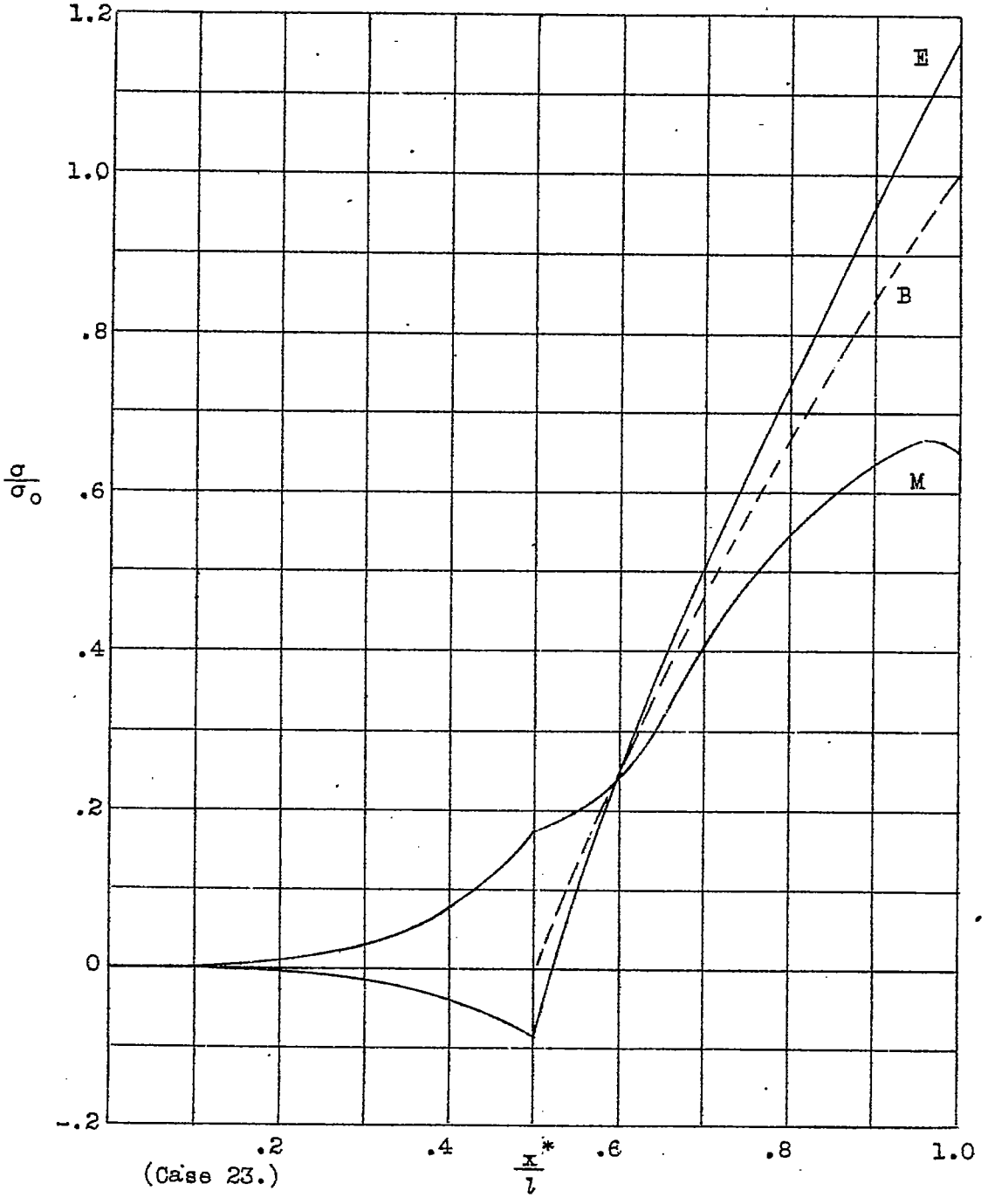

Figure 11(a to b).- Stress diagrams showing effects of taper in beam width and height. (Concentrated load at midspan).
$\left[\left(l/w_R\right)(6G/E)^{\frac{1}{2}} = 7.5;\ w_T/w_R = 0.5;\ m = 2\right]$

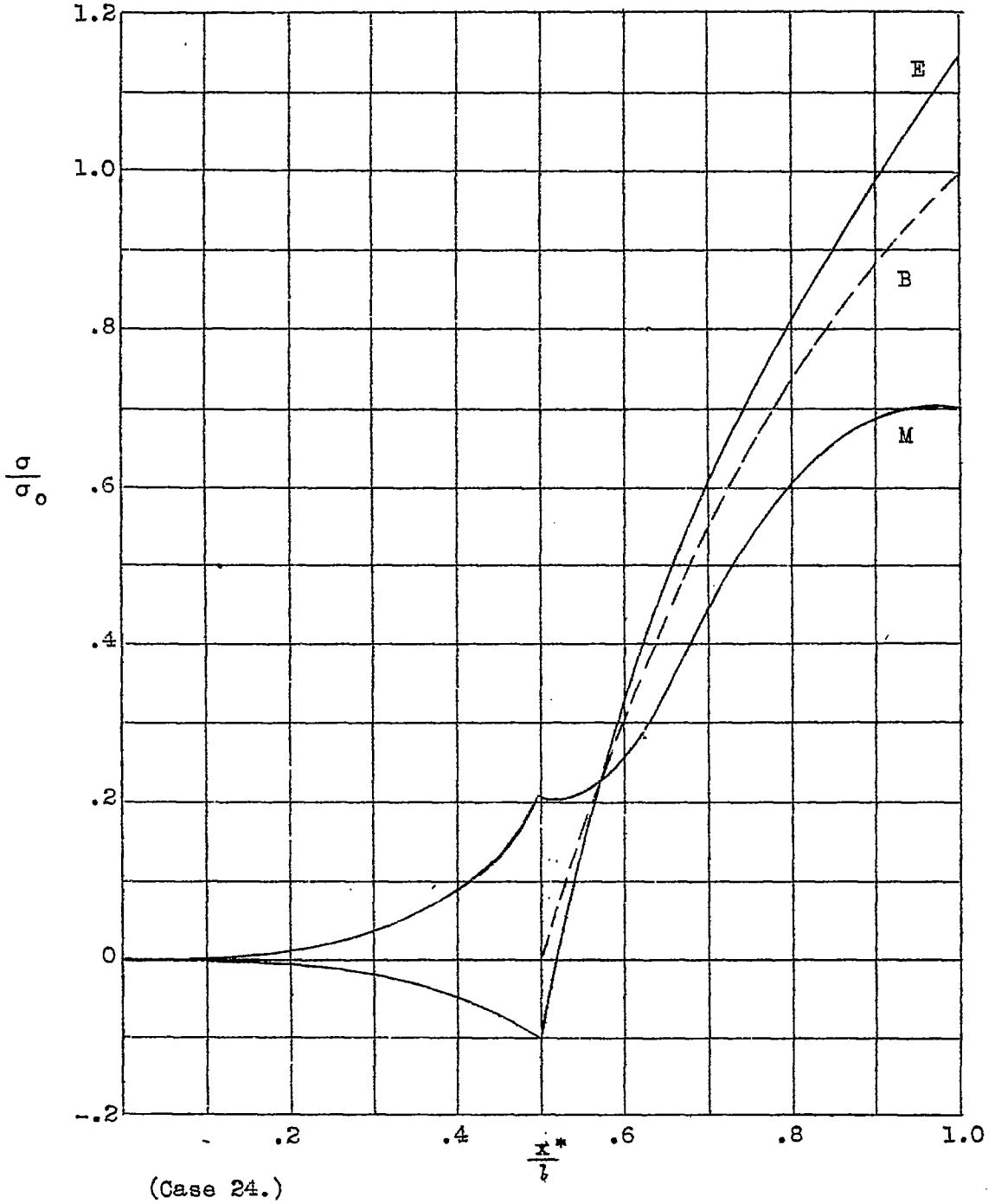

(Case 24.)

Figure 11.- Concluded.

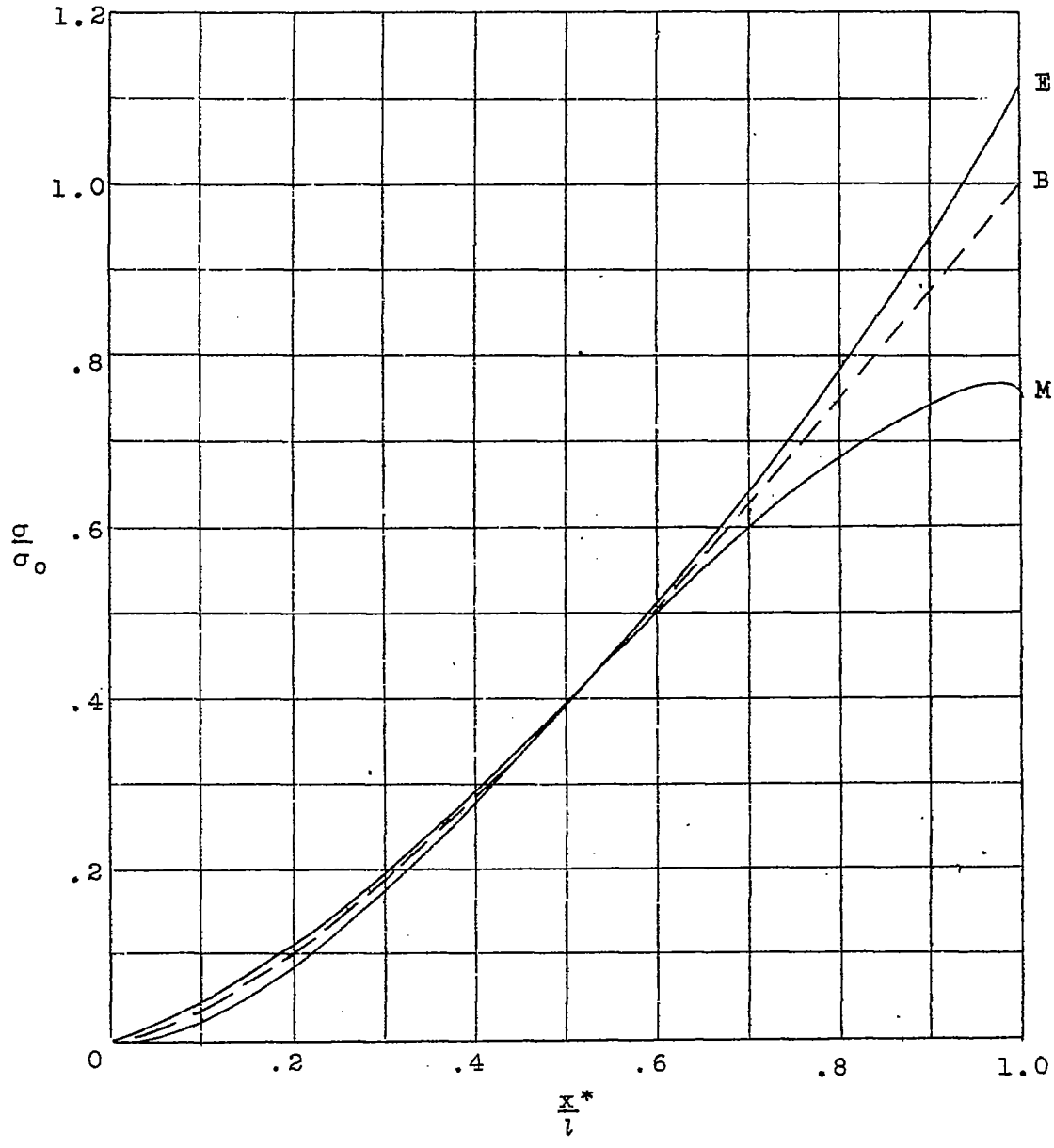

Case 25. $[w_T/w_R = 0.25]$

Figure 12(a to c).- Stress diagram showing effects of increased width taper. (Uniform load distribution.) $[(l/w_R)(6G/E)^{1/2} = 7.5;\ m = 2]$

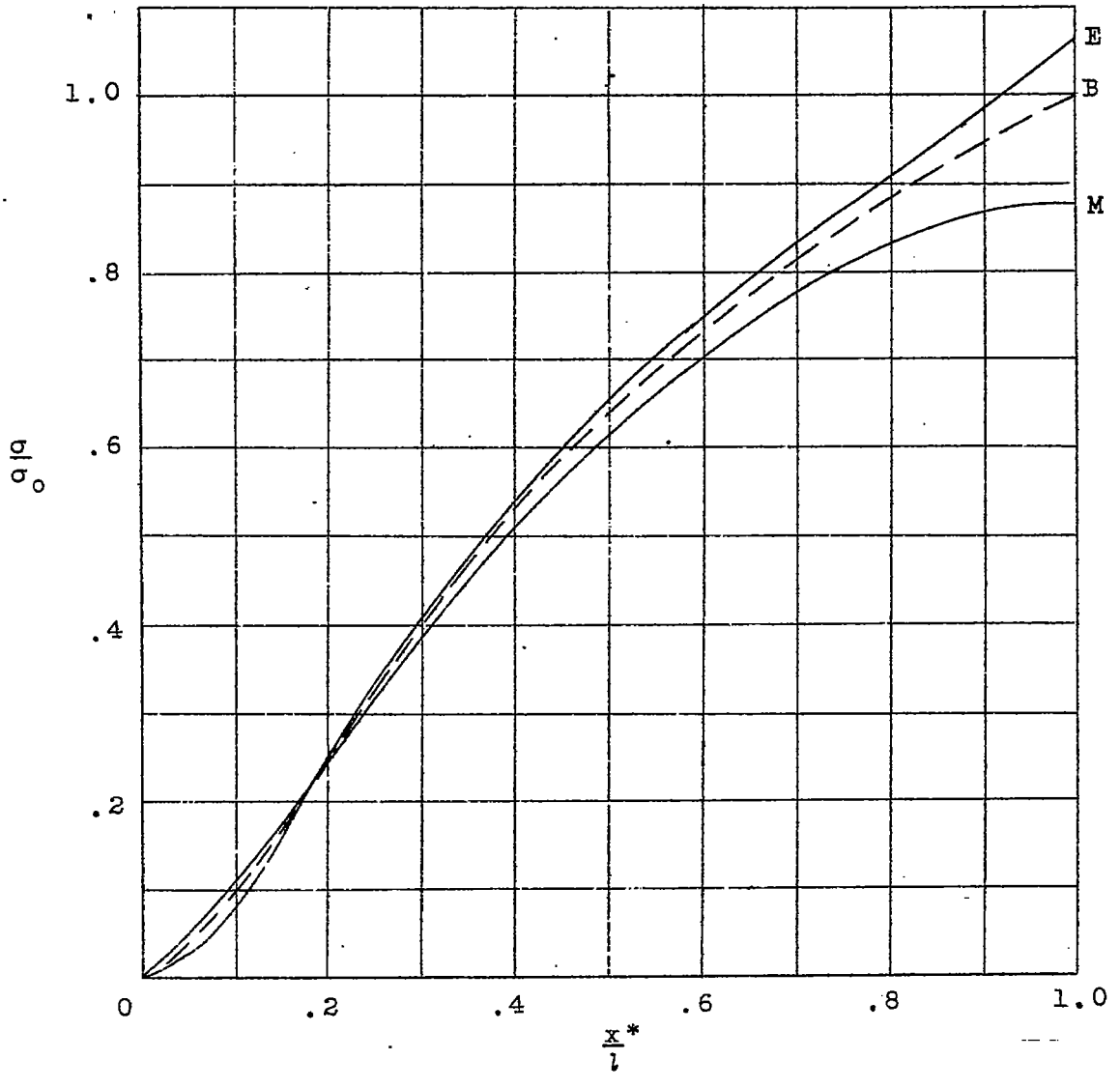

Case 26. $[w_T/w_R = 0.25]$

Figure 12.- Continued.

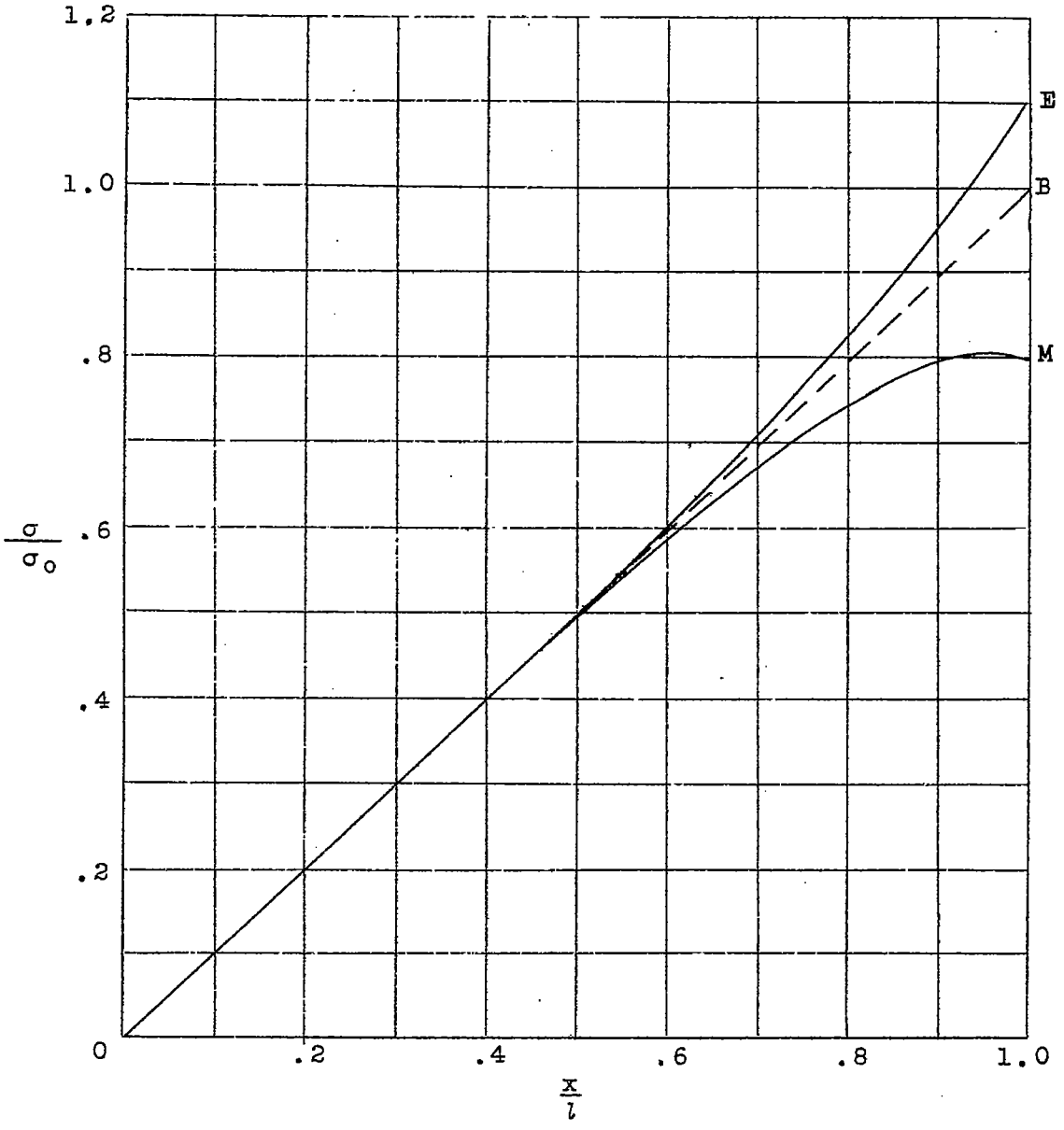

Case 27. $\left[w_T/w_R = 0\right]$

Figure 12.- Concluded.

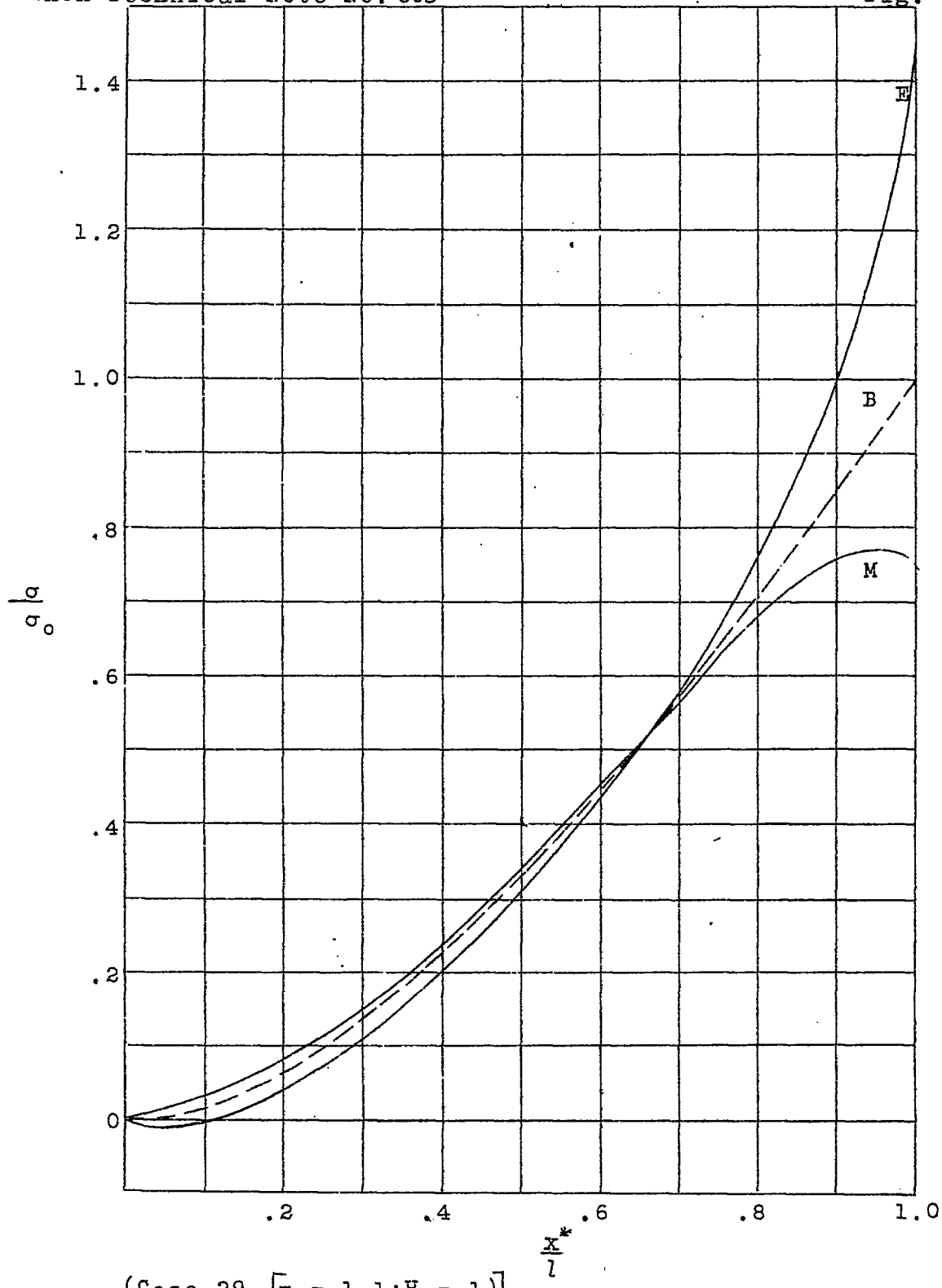

(Case 29, $[m = 1,1; H = 1]$)

Figure 13.- Stress diagrams showing effect of extreme changes of stiffness parameter on (uniformly distributed load) $[(l/w_R)(6\ G/E)^{1/2} = 7.5;\ w_T/w_R = 0.5]$ (a to d)

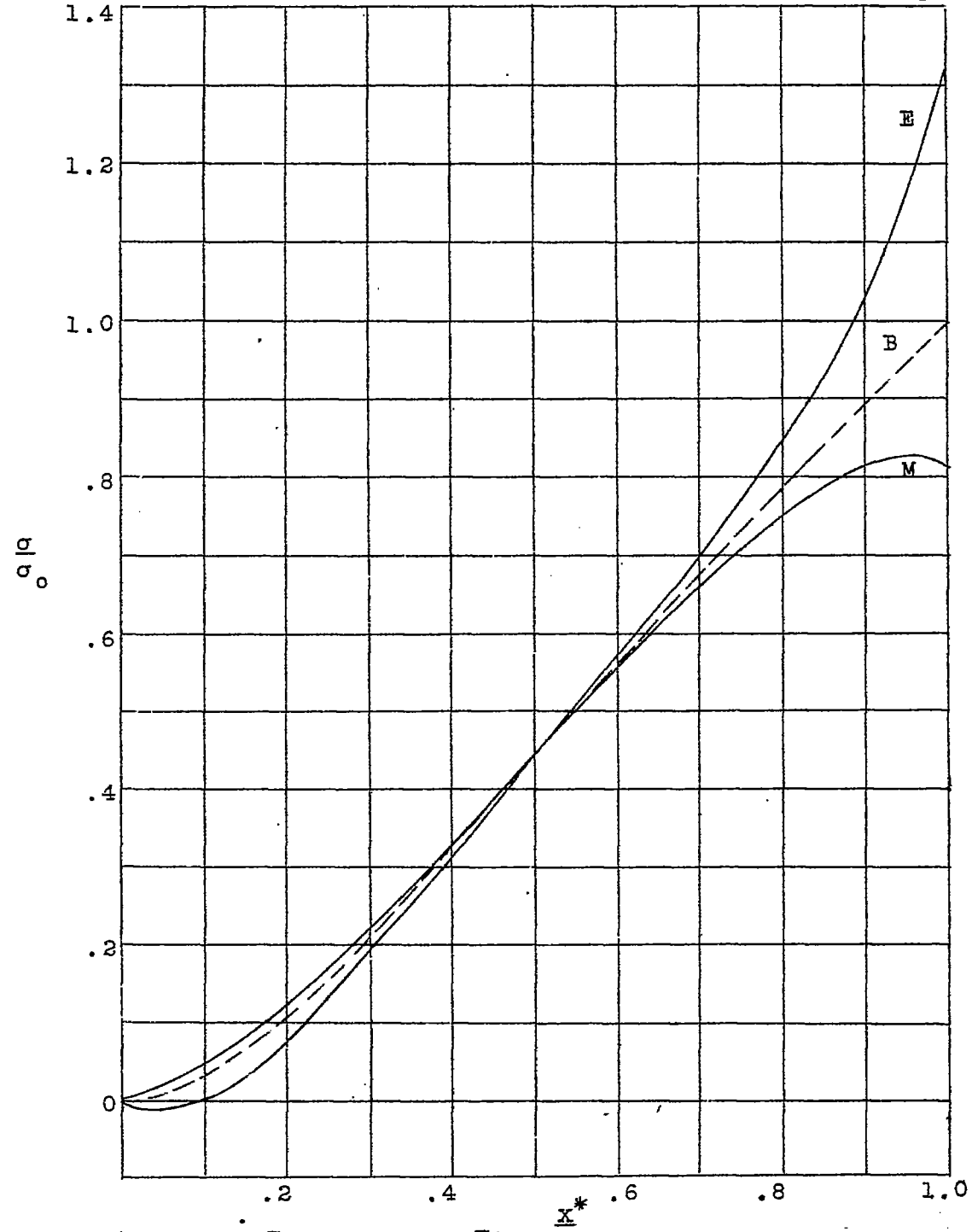

(Case 30. [m = 1.1; H = ξ])

Figure 13.- Continued.

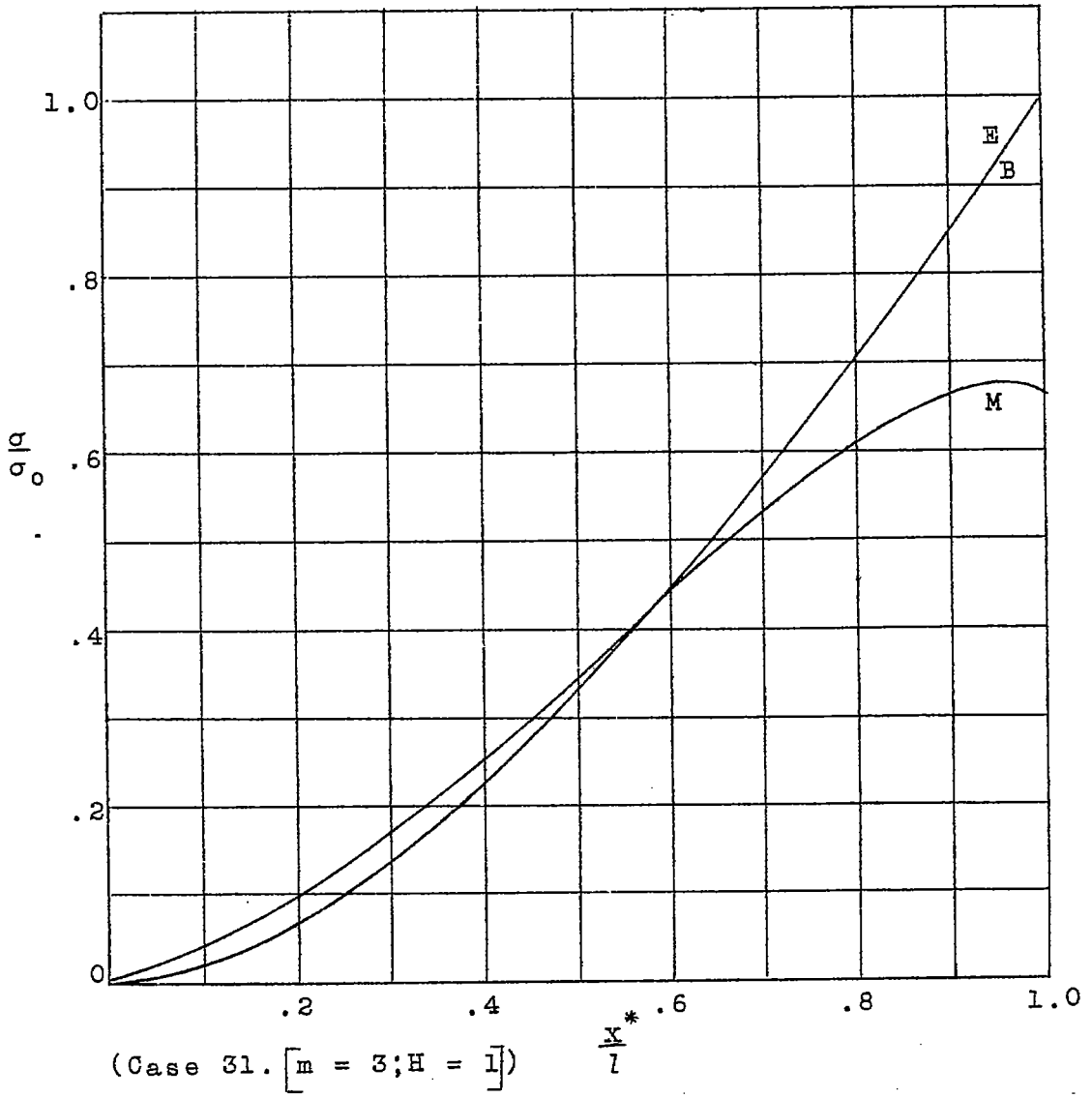

(Case 31. [m = 3; H = 1])

Figure 13.- Continued.

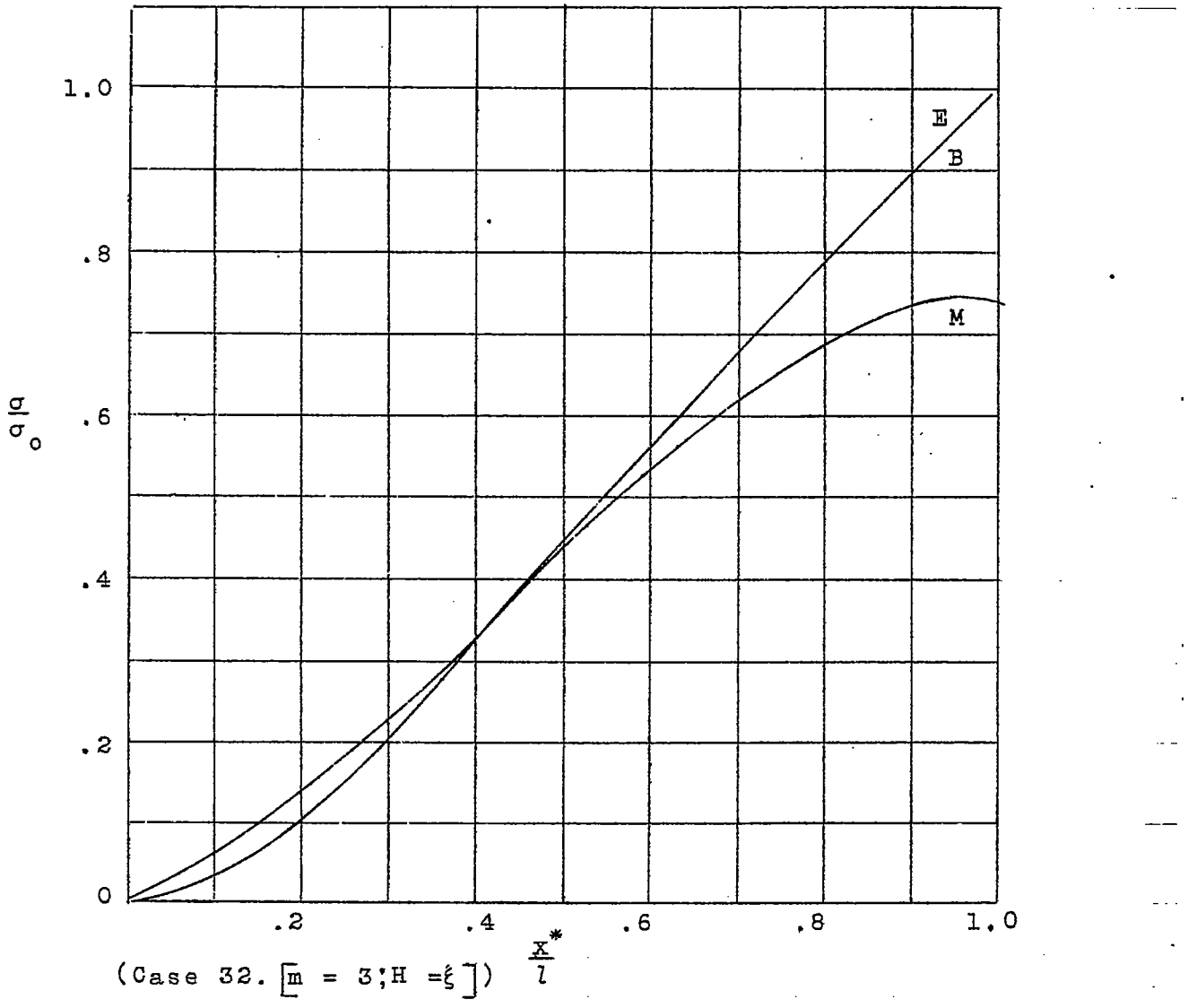

Figure 13.- Concluded.

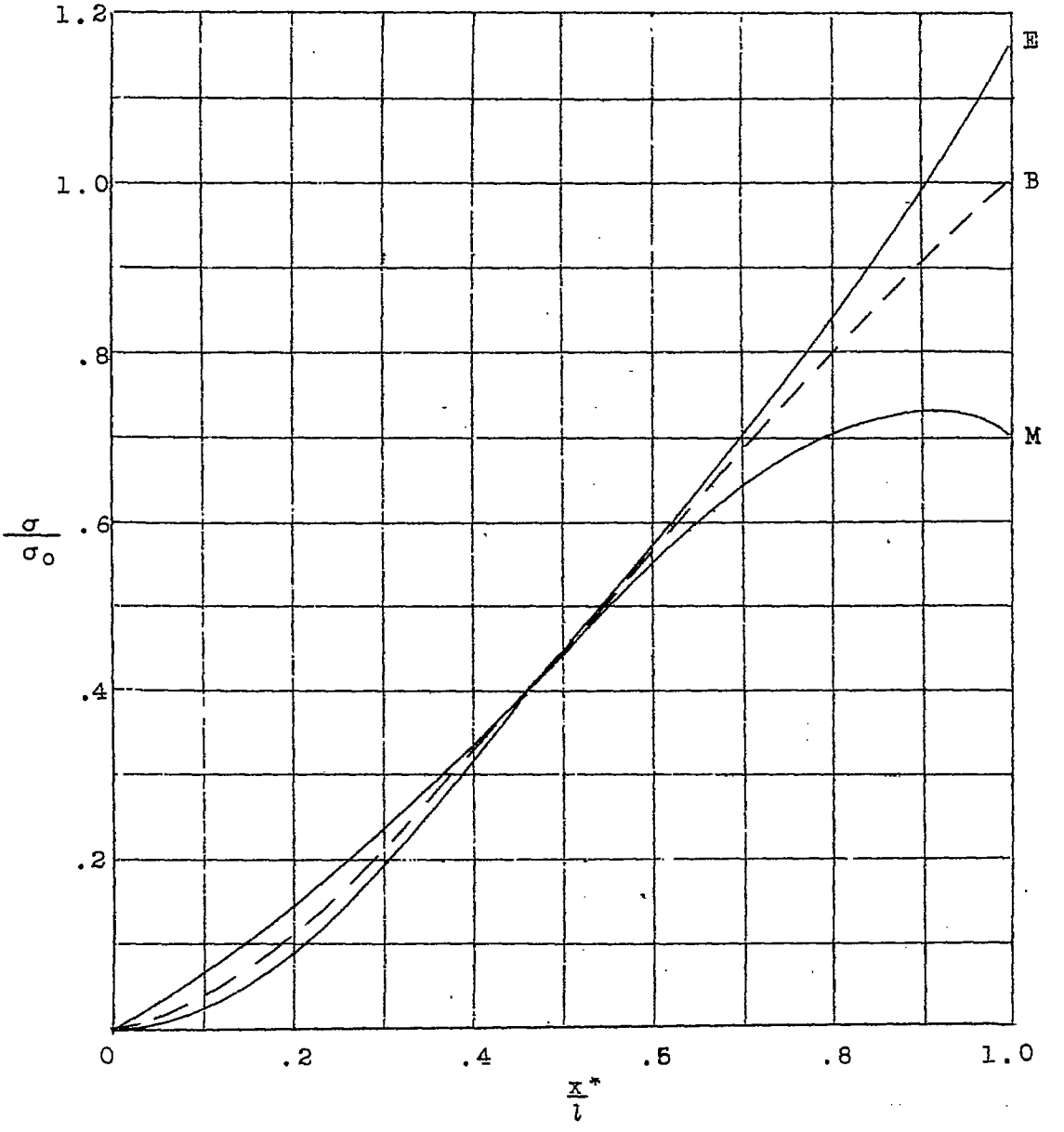

Case 33.

Figure 14(a to b).- Stress diagram showing effect of simultaneous taper in width, height and cover sheet thickness. (Uniform load distribution.) $[(l/w_R)(6G/E)^{1/2} = 7.5;\ m = 2,\ w_T/w_R = 0.5;\ T_T/T_R = 0.5]$

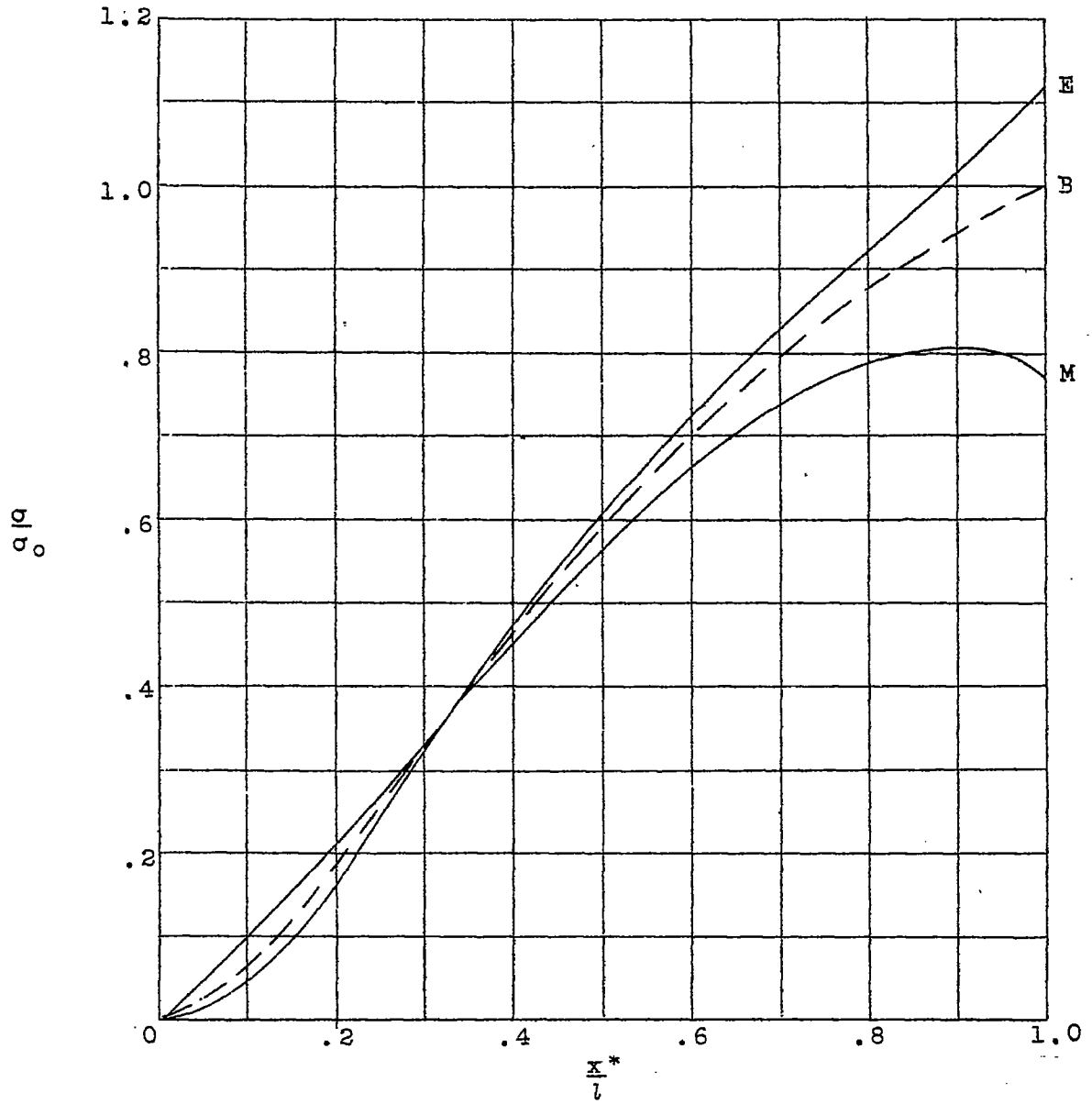

Case 34.

Figure 14.- Concluded.

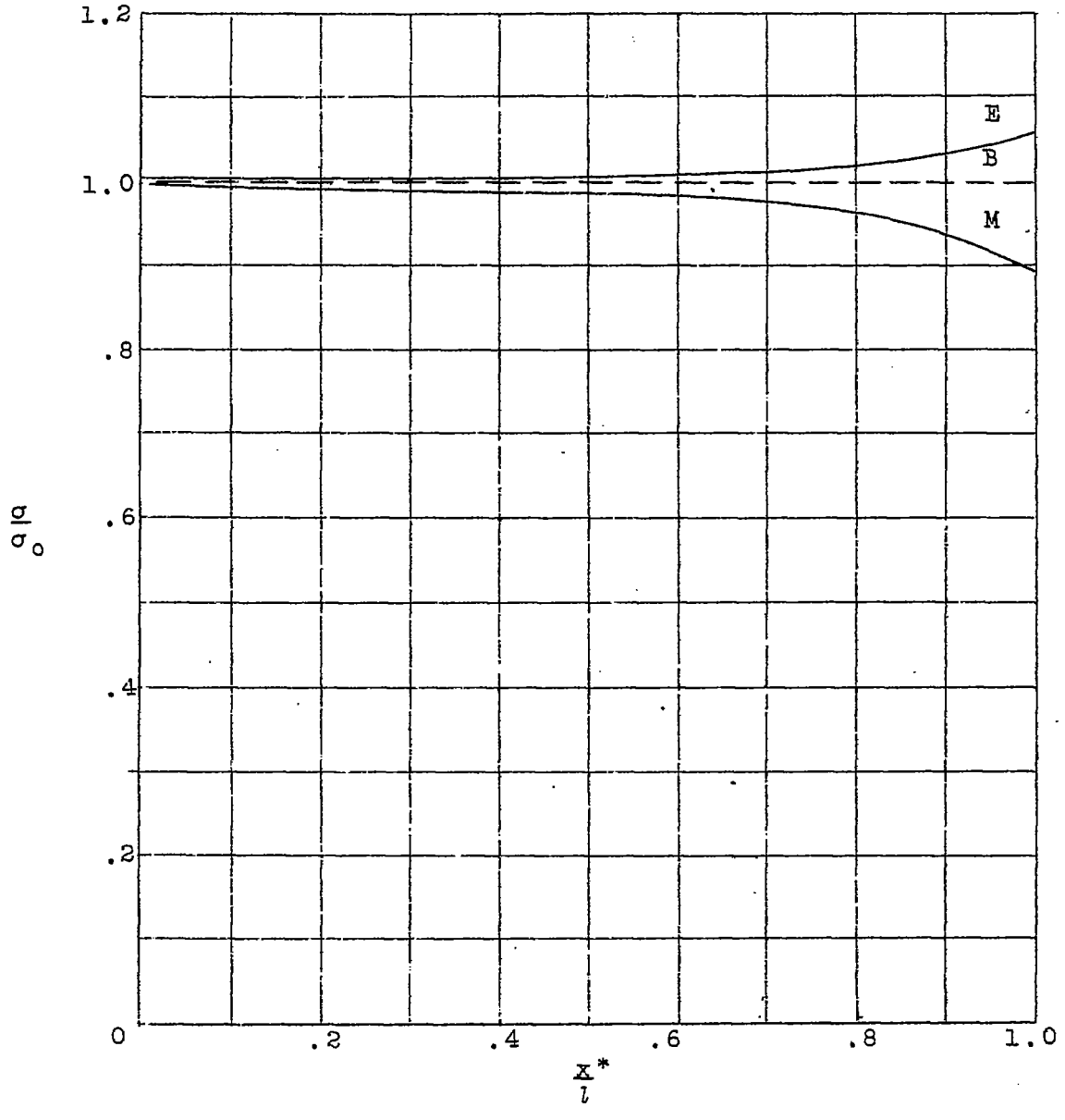

Case 35. $[w_T/w_R = T_T/T_R = 0.5]$

Figure 15(a to b).- Stress diagrams showing effect of cover sheet thickness taper. $[(l/w_R)(6G/E)^{1/2} = 7.5; m = 2]$

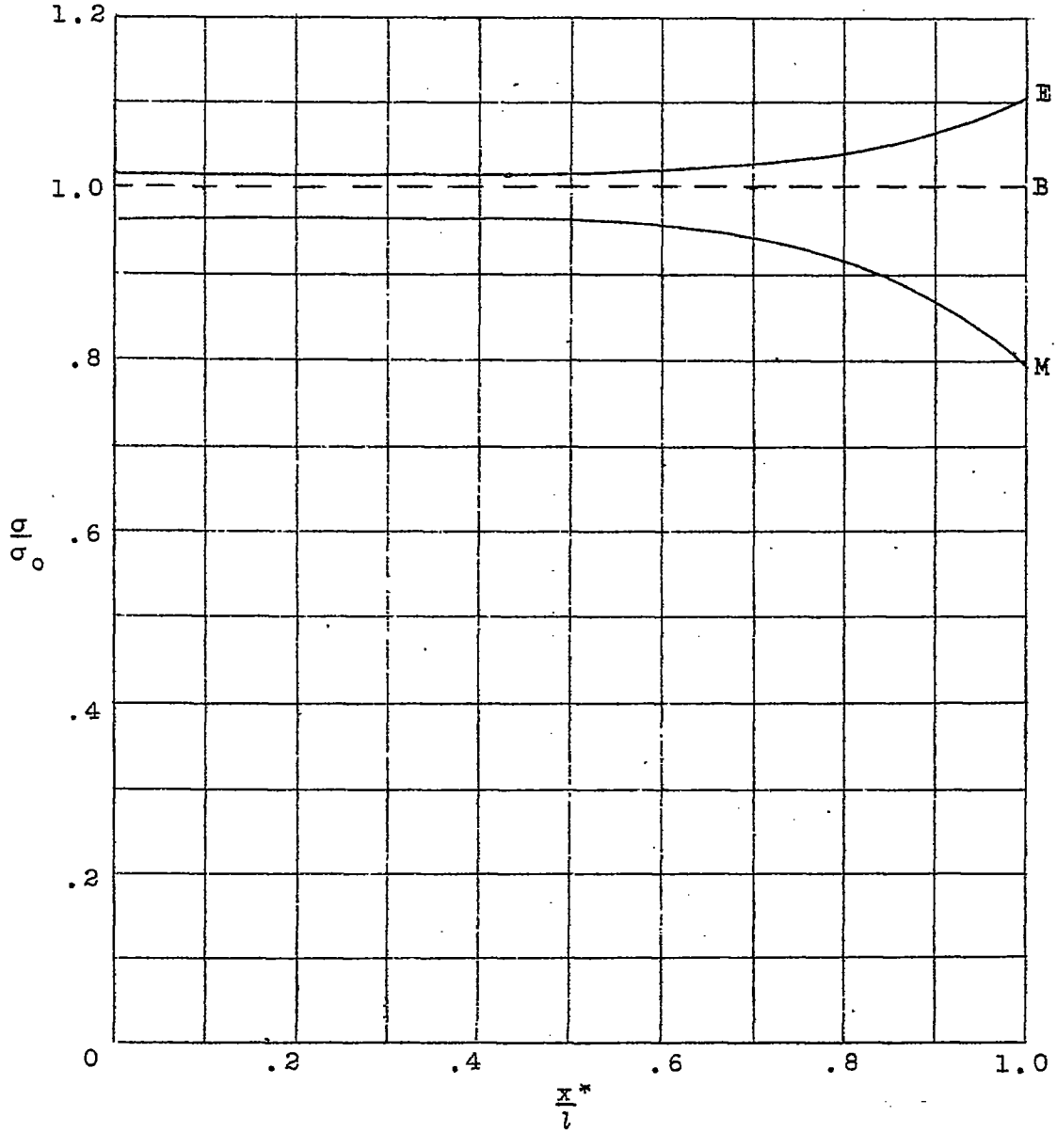

Case 36. $\left[w_T/w_R = T_T/T_R = 0\right]$

Figure 15.- Concluded.

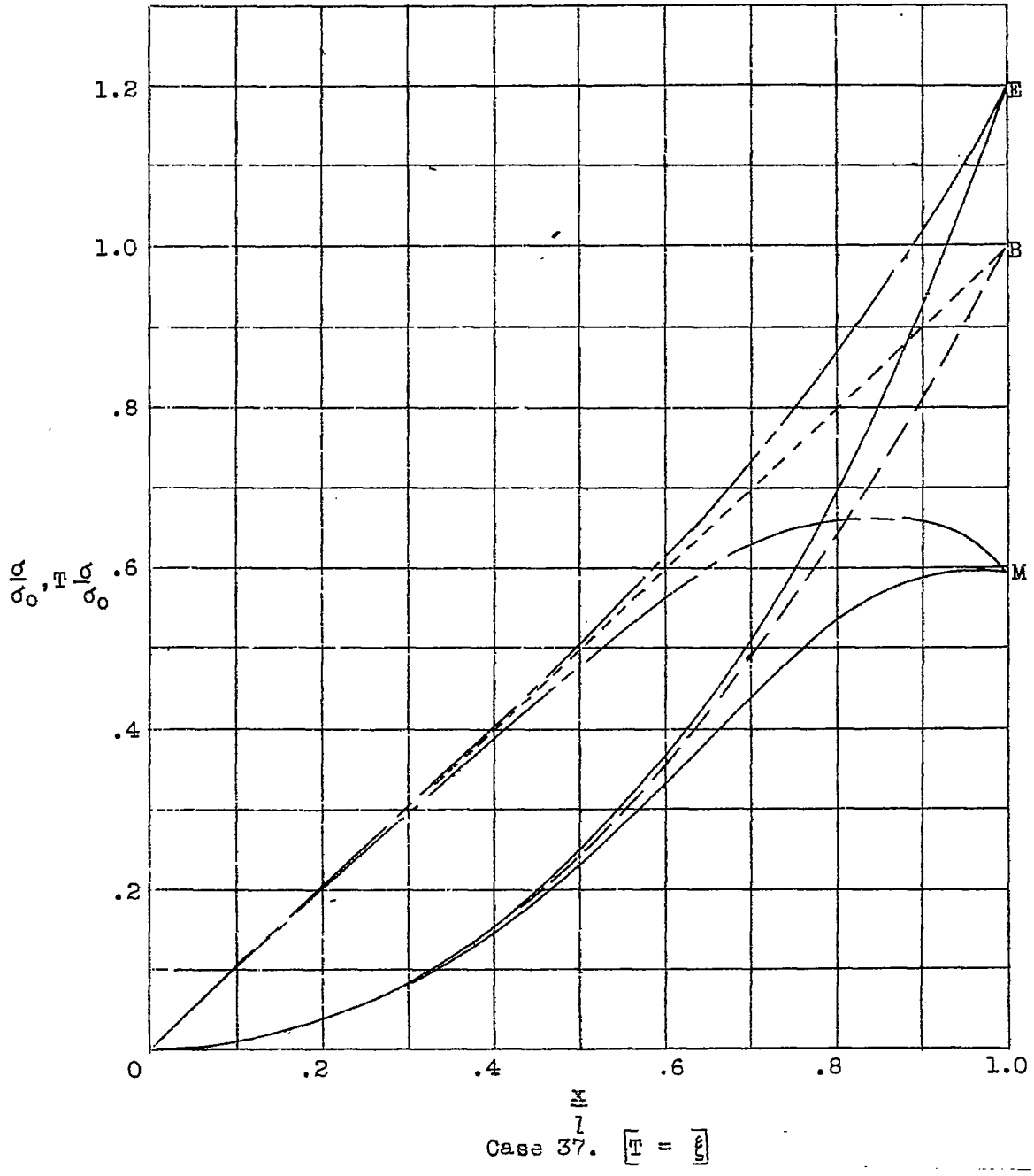

Case 37. $\left[T = \frac{S}{5}\right]$

Figure 16(a to c).- Stress diagrams showing effect of cover-sheet thickness taper, without width or height taper. (Solid lines represent stress resultants; dashed lines, stresses.) $\left[(l/w)(6G/E)^{1/2} = 7.5;\ m = 2\right]$

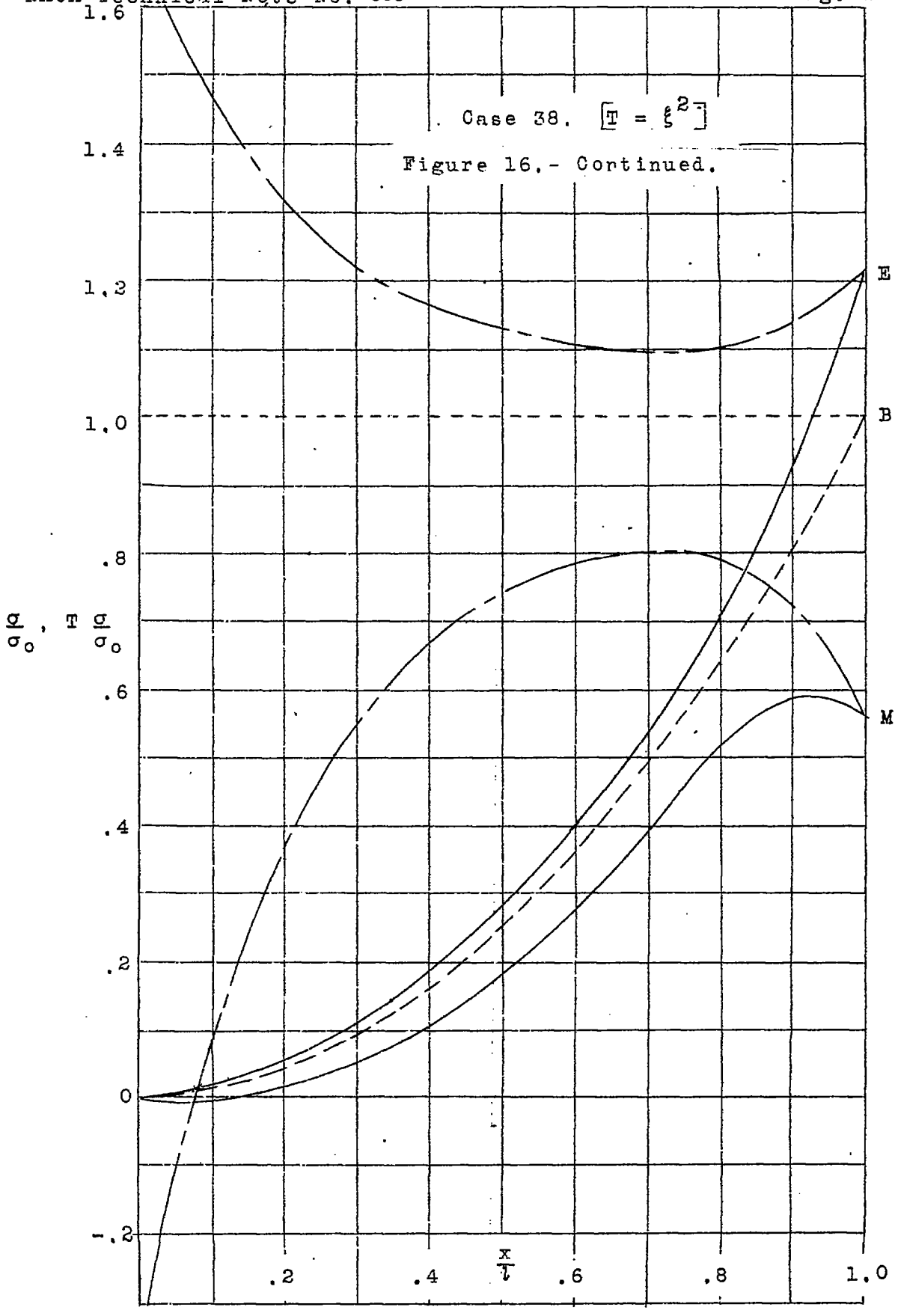

Figure 16.- Continued.

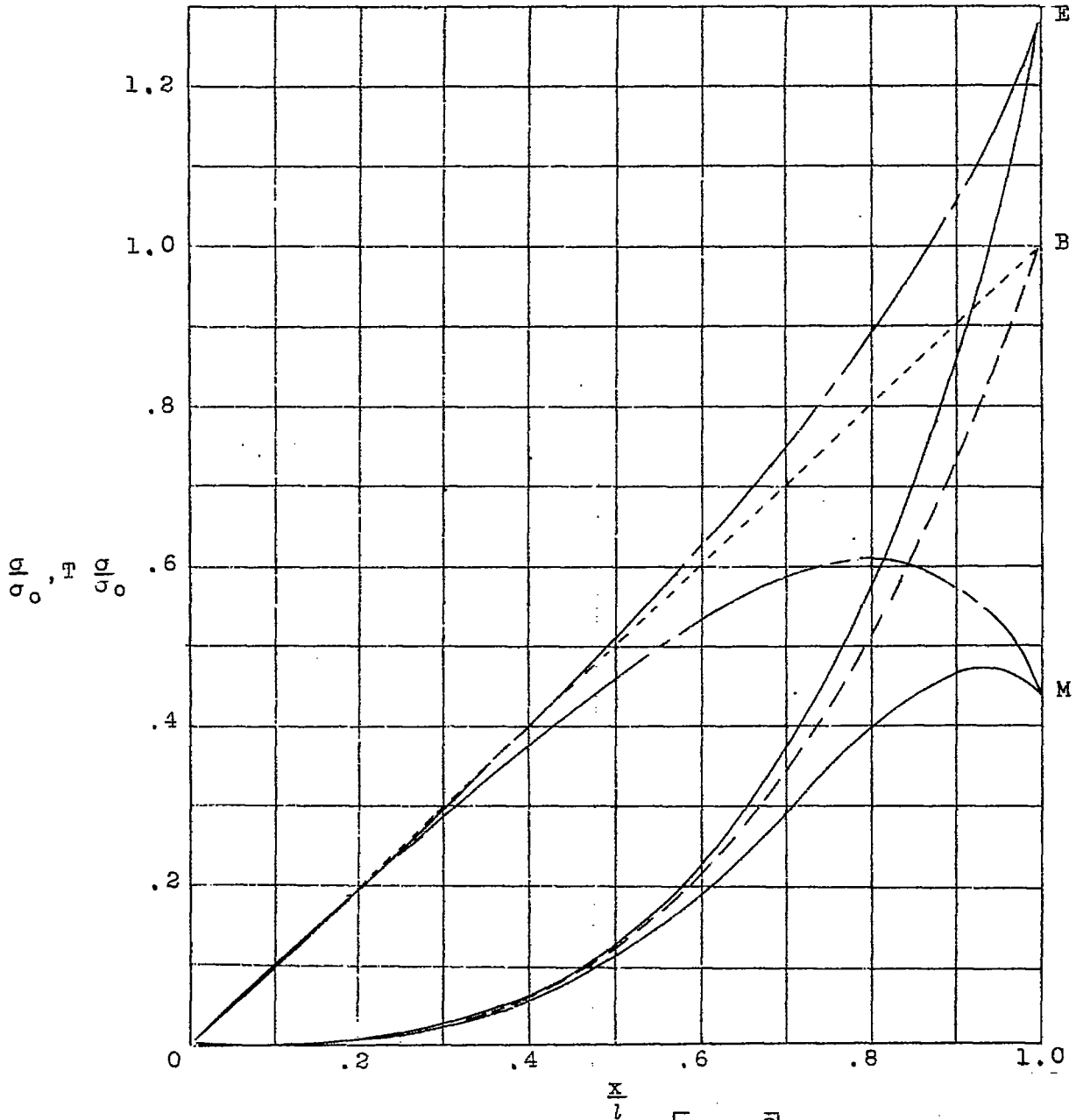

(c) Case 39. $\left[\mathfrak{T} = \xi^{a}\right]$

Figure 16.- Concluded.

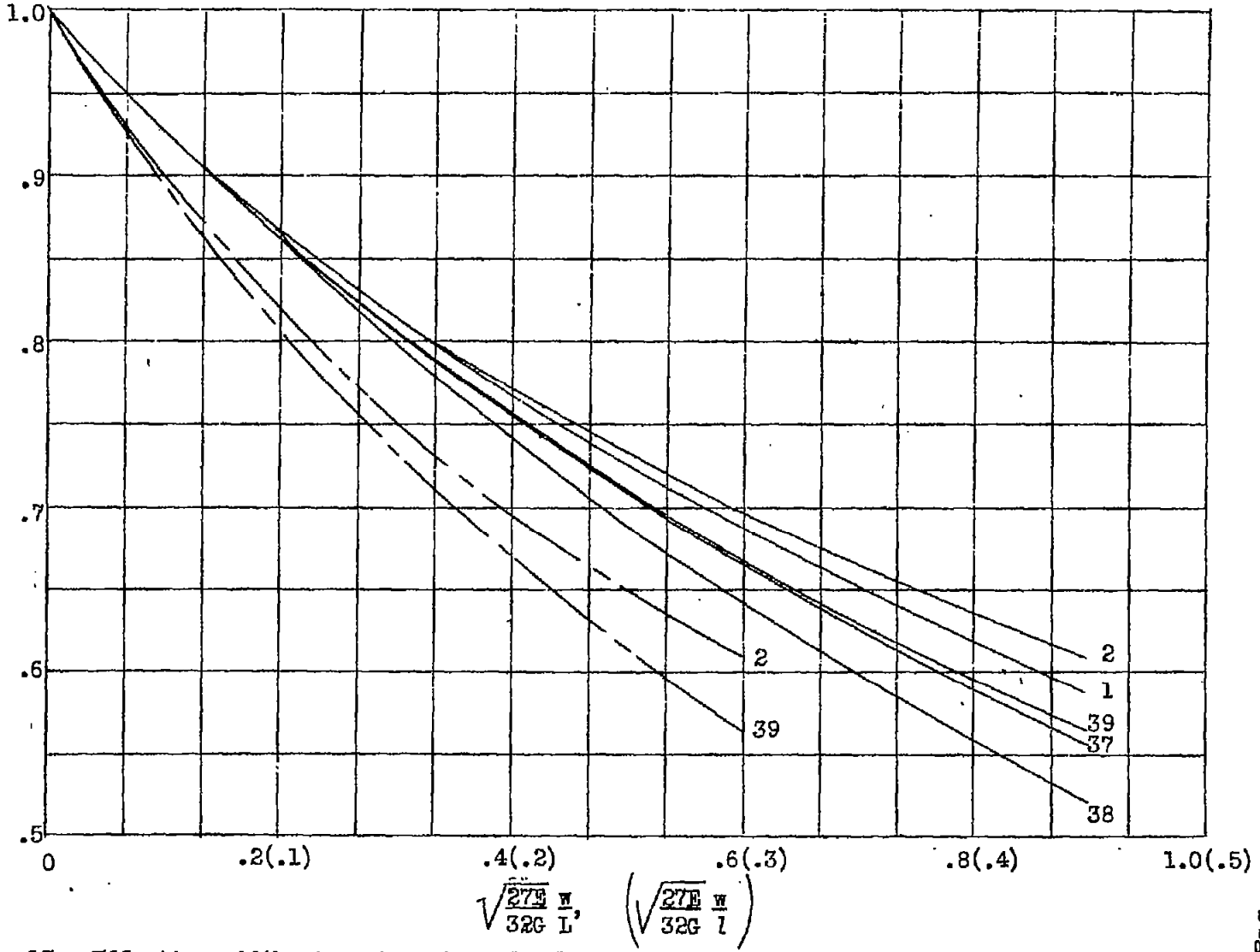

Figure 17.- Effective width at root section for beams with tapered and untapered cover sheet thickness. (Dashed lines represent effective width as a function of $w/_l$ where these lines do not coincide with solid lines.)

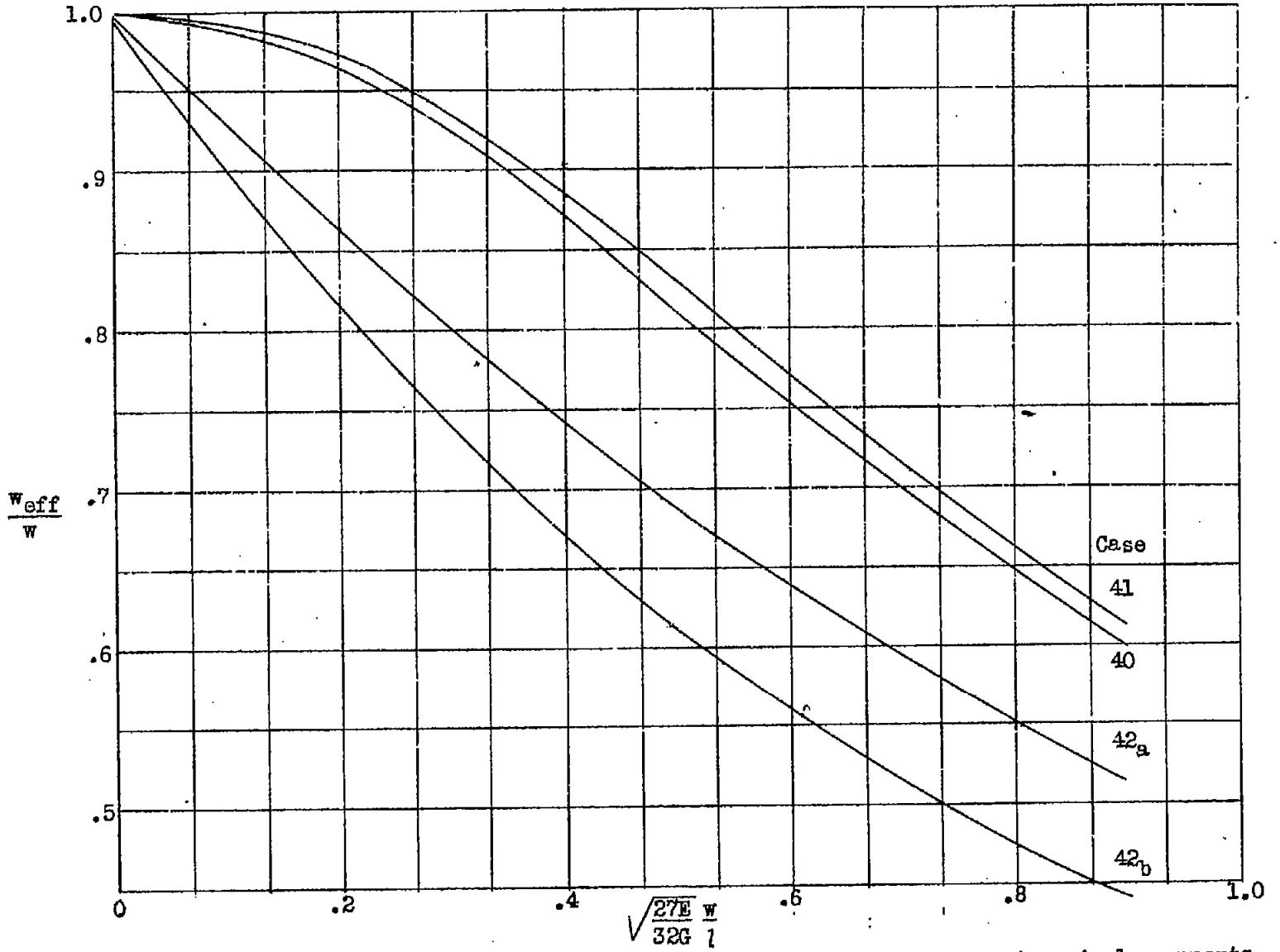

Figure 18.- Effective width at section of maximum bending moment for beams on two simple supports (m = 2).

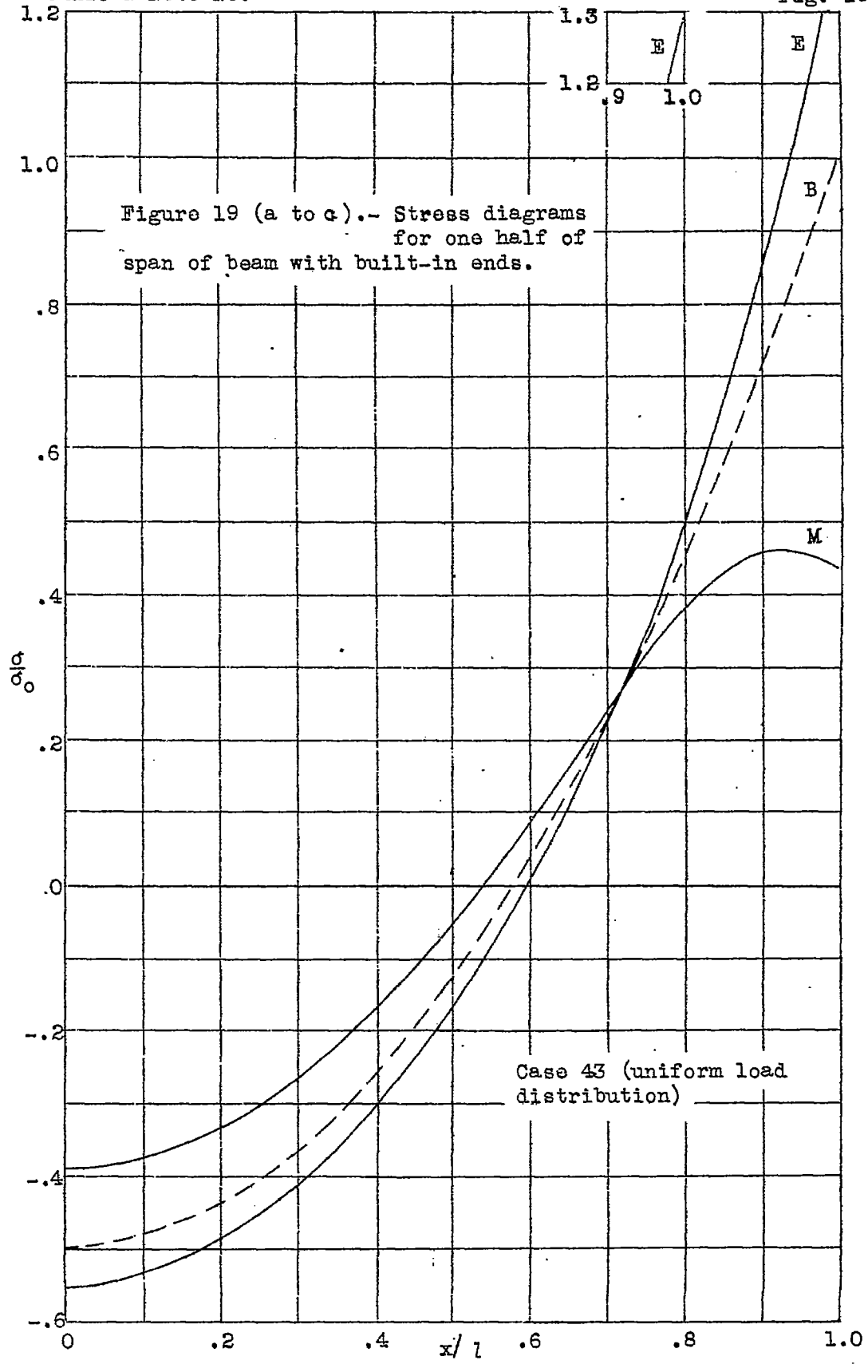

Figure 19 (a to c).- Stress diagrams for one half of span of beam with built-in ends.

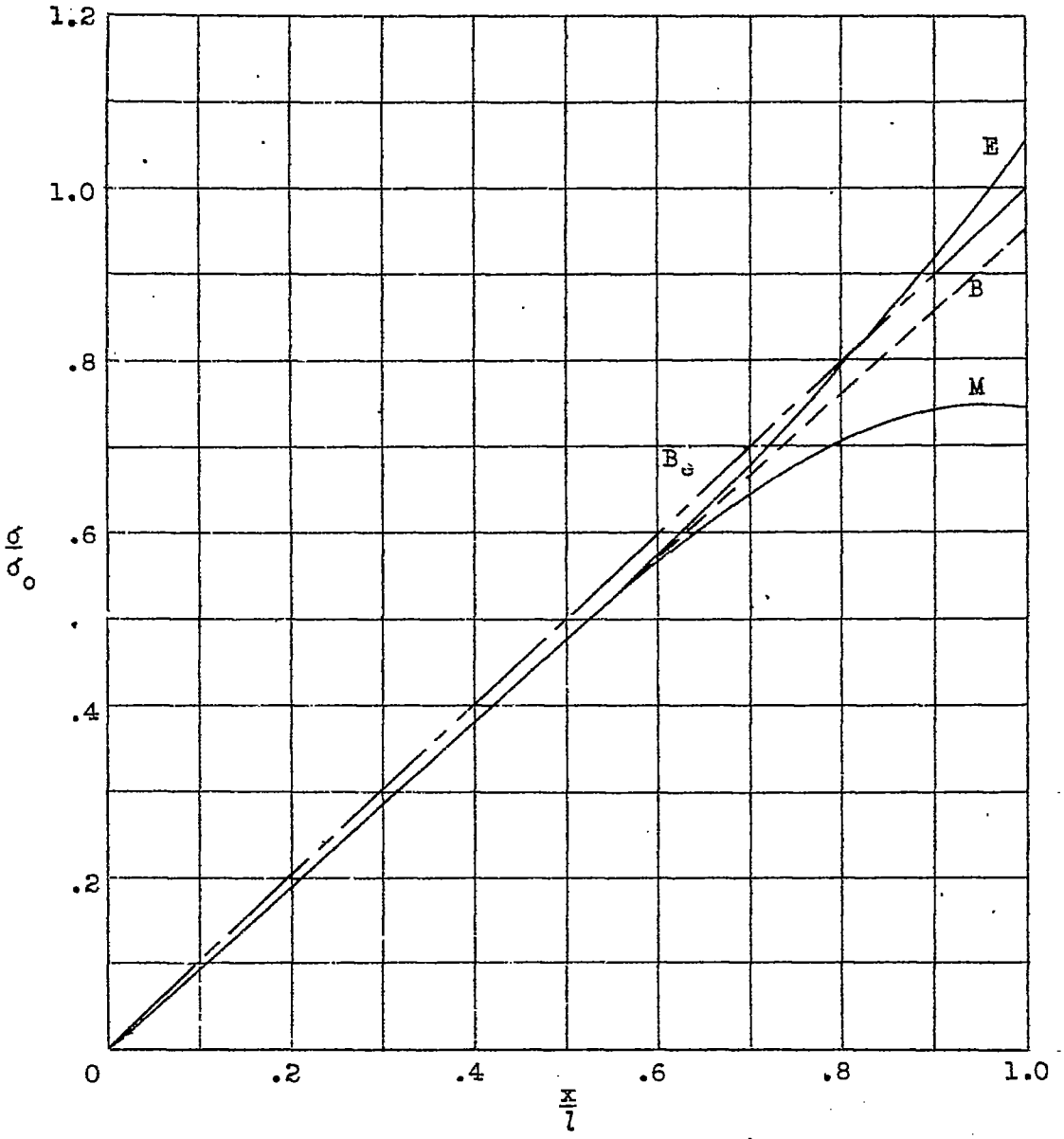

Case 44 (antisymmetrical and deflections)

Figure 19.- Continued.

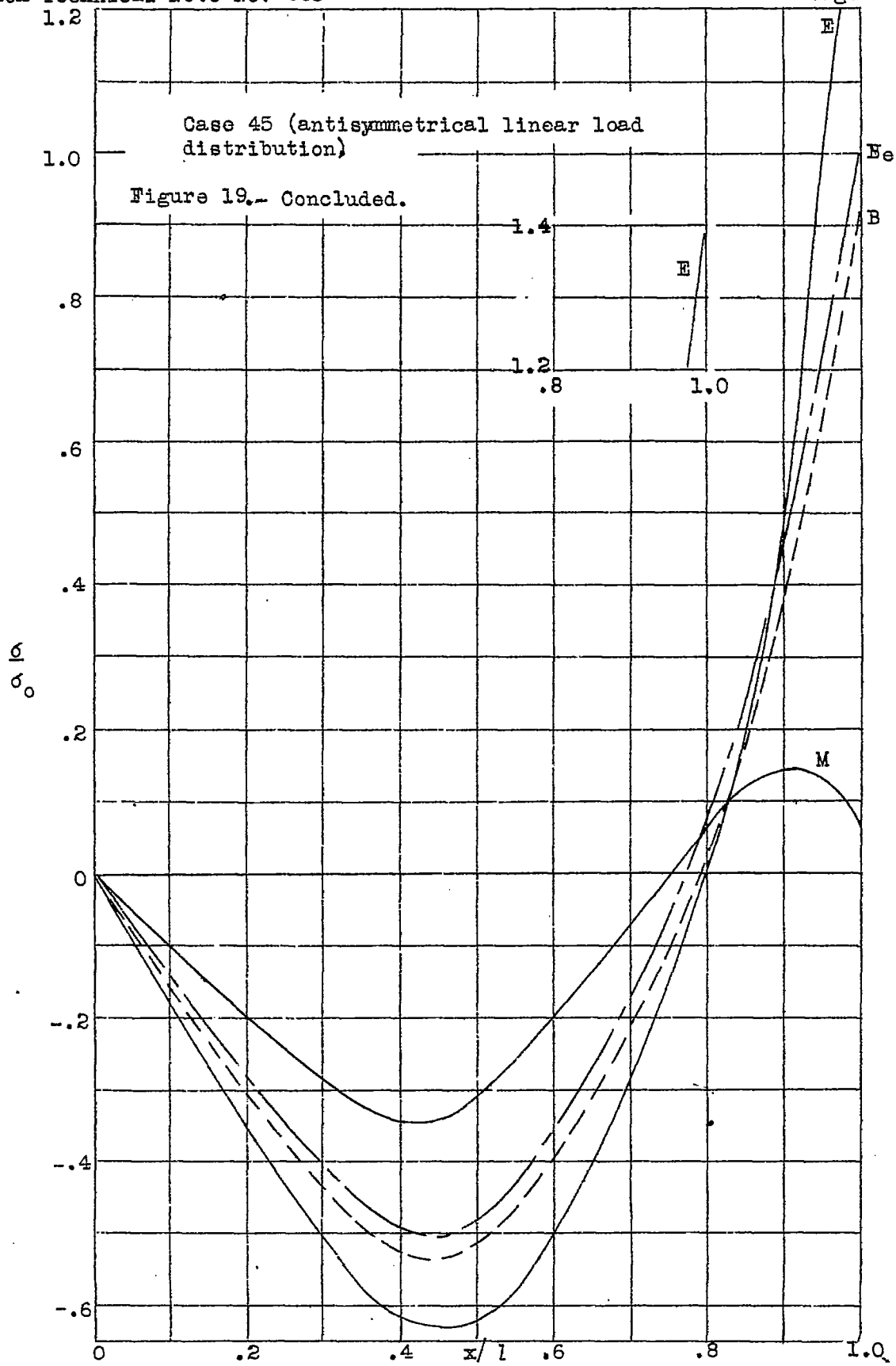

Figure 19.- Concluded.

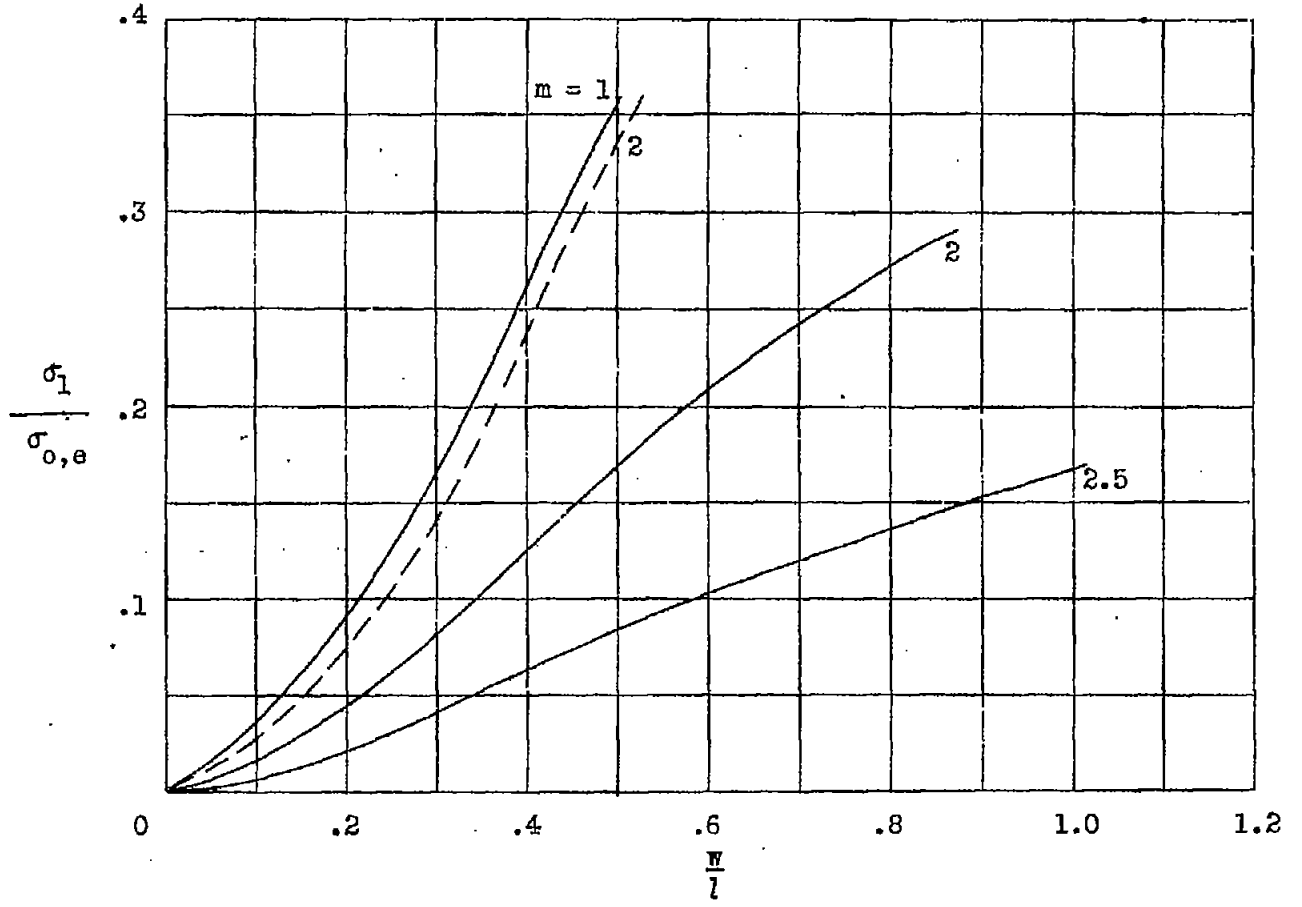

Figure 20.- Relative decrease in edge moment due to shear lag for cases 44 and 45.